PHOTOVOLTAIC THERMOELECTRIC COOLING SYSTEM FOR OFF-GRID VACCINE REFRIGERATOR : AN EXPERIMENTAL STUDY

A Thesis by

NAZIA RODOSHI KHAN

TASNUVA SHARMIN

DEPARTMENT OF MECHANICAL AND PRODUCTION ENGINEERING

ISLAMIC UNIVERSITY OF TECHNOLOGY

May (2022)

PHOTOVOLTAIC THERMOELECTRIC COOLING SYSTEM FOR OFF-GRID VACCINE REFRIGERATOR : AN EXPERIMENTAL STUDY

NAZIA RODOSHI KHAN

STUDENT ID: 170011002

TASNUVA SHARMIN

STUDENT ID: 170011037

Submitted in Partial Fulfillment
of the Requirements
for the Degree of

Bachelor of Science in Mechanical Engineering

DEPARTMENT OF MECHANICAL AND PRODUCTION ENGINEERING

May (2022)

CERTIFICATE OF RESEARCH

*This thesis titled "**PHOTOVOLTAIC THERMOELECTRIC COOLING SYSTEM FOR OFF-GRID VACCINE REFRIGERATOR : AN EXPERIMENTAL STUDY**" submitted by **NAZIA RODOSHI KHAN (170011002)** and **TASNUVA SHARMIN (170011037)** has been accepted as satisfactory in partial fulfillment of the requirement for the Degree of Bachelor of Science in Mechanical Engineering.*

Supervisor

Prof. Dr. Md. Hamidur Rahman
Professor

Head of the Department

Prof. Dr. Md. Anayet Ullah Patwari
Professor

Department of Mechanical and Production Engineering (MPE)
Islamic University of Technology (IUT)

DECLARATION

*I hereby declare that this thesis entitled "**PHOTOVOLTAIC THERMOELECTRIC COOLING SYSTEM FOR OFF-GRID VACCINE REFRIGERATOR : AN EXPERIMENTAL STUDY**" is an authentic report of study carried out as requirement for the award of degree B.Sc. (Mechanical Engineering) at Islamic University of Technology, Gazipur, Dhaka, under the supervision of **Dr. Md. Hamidur Rahman**, **Professor**, MPE, IUT in the year 2022.*

The matter embodied in this thesis has not been submitted in part or full to any other institute for award of any degree.

_____

Nazia Rodoshi Khan

170011002

_____

Tasnuva Sharmin

170011037

ACKNOWLEDGEMENT

In the Name of Allah, the Most Beneficient, the Most Merciful

First of all, I am grateful to ALLAH (SWT), the most benevolent and kind to provide me the strength and ability to write this dissertation. I want to thank my project supervisor, Prof. Dr. Hamidur Rahman Sir, for his strong and patient support through unpredictable problems during the project and his precious advice when I faced difficulties. His generosity, kindness and strong supervision during work made me feel less stressed in confronting unexpected troubles and be more productive in my personal life.

In the next step, I would like express my deep acknowledgment to my father and mother for their continued support and dedication towards my higher study.

Finally, I would like to acknowledge gratefully for the financial support by Islamic University of Technology.

Abstract

The rapidly rising demand of refrigeration technologies mostly in the fields of refrigeration and air conditioning, medical applications and electronic component cooling resulted in much more energy being produced than the requirement. Thermoelectric refrigeration is a novel option that can transform excess power into effective cooling mitigating the problem of current energy concerns. Additionally, the utilization of solar energy as the main power source has ensured the system to be revolutionary and versatile. In comparison to typical cooling methods, thermoelectric coolers have garnered considerable attention for marginal cooling applications in medical science. This research examines thermoelectric freezers for thermal control systems in disciplines of medicine, such as cooling chambers for storing vaccines.

The goal of this study is to construct and experimentally optimize a functional photovoltaic thermoelectric refrigeration system for the purpose of cooling of an optimal volume which works on the principle of Peltier effect to refrigerate and sustain a range of temperature between 2 to 8℃. The capacity of the thermoelectric module has been chosen based on the heat load calculations. The design specification is to cool the respective volume using the forced convection mechanism to a desired range of temperature in less than half an hour and maintain retention of heat for at least the next hour. The design criteria, potential parameters, and the final design of a PV integrated thermoelectric refrigerator are strategically highlighted. An approach is also offered for finding the optimal geometry and power required for operating a small-scale photovoltaic thermoelectric vaccine storage system.

Finally, we note that the novelty of photovoltaic thermoelectric cooling systems have progressively superseded the conventional freezers in medical uses due to their benefits of compactness, innovative usage of renewable energy, versatility, and pollution-free properties. Both modeling and analysis of thermoelectric cooling systems are likely to benefit from this research.

Table of Contents

List of Figures

List of Tables

Nomenclature

LPG	Liquid Petroleum Gas
WHO PQS	World Health Organization: Performance, Quality and Safety
TEC	Thermo-electric Cooler
TE	Thermo-electric
ZT	Figure of Merit
COP	Coefficient of Performance
AC	Alternating Current
DC	Direct Current
PV	Photo Voltaic
MPPT	Maximum Power Point Tracking
T_h , Tc	Temperature of Hot and Cold Side
R	Thermal Resistance
λ	Thermal Conductivity
σ	Electrical Conductivity
K	Thermal Conductivity
R_{cond}	Resistance of Conduction
A	Area exposed to Heat Transfer
L	Thickness along the Direction of Flow
R_{conv}	Resistance of Convection
h_0	Convective Heat Transfer Coefficient
Q_{cond}	Conductive Heat Transfer Rate
Q_{conv}	Convective Heat Transfer Rate
T_s	Temperature of Surface
T_f	Temperature of Fluid
ε	Coefficient of Emissivity
σ	Stefan-Boltzmann Constant
T_{surr}	Temperature of Surrounding
Q_T	Total Refrigeration Load
Q_c	Heat Transfer Rate inside the Chamber
Q_{PL}	Product Load
W_{fan}	Heat generated by Fan
P_e	Power consumed by TE Module
I_e	Current Rating of TE Module
V_e	Voltage Rating of TE Module
Re	Reynold's Number
Nu	Nusselt Number
Pr	Prandtl Number

Chapter 1

Introduction

1.1 Background of the study

Among all the different types of health therapies available today, immunization happens to be one of the most widely used preventive measure for a number of diseases and health conditions [1]. Life threatening chronic conditions are avoided, and millions of lives are saved every year as a result of its use [2]. Vaccines have the ability not just to save lives, but also to transform them by increasing their chances of survival [3]**.** Although vaccination is an absolutely essential health initiative, it has reached a plateau in the past few years. The COVID-19 epidemic along with the disruptions it brought in, have caused sudden disorganization in health services, with 23 million children skipping vaccinations in 2020, 3.7 million more than in 2019 and the largest amount since 2009 [4]. In 2020, more than 17 million infants missed out on receiving the first dose of Diphtheria-Tetanus-Pertussis (DTP). This is a clear indication of inaccessibility to quality health care and the services associated to it. In addition, another 5.6 million received only partial vaccination the same year [5]. Failure to achieve regular vaccination for children is related to more than a lack of consistent vaccine funding [6]. It is also the product of ill-managed and under-equipped health-care delivery systems [7]. In certain nations, health services are scarce outside of metropolitan regions, while in others, buildings, cars, and critical cold chain equipment may be neglected or in disrepair [8]. Vaccine safety may also be jeopardized if vaccines are stored in malfunctioning refrigerators and freezers [3]**.** Another crucial factor in preserving medicinal goods including essential vaccines is having access to grid electricity. It is a matter of fact that, access to electricity basically represents the state of economic progression as well as an indication towards enhanced livelihoods. [9]. Therefore, the estimate of the portion in a region who have direct access to power is indeed a significant metric for an improved socio - economic state. In the past few decades the portion of individuals with access to grid power has risen in a consistent manner. Around 71% people all over the globe had access to electricity in 1990. This percentage eventually increased to

87% by 2016. And still, around 13% population did not have any direct access to grid power. Although such advances in the proportion of the population having access are noteworthy for nations with high population growth, a lot of locations throughout the globe are still seriously underperforming. Significant gains in access will continue to be a serious concern for several nations over the next few decades [10]. As can be seen from figure no. 1, a major portion of population in several developing countries is still without any access to electricity. However, even in locations that have access to grid power, the energy consumption has outgrown availability, leading to unstable electricity that is inadequate for uninterrupted refrigeration operations **[3]**. It is indeed a severe difficulty that puts the continuation of the vaccine cold chain at risk of being compromised.

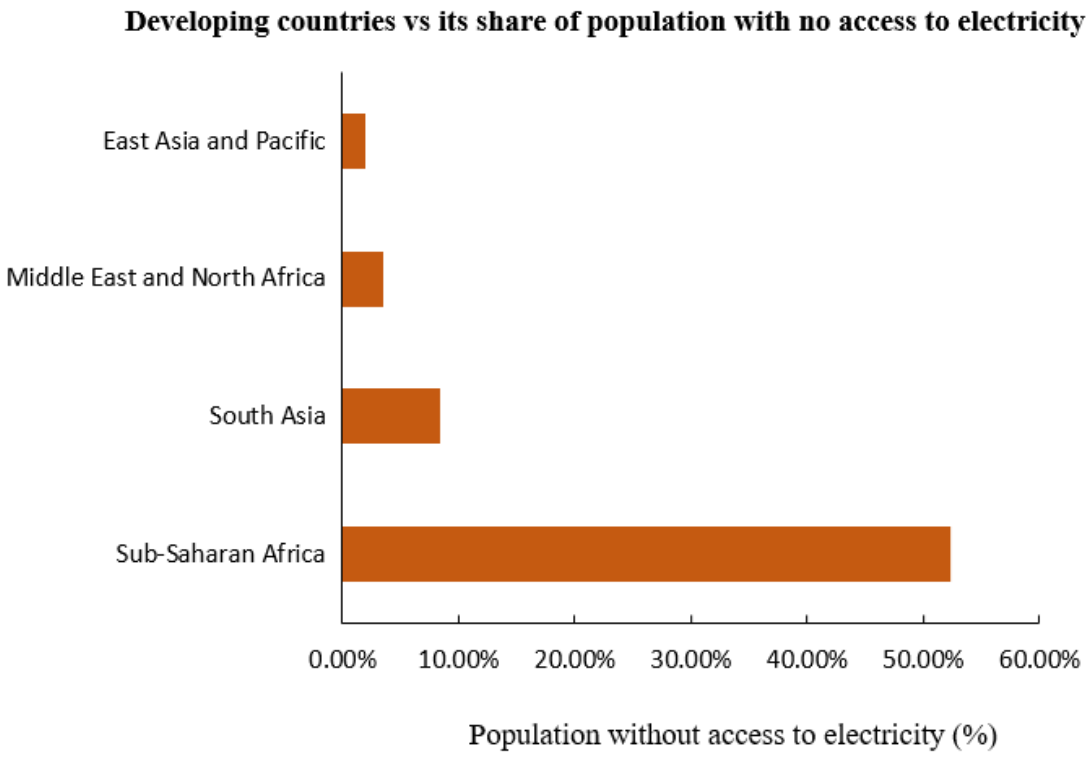

Figure 1: Percentage of population of developing countries without any access to electricity [11].

These two key concerns are substantial impediments to providing maximal immunization, particularly in developing countries with insufficient healthcare infrastructure. The issue regarding inaccessibility of electrical power in remote areas can be solved using solar power to a large extent. Solar energy paves the way towards further development especially in the applications of domestic cooling, heating, ventilation and in several other areas in the healthcare system. Solar driven medicine storage boxes have garnered significant attention and considerations from all around the globe as they are not only capable of producing effective cooling but also can be a great alternative to conventional refrigeration systems given the fact that, they do not emit any greenhouse gases or any other form of contaminants.

The relevant research was carried out with the goal of discovering answers to issues such as inaccessibility to excellent healthcare systems, lack of electricity in remote areas throughout the globe, and loss of potency owing to improper temperature regulation. Therefore, the current research comprises of a combination of tests that had been carried out under several operating conditions to establish a thermoelectric cooling system that will be sufficient for powering small-scale vaccine refrigerator using solar energy extracted from photovoltaic panels.

1.2 Research Problem Statement

A number of refrigeration systems have been developed for vaccine storage and maintenance purposes till today. With the help of advanced technology, several options have been developed over the years to sustain and ensure vaccine refrigeration [12]. The vapour compression refrigerator, absorption-type refrigerators and traditional cold boxes are the most often used cooling systems for vaccinations at health posts [13]. In the following figure no.2 the corresponding annualized costs of these refrigerators including both operations and capital have been represented with information acquired from WHO.

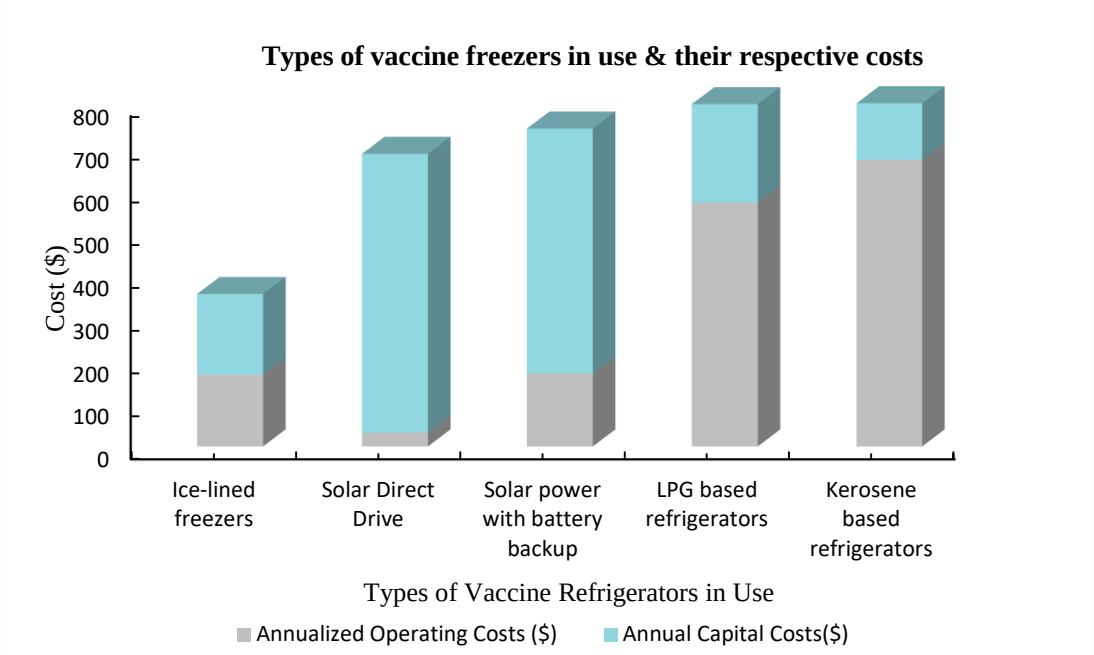

Figure 2: Types of vaccine refrigeration systems in use and their corresponding annual operating as well as capital costs [14].

From this figure, it is evident that, solar direct drive as well as solar power with battery backup refrigerator incur considerably low amount of annualized costs.

Mechanical pumps are used in the vapour compression system to activate the compression and subsequent expansion of certain working fluids [15]. This method has the benefit of being able to refrigerate huge loads efficiently. However, because of the compressor, the system is heavy, expensive, and loud during operations. As a result, the technology is not ideal for or easily transportable to isolated places [7]. Another typical way is to cool the designated chamber using re-freezable ice packs. The cooling lifespan of these systems is determined by how long the packs remain frozen and how effectively the chamber is insulated. While the cost is often modest, system resilience is a concern. Temperature control and regulation are not possible with this kind of cooler, which is why they are not recommended for long-term storage. The propensity of passive vaccine coolers to freeze vaccines when vaccine vials come into close contact to the ice packs is a frequently neglected issue. Freezing destroys the efficacy of vaccines and makes them ineffective [16]. The large percentage of absorption-type refrigerators use both kerosene and packaged LPG to power the corresponding refrigeration cycle. These kinds of fuels have a tendency to pollute the

environment. In addition, they are subjected to inconsistency and disruptions owing to a variety of factors such as inadequate scheduling, limitation in terms of fuel availability and diversion towards other purposes. These refrigerators are also inefficient, have poor temperature control, need periodic inspection, and have a constrained ice-making capacity. In addition to that, they have not been able to fulfill all the requirements regarding health care policies provided by WHO PQS [17].

Whereas, refrigerator powered on solar drive have consistently been improved leading to an increase in their use in assuring quality health care system in several countries around the world [17]**.** As, solar power is one of the fundamental renewable resources of energy, it plays a vital role in mitigating the current energy crisis that exists worldwide.

Although, solar power is not constant throughout its operational duration in different applications, it possesses the potential for developing a cooling system which can be sustained for considerable amount of time during the day. Moreover, solar energy driven refrigerators were initially designed based on the principle of thermoelectric effect to be utilized in the developing countries. The reason behind it was to establish a cooling system for prevention of deterioration of medicinal good that will be durable and will not require skilled personnel for operating. Another important aspect of using solar powered refrigeration system which makes it even more attractive is the fact that, these systems do not incorporate huge costs. They are economically viable to a great extent. As it is evident from figure no.02, both solar direct driven and solar drive with battery backup refrigeration systems incur considerably low capital as well as operational costs on annual basis.

In today's world, it is absolute necessary to explore and support such renewable resources as much as can be possible given the current energy crisis around the globe which cannot be left without attention.

Generally, solar driven vaccine refrigerators are used in two major ways. One is operated directly using solar power and the other uses solar power with an addition of a battery for additional assistance. Both have been demonstrated through schematic diagrams in the following.

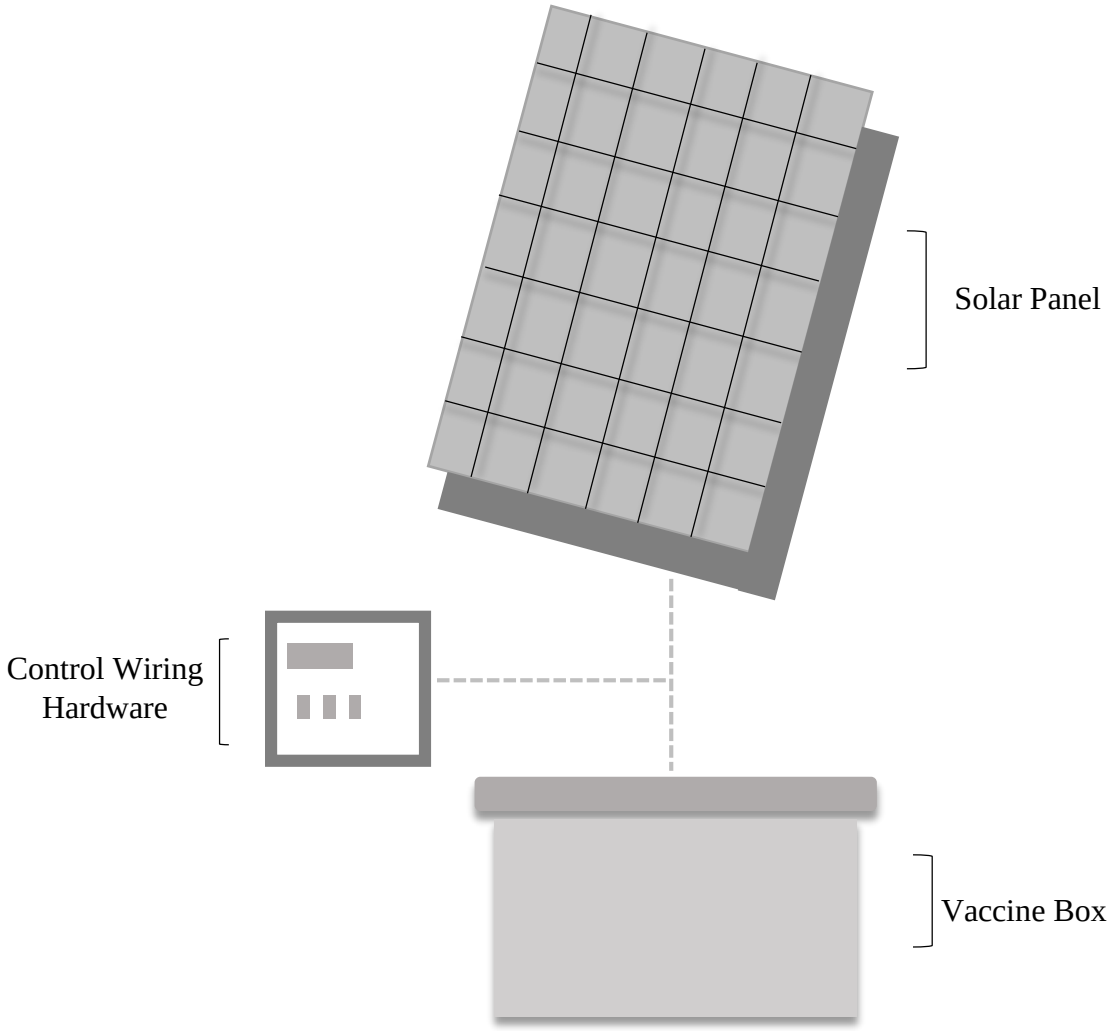

Figure 3: Schematic diagram of Solar Direct Drive Refrigerator.

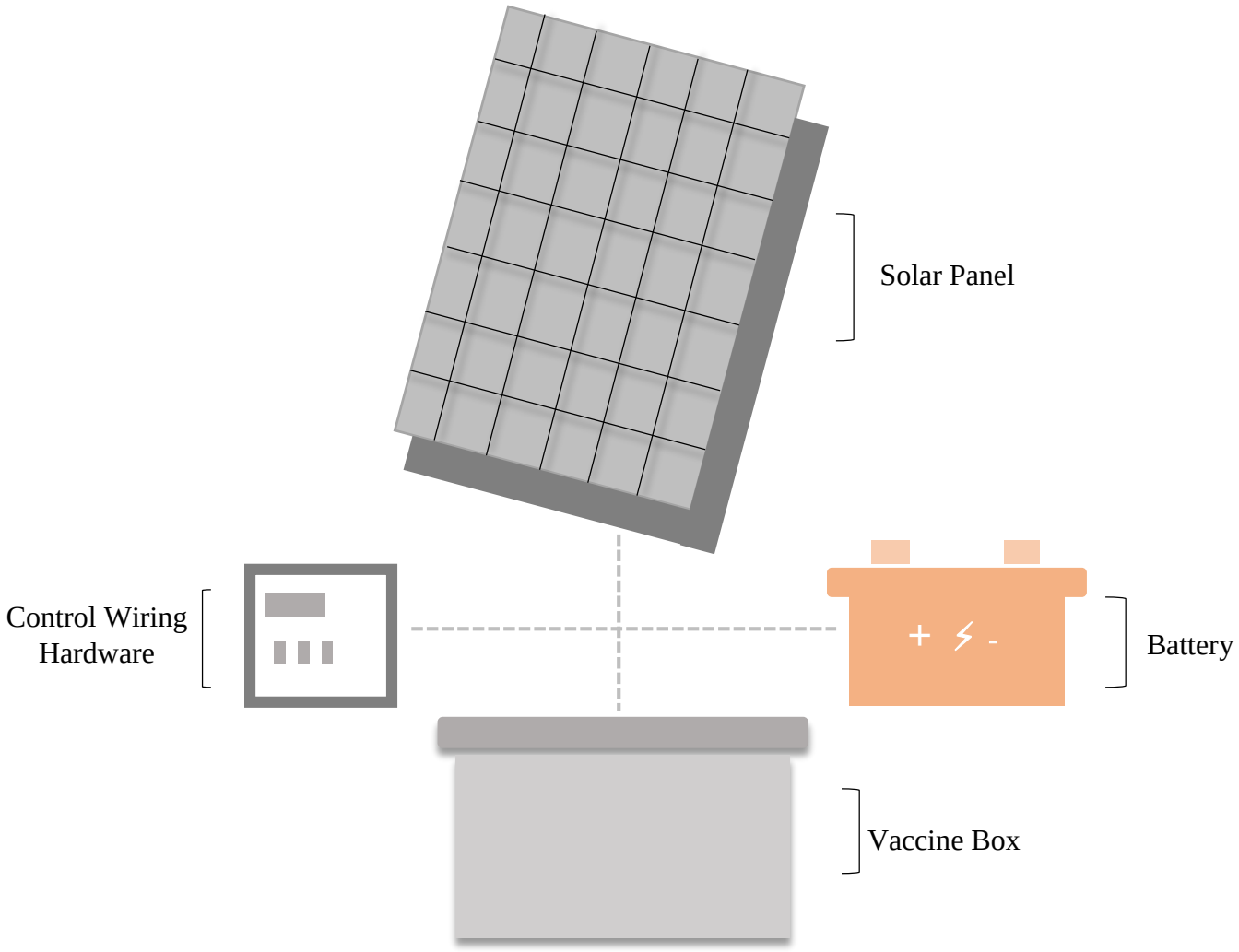

Figure 4: Schematic diagram of Solar Drive with Battery Backup Refrigerator.

One greatly effective and novel approach towards overcoming several issues mentioned is use of thermoelectric refrigerators [18]. The principle of thermoelectric modules can result in effective cooling which has garnered considerable attention [19]. Thermoelectric cooling devices, often introduced as thermoelectric coolers (TECs), provides the benefits of great stability incorporating no moving parts which ensures compactness of the system with an absence of working fluid leading to operation without any emission of any kind. It further possesses convenience regarding the source of energy to be supplied to the system. Both grid electricity as well as renewable resource can be incorporated. The primary drawbacks of such systems are that they have lower efficiency and often cannot be implemented in a cost effective manner. Although, they fulfill power demand and provide both system resilience and noiseless operation [20]. The actively cooled vaccine freezers based on the thermoelectric effect handle the temperature control problem by employing the thermoelectric module to manage the interior temperature, avoiding vaccine spoilage. Vaccines are important commodities, particularly in third-world nations, thus it is critical to minimize efficacy loss due to inadvertent freezing or heating [16]. Although, in our study, we mainly focused on designing and analyzing a system working on the principle of thermoelectric effect primarily for the purpose of storing vaccines, further improvisation in the design may facilitate utilization of the system for transporting the medicinal goods as well.

The "Seebeck effect" and the "Peltier effect" may be used to create cooling via TE techniques, which use the principles of creating electricity and the principles of producing cooling. DC voltage differential across TE module allows electric current to flow, which absorbs heat from one side and releases it from the other side, as seen below in the figure no.3. As a result, on one face of the module, cooling effect will be generated while on the other heating effect will be generated. While a temperature gradient exists between the module's two junctions, a voltage difference is formed across the module, resulting in the delivery of electrical power. A thermoelectric module is made up of a limited number of thermocouples composed of two semiconductor materials of dissimilar kind that generate a low thermoelectric power but a large electric current. It has the benefit of being able to work with a low range of energy source, making it useful for converting solar energy into electricity [21].

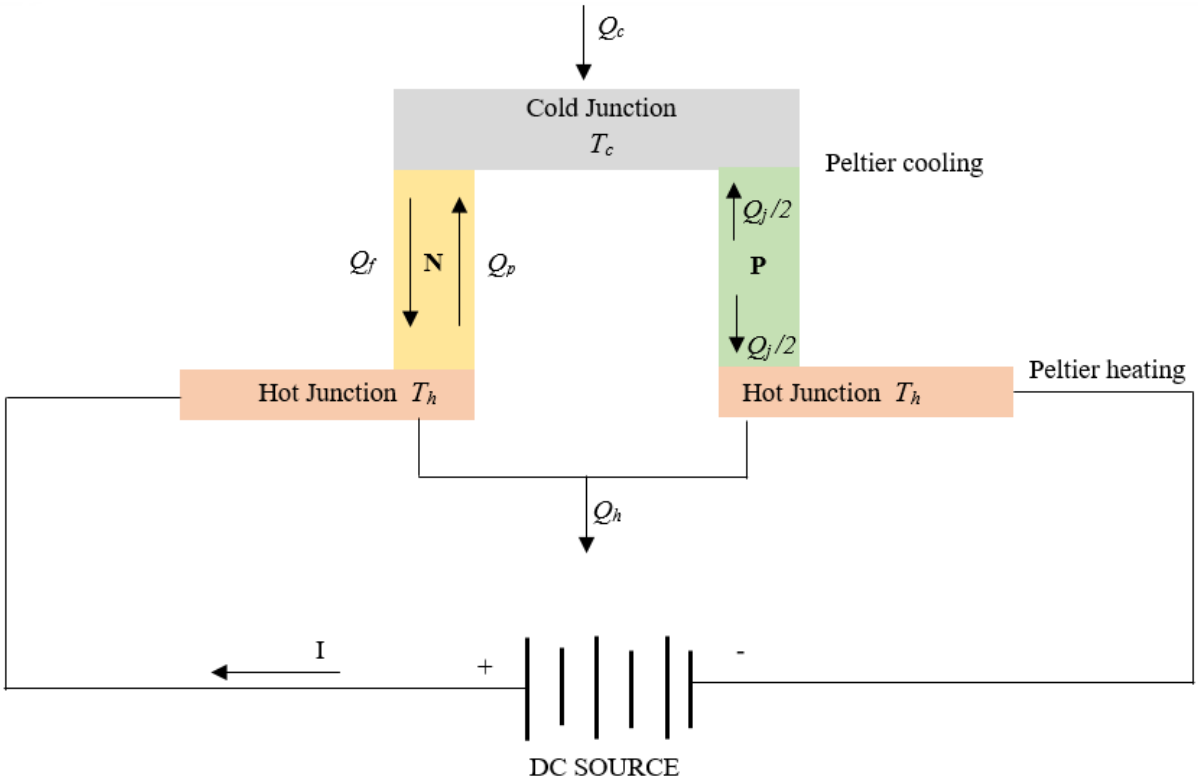

Figure 5: Schematic of working principle of Thermoelectric module.

A thermoelectric cooler basically incorporates several components and creates a temperature gradient based on the thermoelectric principle. When the operational temperature range of a thermoelectric device is exceeded, the equipment will no longer function properly. To disperse the heat created or absorbed at the two junctions, all thermoelectric modules need heat sinks. There are three fundamental components in a cooling/heating unit: the thermoelectric module, a number of fins for ensuring proper dissipation heat on the heated side of the module and the cooling component on the cold side [22].

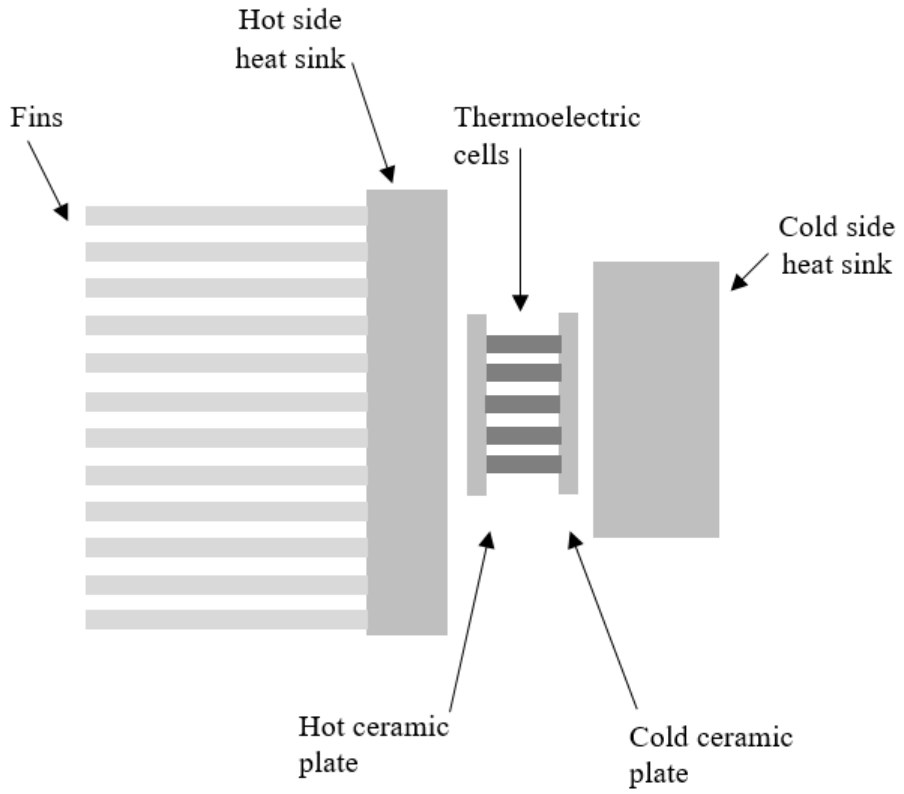

Figure 6: Components of a Thermoelectric Cooler.

The efficiency and performance rating of a thermoelectric cooler is determined by a number of parameters. These include – the current (I) applied at the semiconductor materials, the temperatures on both the hot and cold faces (T_h , T_c), thermal resistance (R) between the surface and the cold side of the module, thermal and electrical conductivities (ƛ, σ) and the thermal conductance (K). The figure of merit, cooling capacity, and COP are metrics that define the features and performance of a TE cooler [21].

1.3 Goals and Objectives of the study

Setting a few clear aims or objectives has a significant impact on the amount of value that may be added to any experimental investigation. Likewise, our approach to experimental analysis, followed by implementation, was heavily affected by some of the objectives that we had tried to accomplish throughout the research.

The objectives of the experimental analysis include-

- Determining the optimized geometry that will facilitate effective cooling as well as enhanced performance.
- Determining the relevant power requirements that is needed to be fulfilled in order to operate a small-scale refrigeration system based on thermoelectric principle.
- Constructing the experimental setup and analyzing its performance for a number of cases to understand the variation in outcome that eventually will lead towards obtaining the ultimate geometrical optimality.
- Finding out several design criteria as well as potential parameters to finally design the thermoelectric refrigeration system in accordance to the desired temperature range.
- Examining the performance of the thermoelectric refrigeration system for the case of photovoltaic integration and analyzing its performance.
- Examining the performance of the system in different testing criteria after photovoltaic integration to have a clear understanding on the outcomes of the distinct cases.
- Combining the experimental analyses for both cases of utilization of grid electricity and solar power as the main source of energy to the system.
- Finally, studying the outcome of all stages incorporating all the testing cases to determine whether or not the system gives effective cooling within adequate duration facilitating noiseless operation.

In this experimental study, our main focus was to design and analyze the performance of a small-scale photovoltaic integrated refrigeration system that will ensure the generation of effective cooling using renewable resource for using in medical applications. It is important to mention that, our aim was to incorporate the analyses of a small-scale thermoelectric refrigeration system for both the utilization of grid electricity and solar power separately which is the novelty of the experimentation.

1.4 Scope and limitation of the study

1.4.1: Scope:

Previous studies incorporated extensive analysis of thermoelectric cooling systems using either grid electricity or solar power. This study aims towards a novel approach where it analyzes a small-scale refrigeration system working on the principle of thermoelectric effect in two stages. The first stage utilizes grid power and optimizes the total geometry which further ensures proceeding towards the second stage which incorporates Photovoltaic integration on the optimized geometry and brief experimental analysis on it. Our study included experimenting on the setup in several design criteria and analyzing the performance based on a number of parameters. The parameters that were taken into consideration were - ambient average outside temperatures on all sides of the vaccine box, initial ambient conditions before initializing each testing procedure, voltage and current ratings on both load and battery sides, temperature and humidity readings inside the cooling chamber, temperature readings of the TEC module, irradiation readings throughout the testing duration, time required for the system to reach to the desired range of temperature as well as time required for it to hold the cooling within the chamber and difference between the initial ambient temperature inside the chamber and the lowest temperature achieved in there. As the study has been conducted in such a broad retrospect, it is noteworthy that it possesses the capability of being a brief and sophisticated study of its first kind. In addition to that, this study has the potential for further improvisations which will only add to its operational potential.

1.4.2: Limitations

As the study was solely based on experimentation, it naturally comprised of its own experimental constraints as well as several challenges. Some of the challenges include -

- **Lack of compactness of the experimental setup -** The electrical components reside outside of the box at the current state of experimentation. To make the setup more mobile and convenient to study upon, all the electrical wirings can further be organized.
- **Low efficiency of TEC -** Efficiency of thermoelectric cooler is not as high as vapour compression refrigerators. Further improvisation such as incorporating multiple TEC

modules can positively affect the outcome by increasing the lifespan of the cooler and sustaining its efficiency for prolonged period of usage.

- **Unreliable backup system -** The existing backup system is not quite stable to provide consistent power to the system. Further study of the backup system especially during the night can give clearer understanding regarding the requirement of a stable backup system.
- **Effect of shading -** The current location of the solar panels affected the performance of the system due to effect of shading resulting from surrounding building structures as well as trees.
- **Lack of performance testing in varying weather conditions -** As the time when the experimental study had been conducted was during summer, testing the setup on varying weather conditions was not possible. Further experimentation during all possible weather variation will definitely incorporate greater understanding about the potential of the current experimental setup.

1.4 Methodology of the study

The experimental study aimed to achieve geometrical and performance optimization. Therefore, to obtain that, it incorporated two different stages which were- **i)** Volume Optimization and **ii)** Photovoltaic Integration.

- **Volume optimization –** This was the first stage of experimentation. Several test cases were taken into consideration and extended experimentation for each of the cases were conducted. All the test runs have been conducted using grid electricity as the main power supply. A total of 5 test cases were involved in this stage which based on both the inclusion and exclusion of insulation on full and half volume of the dedicated cooling chamber.
- **Photovoltaic Integration-** This stage had been approached only after an optimized condition was achieved from the perspective of geometrical optimality. Both the cases of solar direct drive and solar power with inclusion of a backup system were investigated. These two conditions utilized solar panel with automatic tracking mechanism as well as solar panels without a tracking mechanism.

1.6 Contribution of the study

The relevant experimental study has combined the analyses of both on grid and off grid power resource for studying the experimental setup. Therefore, it can be said that, this particular concept of thermoelectric cooling has been analyzed taking two vast methodologies into consideration and respectively combined the outcome of those to determine the condition of best possible utilization of the concept of thermoelectric cooling. This is the novel approach of the study which brought about an extensive experimental background that has the potential of paving the way for further investigation as well as analysis on this particular reference. In other words, it can be said that, this particular study has become quite a sophisticated and novel reference for implementing further extension of similar work.

1.7 Organization of the thesis

The thesis work has been organized in a consecutive manner where it has been first introduced and then the inspiration of conducting the experimental study has been discussed. Further, methodological framework has been included and very descriptively discussed followed by an elaborated literature review regarding the concept of thermoelectric cooling and several parameters that affect its concept. Next, the outcome from all the test cases in both the stages has been presented in a sequential manner and analyzed based on the parameters taken into consideration. Moreover, the result section discusses about some of the constructive improvisations which can enhance the overall performance of the setup considerably. Finally, the study is concluded reflecting on the current progress of the developed system as well as the further future extension associated to the study.

Chapter 2

Literature Review

In the following section, a brief discussion on thermoelectric refrigeration system as well as several parameters critical to the selection of thermoelectric materials will be provided. Additionally, a number of other selection criteria and parametric review will be discussed.

2.1 Thermoelectric Materials

It is crucial to select thermoelectric materials in a way that it can facilitate the production of thermoelectricity which eventually will ensure that adequate cooling effect is being produced in response to the thermoelectric effect. A good thermoelectric material should possess several specific qualities according to the Wiedemanne-Franz law [23]**.** After doing a brief review on a number of research studies based on this specific criteria, it has been noted that, there are about three major qualities that a good thermoelectric material is supposed to inherit as discussed by Sarbu et al. [21] . The first one being a high seebeck coefficient basically implies that the amount of thermoelectric voltage being generated in a material as a response to the application of a temperature gradient across it should be high in order to provide greater efficiency in thermoelectric coolers. The second one being a high electrical conductivity which basically implies that, the material should have the capability to carry larger amount of current which again is required to ensure greater performance rating is being achieved from a particular thermoelectric cooler. And the third one being low thermal conductivity which implies that, the selected element must have lower capacity of transmitting heat so that, it can be ensured that both sides of the thermoelectric element will have a potential difference in temperature that in other words is an indication of generation of greater voltage difference resulting in achieving higher energy efficiency in the thermoelectric material. Thus, based on all three parameters, a measure established for selecting the best suitable material for generating thermoelectric effect is known as Figure of merit, Z. Another general form of this quantity is the product of figure of merit of a material and the absolute temperature between the hot and cold sides of the module; described as a dimensionless quantity and represented by ZT. Therefore, it is evident that, the higher the value

of figure of merit is, the higher the efficiency will be. As mentioned by Zhao et al. [20] the best possible figure of merit achieved for commercial thermoelectric applications is 1.

A few example of such thermoelectric materials are semiconductors. Bi_2Te_3, $Si_{80}Ge_{20}$ and PbTe possess decent thermoelectric characteristic as mentioned by Hogan et al.[24] Other best possible values of ZT obtained remain within the range of 1-2. Zhao et al. [20] also mentioned that, a system incorporating thermoelectric element having the value of ZT to be 1, operates on a 10% carnot cycle efficiency whereas, a system incorporating another element of ZT value of 4 can operate on 30% carnot cycle efficiency. According to Hogan et al. [24], the best possible value of ZT is 3. Bell et al. [25] mentioned that when the value of ZT reaches 2, the system becomes attractive in terms of providing adequate cooling as well as enhanced temperature control. But it is not recommended to use materials with really high values of ZT such as 4 because that will incorporate a set of complexities into the system as discussed by Francis et al.[26]

Among several other types of thermoelectric materials, ceramics have proven to be highly functional. Elghool et al. [27] conducted a study on a number of n-type and p-type materials. The n-type materials were $SrTiO_3$, ZnO and $CaMnO_2$. Likewise, the studied p-type materials were $Ca_3CO_4O_9$ and $NaCO_2O_4$. Among these, $CaMnO_2$ showed best results. Zhu et al. [28] mentioned in their analysis that oxides show great thermoelectric properties as they incorporate low cost and provide greater chemical stability.

Another type of thermoelectric material is polymers. They inherit good thermoelectric characteristics because of low thermal conductivity. But their performance as a suitable thermoelectric material is generally hampered as they possess low electrical conductivity and seebeck coefficient as described by Choi et al. [29]

2.2 Coefficient of Performance

The COP of a thermoelectric cooler can be enhanced through a number of ways. According to Sabah et al. [30], it can be enhanced significantly by reducing thermal contact as well as electrical resistances. Chen et al. [31] mention, COP can be increased by using materials that have negative Thompson effect. The COP can also be enhanced by utilizing multistage thermoelectric modules as mentioned by Enescu et al. [32]

2.3 Performance enhancement

According to an experimental analysis conducted by Astrain et al. [33], testing on a prototype based on thermoelectric refrigeration gave COP values with the range of 0.3-0.5 which was possible after making necessary modifications in contact resistances of the module as well as the thermal interfaces. Astrain [34] conducted an experimental study to understand how the temperature control systems were affecting overall energy consumption by the system and its COP rating. It was found that only by controlling the voltage, total energy consumed by the system could be reduced by 32% and COP of the system could be increased by 64%. According to a study conducted by Liu et al. [35], they found that if heat sinks with greater efficiency can be incorporated to the thermoelectric module, it can act as an alternative for enhancing the overall performance of the cooling system.

2.4 Photovoltaic Integration

The Photovoltaic integration stage of this study was conducted by considering some parameters that effect the solar panel performance and efficiency. Some other crucial factors under consideration were the effect of the structure of Monocrystalline and Polycrystalline materials on solar cell performance, effect of shading losses on solar module performance and performance of solar panels applying Solar Tracking Device. In the study of Jumrusprasert et al. [39], it is claimed that monocrystalline and polycrystalline solar cells installed on fixed-panel rigs with a 30 degree south-facing tilt angle give 6.8% and 5.7% efficiency for monocrystalline and polycrystalline, respectively. Anand et al. [40] has stated that because of the fluctuation of solar energy induced by shade, integrating large-scale PV into the power grid poses significant complications. The real power generated by a solar PV array may fall substantially below the designed level due to shading, resulting in a full "loss of load" at times. Dust settlement in panels, passing clouds, and shadows of neighboring mounting structures are the main causes of shading. It can also cause charge controllers and Maximum Power Point Tracking (MPPT) systems to malfunction. According to a study of Azhar et al. [41] the implementation of tracking technologies when compared to modules at a fixed angle, letting solar modules to follow the path of the sun (and maximize the incident

angle of sunlight on their surface) can improve power generation by roughly a third, and some claim by as much as 40% in some regions.

Dai et al. [36] conducted an experimental study based on the principle of thermoelectric refrigeration using solar power as the power supply with a battery backup. The results obtained were that, the lowest temperature reached was 5-10℃ and the COP was about 0.3. Abdul et al. [30] conducted an experimental study on a portable solar thermoelectric refrigerator and found that the cooling chamber was capable of lowering the temperature from 27 to 5℃ within 44 minutes.

Chapter 3

3. Methodology

This section contains a detail brief on the experimental study. It incorporates all the details regarding the methodological framework, experimental sequence and the parameters that have been studied. Additionally, it also contains the details regarding every test cases that have been performed. The details include a brief about the experimental procedure, the readings that were taken during the testing and the parameters that were selected to study for grasping better understanding of the experimentation.

3.1 Methodological Framework

The methodological framework of the experimental study comprises of four separate sections. These include- Process specifications, Electrical design, Thermal design and Mechanical assembly.

- **Process Specifications -** Mainly focuses on specifying the problem statement which incorporates information such as; the operating conditions of the testing processes as well as some selection criteria in order to select the cold box, TEC, insulation materials and PV panels.
- **Electrical Design -** Majorly focuses on designing and establishing the electrical circuit using main source of power and other accessories such as AC/DC converter, battery, charge controller, necessary wirings etc.
- **Thermal Design -** Briefly focuses on analyzing the transfer of heat in the system involving all electrical and mechanical equipment.
- **Mechanical Assembly -** Finally, ensuring that all the corresponding components within the experimental setup have been assembled in a manner that facilitates extracting the best possible performance of the system.

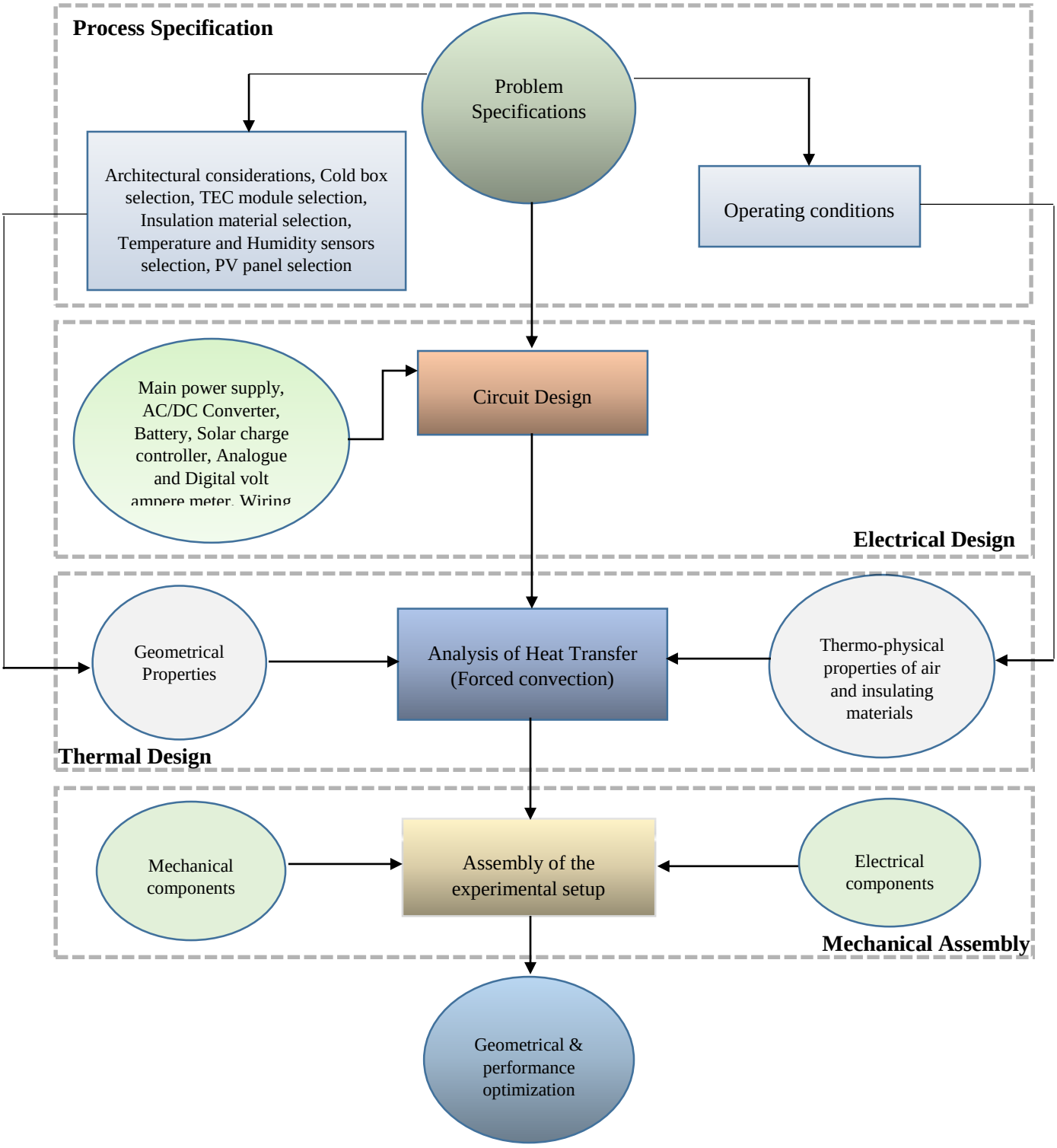

Figure 7: Methodological framework of the experimental study.

3.2 Experimentation Sequence

The total experimentation have been conducted into two separate stages- Volume optimization and PV integration. The main purpose for conducting this experimental analysis is to achieve geometrical and performance optimization.

- **Stage 1- Volume Optimization:** This particular stage mainly involves testing the experimental setup under varying conditions. This stage of experimentation was implemented using grid electricity as the main power supply. It consists of five test cases on total based on two separate segments – full volume and half volume study. After analyzing the outcome from all these cases, the optimal geometrical conditions were determined. The five test cases include-
  - Full volume without insulation;
  - Full volume with insulation on four sides;
  - Full volume with insulation on five sides;
  - Half volume without insulation &
  - Half volume with insulation.

- **Stage 2- Photovoltaic Integration:** This stage was approached using the optimality found in stage 1. The experimentation in this particular section was based on two types of solar systems- Solar panels without any tracking system and solar panel with automatic tracking system. In this stage, two separate test cases have been conducted, which include-
  - Solar direct drive with no backup system &
  - Solar power with battery backup system.

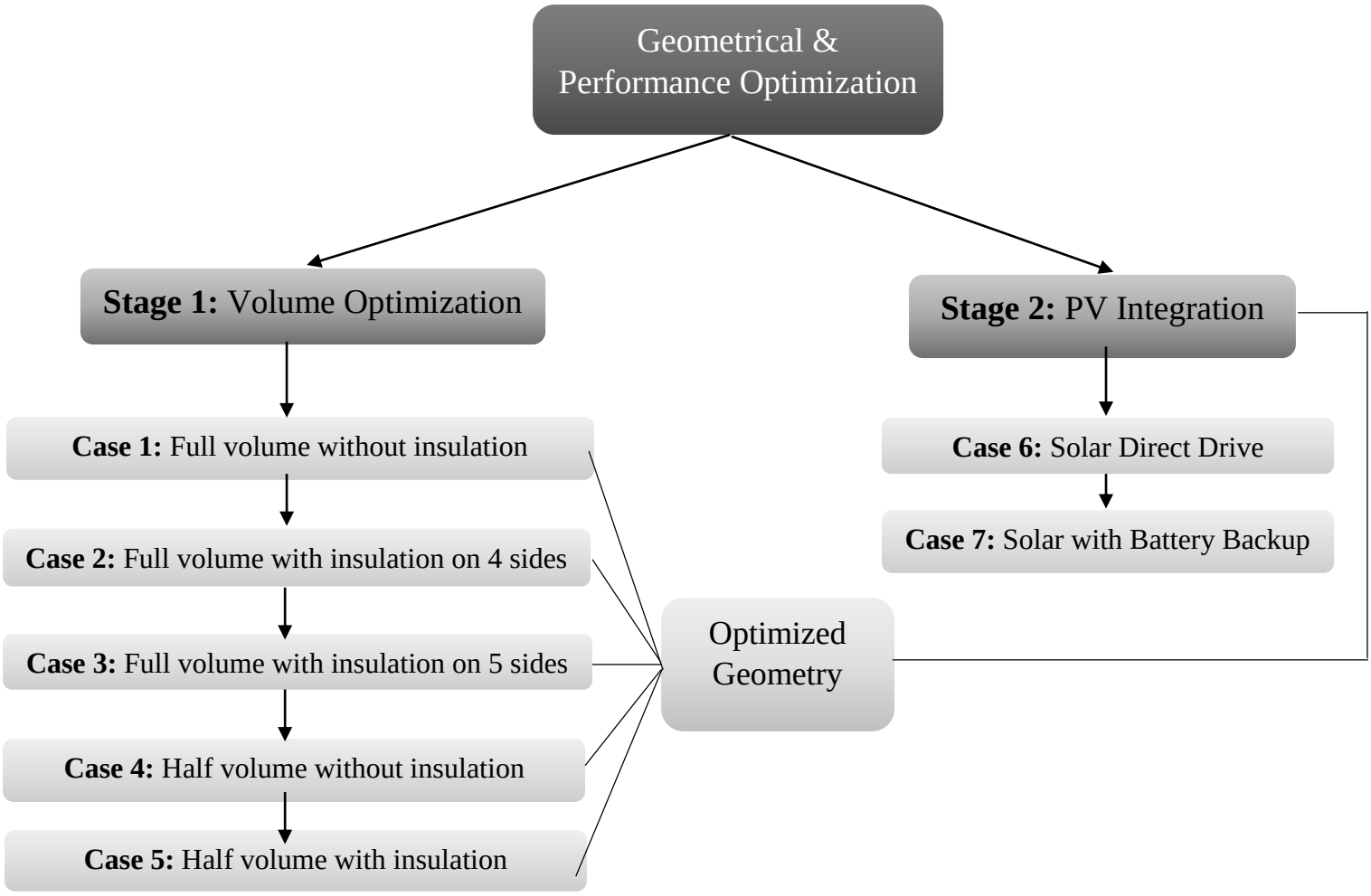

Figure 8: Experimentation sequence.

3.3 Studied Parameters

As mentioned previously, while conducting the second stage which was PV integration, several parameters have been taken into consideration. Evidently, these parameters had significant effect on the performance of the thermoelectric cooling system after incorporating photovoltaic system in it. The major factors that determine the performance of the system include -

- **Solar radiation -** It depends on both the ambient temperature and solar irradiation. These two factors change on a daily basis. The magnitude of solar radiation therefore varies from day to day.
- **Photovoltaic panel -** Photovoltaic panels are generally used for producing power from solar energy. Electricity generated from the PV panels depend on a number of input parameters. These parameters are-
  - **Efficiency:** The generation of electricity depends upon the efficiency of the panel. The more efficient a panel is, the more power can be extracted utilizing it.
  - **Surface area:** The greater the surface area, the greater will be the magnitude of exposure to sunlight.
  - **Number of Cells:** The amount of power produced by the panel will highly depend on the number of cells present in the solar panel.
- **Thermoelectric cooler -** The temperature gradient across the thermoelectric module depends on a set of input parameters such as;
  - **Thermal conversion rate of the TEC**: A TEC with higher conversion rate will be able to provide greater cooling within shorter duration of time.
  - **Surface area of both the heat sink and the cooler:** Greater surface area of the heat sink as well as TEC will ensure effective and higher rate of heat transfer for establishing effective cooling.
- **Cooling effect -** The outside temperature due to the generated cooling effect depends upon volume of the cooling chamber as well as the initial ambient temperature inside it.

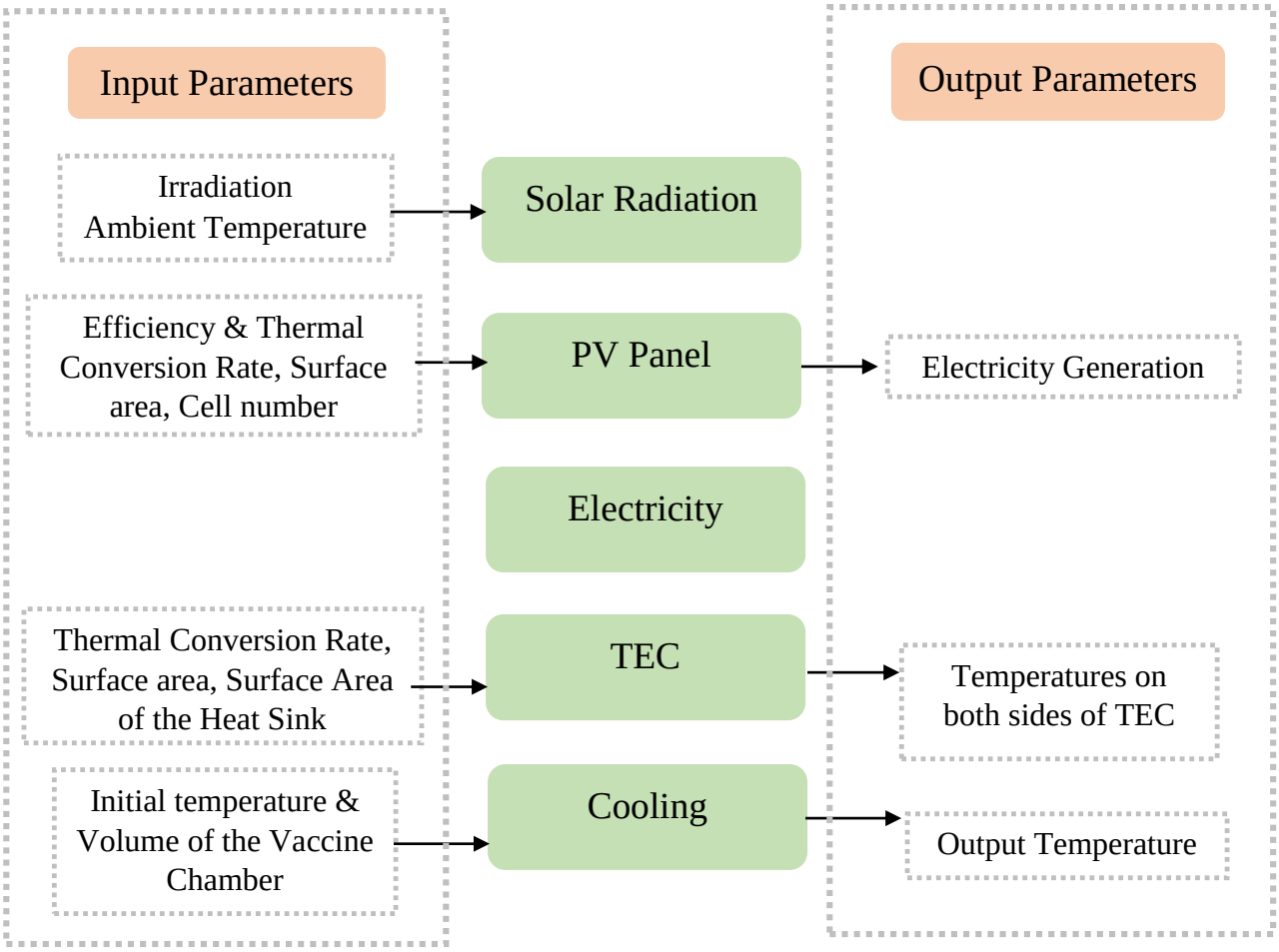

Figure 9: Parameters that have been studied.

3.4 Experimentation Procedure in Detail

This section provides sequential details regarding the implementation of the experimentation. It gives an insight on the gradual designing and development of the experimental study in terms of the procedures that have been followed.

3.4.1 Initialization

Before proceeding towards the experiment, a number of steps had been followed to implement a strategic flow of work. The first step taken was the selection of a cold box with specified storage capacity. The cold box selected was of a capacity of 25L. A theoretical calculation had been done in order to determine the cooling load requirement of the system. The calculation was done extensively in determining the total amount of heat transfer as it took all three modes of heat transfer (conduction, convection and radiation) into consideration. The load calculation provided with a general idea about the power requirement of a small-scale thermoelectric cooling system.

3.4.1.1 Mathematical Formulation

- The resistance due to conduction is given by the equation -

$$\mathbf{R_{cond}} = \frac{\mathbf{L}}{\mathbf{kA}} \qquad [1]$$

  Here, k is the thermal conductivity of material, A is the area exposed to heat transfer and L is the thickness of body in the direction of flow.

- The resistance due to convection is given by the equation -

$$\mathbf{R_{conv}} = \frac{\mathbf{1}}{\mathbf{h_o A}} \qquad [2]$$

  Here, h_o is the convective heat transfer coefficient and A is the area exposed to heat transfer.

- Conductive heat can be determined by the equation-

$$\mathbf{Q_{cond}} = \mathbf{-kA}\frac{\mathbf{dT}}{\mathbf{dx}} \qquad [3]$$

- Convective heat can be determined by the equation -

$$\mathbf{Q_{conv} = hA\ (T_S - T_f)} \quad [4]$$

- Heat transfer by radiation is determined by -

$$\mathbf{Q_{rad} = \varepsilon\sigma A[(Tsurr)^4 - (Tsurf)^4]} \quad [5]$$

- Transmission load determined using the equation –

$$\mathbf{Q_T = Q_{cond} + Q_{conv} + Q_{rad}} \quad [6]$$

- Q_T (the refrigeration load) is the total rate of heat gain of a refrigerated space and in this study, it was based on the following expression -

$$\mathbf{Q_T = Q_c + Q_{Pl} + W_{fan}} \quad [7]$$

Here, Q_c is transfer of heat through the entrance of the vaccine chamber, Q_{Pl} is product load which basically implies the amount of heat that has been evacuated out of the products in the refrigerated chamber and W_{fan} is the heat generated by the fan placed right below the cold side of the thermoelectric module.

- The power consumed by the thermoelectric cooler is determined by -

$$\mathbf{P_e = I_e \times V_e} \quad [8]$$

Here, I_e and V_e are the current and voltage ratings of the thermoelectric module.

- To calculate the heat transfer coefficient the following correlations have been utilized [13].

$$\mathbf{Nu = 0.664 Pr^{1/3} Re_L^{1/2}} \quad [9]$$

$$\mathbf{[0.6 \leq Pr \leq 50]}$$

$$\mathbf{[Re < Re_{x,c} \approx 5 \times 10^5]}$$

3.4.1.2 Calculation, Instrumentation and Measurement

Prior to the initiation of experimentation some theoretical calculations were conducted in order to evaluate the system components quantitatively. Accordingly a cooling load calculation was done for accurate determination of the quantity of mechanical and electrical components required for the experimentation. After the components were finalized, the dimensions and measurements were taken carefully for further accurate calculation. Finally, a CAD model was also designed for proper visualization of the system.

Components	Quantity	Dimensions
25 liter Cold Box	1	**Outer Measurement-** Length: 505 cm Breadth: 335 cm Height: 315 cm **Inner Measurement-** Length: 393 cm Breadth: 273 cm Height: 247 cm
12V-10A TEC module	1	**Dimensions of the Bottom Circulating Fan adjacent to the Bottom Heat Sink:** Opening Diameter of the fan: 3.8 cm Length of the casing: 3.8 cm Breadth of the casing: 3.8 cm Height of the Casing: 1.1 cm Diagonal Distance of the Casing: 5.4 cm No. of Blades of the Fan: 9 **Details on Bottom Heat Sink:** Length: 6.1 cm Breadth: 4.6 cm Total Height with Fins: 3.1 cm Base Thickness/Height without Fins: 0.8 cm **Details on Fins of Bottom Heat Sink:** Height of each fin: 2.3 cm Distance between two adjacent Fins: 0.6 cm Thickness/Breadth of each Fin: 0.1 cm Number of Fins: 9 **TEC/ Peltier Chip:** Length: 4 cm Breadth: 4 cm Height: 0.38 cm
120W monocrystalline solar panel	3	Length: 58 cm Breadth: 26 cm
375W monocrystalline auto-tracking solar panel	1	Panel Area: 1.736 m^2
12V DC Lead Acid Battery	1	-
Solar Charge Controller	1	-
Analog Volt-Ampere Meter	1	-
Digital Volt-Ampere Meter	1	-
Polystyrene Sheets (Insulation)	10-15	Thickness: 1 inch
Fluke Temperature Sensor	1	-
Digital Data Logger	2	-
Inverter	1	-
Wiring	10-30	-

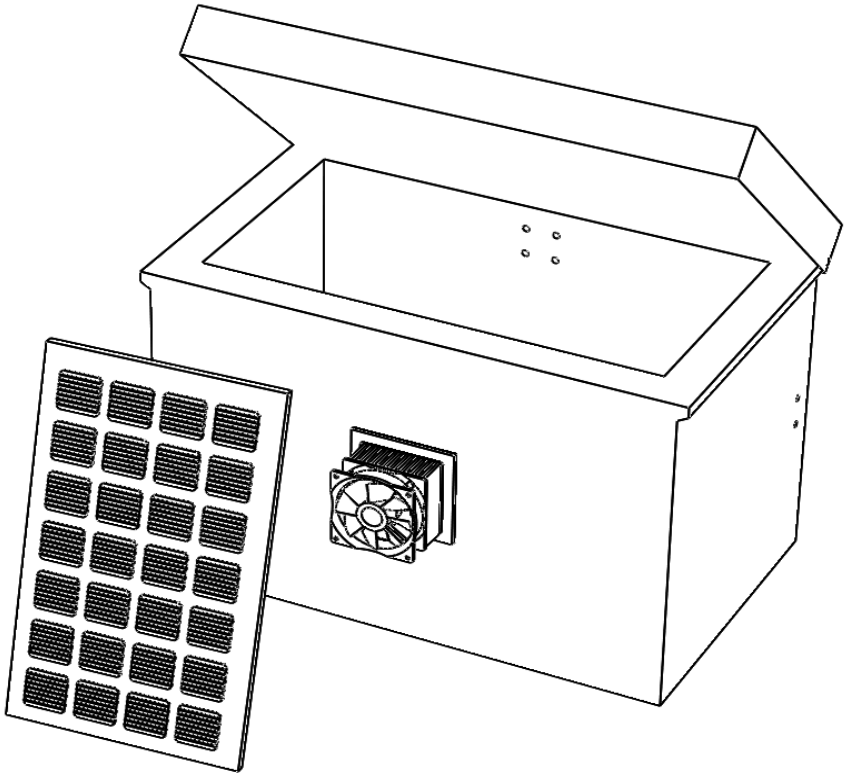

Figure 10: A Simple CAD Model of the System.

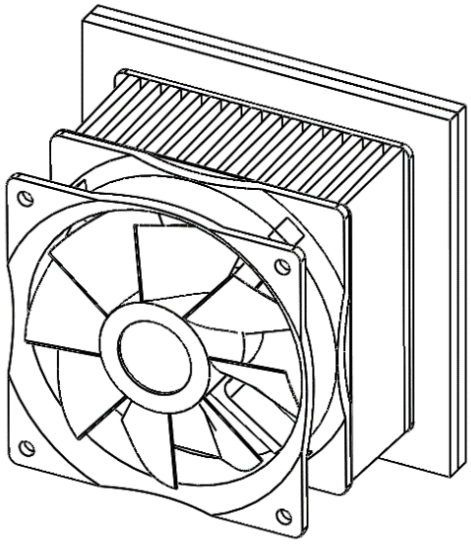

Figure 11: Isometric View of the TEC Module

3.4.2 Implementation

3.4.2.1 Detailed description on Experimentation

Initially, an overall volume of 25L had been chosen as the vaccine storage. This storage was finalized based upon the theoretical cooling load calculations. A series of sequential tests were performed for volume optimization. From test run 1 to test run 5, a series of tests had been conducted with and without the presence of insulation for both the cases: i) Full volume and ii) Half volume. These tests also signify an overall analysis on the performance of the vaccine cooler on given variations of the thickness of insulation. Test run 6 and 7 signifies an overall analysis of performance of the vaccine cooler after Photovoltaic panels had been integrated. The solar integration had been established in two kind of panels: i) Monocrystalline panels ii) Monocrystalline panel with auto tracking system.

3.4.2.1.1 Test Run 1: Full volume without insulation

This test involved testing on the full volume vaccine storage without using any insulation. The cold storage was required to be kept at the optimum range of temperature; 2-8℃. It had been ensured by exposing the storage to the cold side of the Thermoelectric cooler. The hot air from within the storage was then extracted via the fans attached to the cooler and released to the atmosphere. To ensure greater rate of transfer of heat and uniform circulation of air inside the control volume of the chamber, forced convection was utilized through a miniature fan that resides right below the TEC module. For an understanding of how temperature and humidity was changing as the test proceeded further, a set of data at a specified interval had been recorded using two sets of Data loggers. These loggers recorded both the Temperature and the Humidity of the system. One logger recorded the data for both temperature and humidity through temperature and humidity sensors placed inside the chamber while another one recorded temperature of the TEC through the temperature sensor placed around the heat sink in the TEC. The height of both the probes inside the chamber were exactly 3.9 cm from the bottom of the cold box. The main source of power for this case was grid electricity that basically drove the system through an inverter. A 12V lead acid battery had been used as a backup for the system. Additionally, one analogue voltmeter and one ammeter were included in the main circuit to record the current and voltage ratings of the battery.

Similarly, one digital volt- ampere meter had been used to check the current and voltage ratings on the load side. The time taken to reach the desired temperature as well as the time taken for the heat retention process were also recorded simultaneously. Moreover, the average ambient temperature had been recorded on the outside of all four sides of the vaccine box through a Fluke sensor thermometer.

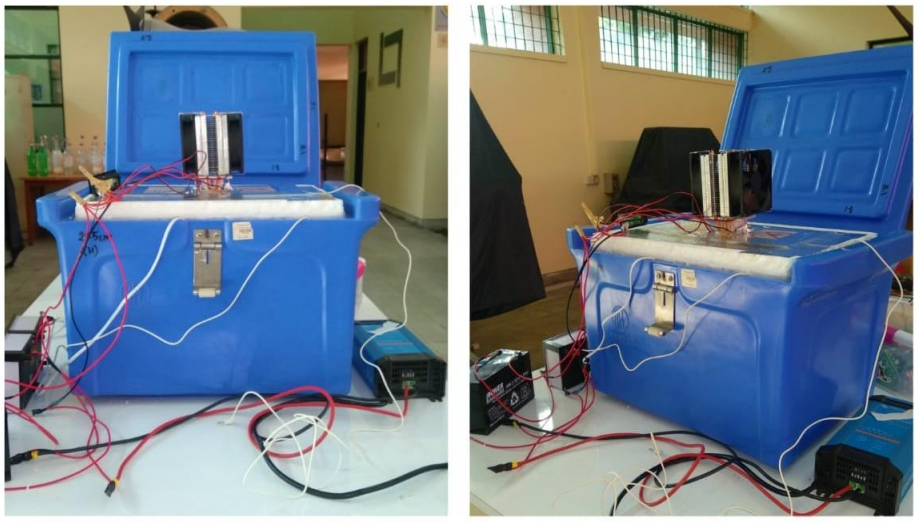

Figure 12: Testing on full volume without insulation.

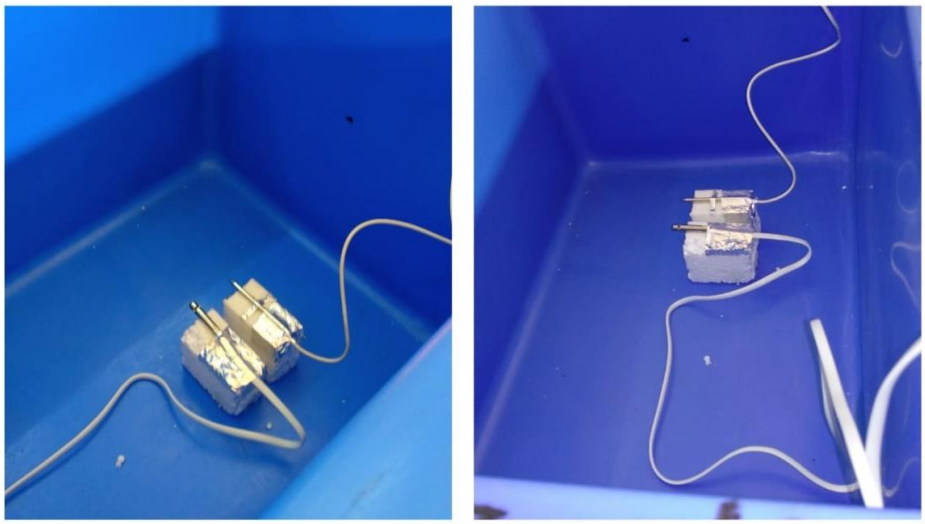

Figure 13: Temperature and humidity sensors placed within the chamber at a height above the base.

3.4.2.2 Test Run 2: Full volume with insulation on four sides

After conducting the first test run it was observed that the insulation material of the cold box was not efficient enough for retaining the desired temperature in the system. Based on this observation, a layer of Polystyrene Sheet (insulation material) was integrated in the box for providing sufficient insulation. Initially, the Polystyrene layer was installed inside the cold box on its four sides (front, back, left and right). The thickness of this insulation layer was 1 inch on each side. Similar to the previous test run the Temperature and Humidity sensors were placed on the bottom side of the box. The tip of the Temperature Sensor Probe was carefully placed at the center coordinate of the half-volume of the box. The height of both the probes were exactly 3.9 cm from the bottom of the cold box. It was measured that the existing volume of the system during this test run was 18 liter. After the completion of the fabrication and assembly, the rest of the test run was conducted following the steps of the previous test run. Accordingly the necessary parameters were recorded precisely and strategically. The design parameters included the temperature and humidity reading of the cold chamber, the temperature reading of the cold side of TEC, the voltage and current ratings of both the source and load side, the average ambient temperature reading of all the four sides of the cold box. The result of the data set from this test run significantly impacted to the subsequent improvement of the design process of the system for further research and development.

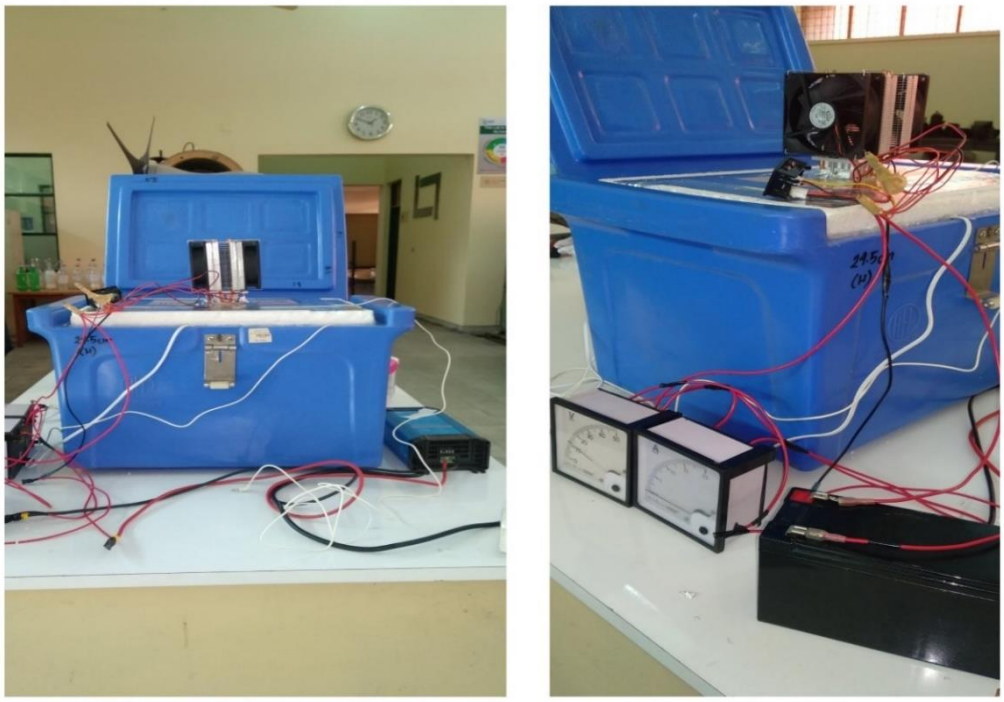

Figure 14: Testing on full volume with insulation (on four sides).

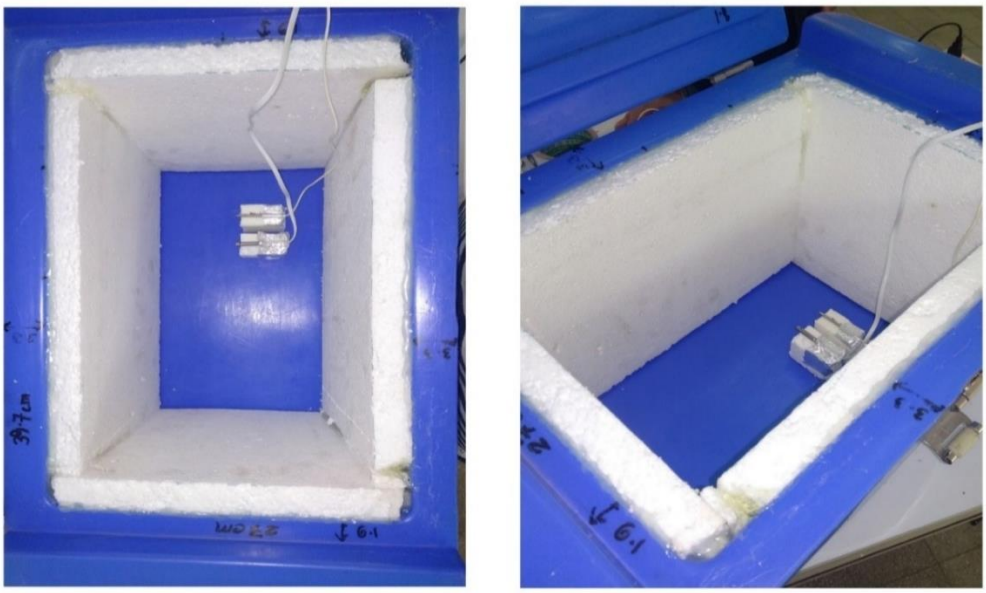

Figure 15: Temperature and humidity sensors placed within the chamber at a height above the base.

3.4.2.3 Test Run 3: Full volume with insulation on five sides

This test run involves the installment of insulation of Polystyrene Sheet on five inner sides of the cold box (front side, back side, left side, right side and bottom side). This additional insulation layer on one more side was introduced to the system for attaining better performance than the previous run. The thickness of the insulation layer was 1 inch on each side. Similar to the previous test run the Temperature and Humidity sensors were placed on the bottom side of the box. The tip of the Temperature Sensor Probe was carefully placed at the center coordinate of the half-volume of the box. The height of both the probes were exactly 6.44 cm from the bottom of the cold box. It was measured that the existing volume of the system during this test run was 15 liter. After the completion of the fabrication and assembly, the rest of the test run was conducted following the steps of the previous test run. Accordingly the necessary parameters were recorded precisely and strategically. The result of the data set from this test run significantly impacted to the subsequent improvement of the design process of the system for further research and development.

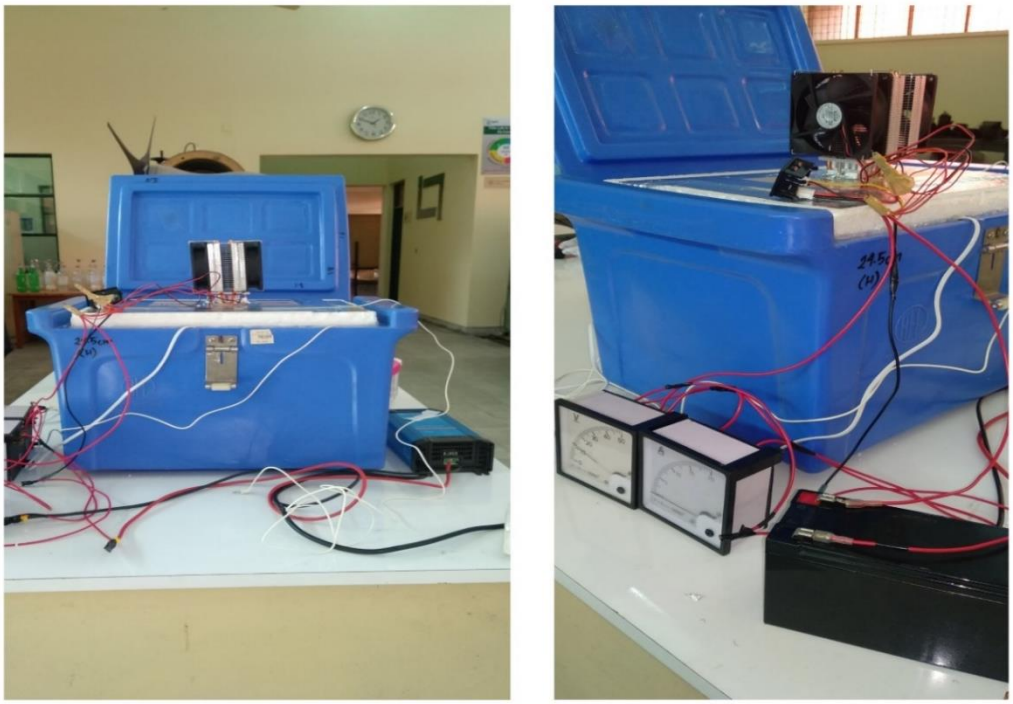

Figure 16: Testing on full volume with insulation (on five sides).

Figure 17: Temperature and humidity sensors placed within the chamber at a height above the base.

3.4.2.4 Test Run4: Half volume without insulation

This experiment involved testing on the half volume vaccine storage without using any insulation. The storage volume for this case was 13.7L. For minimizing the total volume space of the cold box a number of layers of polystyrene sheet had been attached to the bottom face. Between these layers, a single layer of air gap had been introduced as well as part of the enclosure. This layer of air gap had been utilized for its dual functionalities. It was utilized as part of the enclosure as well as provided adequate thermal resistance since it is a poor thermal conductor. This was established with the hope of achieving the best possible cooling performance. The polystyrene enclosure had been carefully attached to the insides of the PVC box so that air leakage of any kind could be prevented. Two sets of Data loggers recorded the temperature and humidity of the system at a specified interval throughout the testing duration similar to the previous test runs. This was done to keep track of the change in temperature and humidity of the system. One logger recorded the

data for both temperature and humidity through temperature and humidity sensors placed inside the chamber while another one recorded temperature of the TEC through the temperature sensor placed around the heat sink in the TEC. The temperature and humidity sensors had been placed at the center of half of the total storage towards right when seen from the top. The temperature sensor was placed at a distance of 15.4cm from the bottom face. Both the temperature and humidity sensors were kept at a distance of 4.5cm apart from each other. Grid electricity was the primary source of power in this situation, which was used to power the system via an inverter. As a backup, the system was powered by a 12V lead acid battery. In addition, the main circuit contained one analogue voltmeter and one analogue ammeter for recording the battery's current and voltage ratings. On the load side, a single digital volt-ampere meter was utilized to assess the current and voltage ratings. A Fluke sensor thermometer was also used to record the average ambient temperature on the outside of all four sides of the vaccine box.

Figure 18: Testing on half volume without insulation.

3.4.2.5 Test Run5: Half volume with insulation

This experiment involved testing on the half volume vaccine storage with insulation. The storage volume for this case was 7L. Polystyrene had been used as the insulating material. The insulation had been kept of a thickness of 2.54cm. The cold chamber was surrounded by two layers of polystyrene from all four sides and approximately three layers of it from the bottom face. Each layer of insulation was joined to the adjacent layer with the help of an adhesive. Any gaps within the systems that could have contributed to air leakage had been sealed with carefulness so that maximized cooling could be obtained. The aim for such enclosure of insulating materials was to ensure minimum heat loss from the system so that adequate amount of cooling could be achieved within a moderate duration that could be sustained for a good amount of time within the cold box. Similar to previous test runs, two sets of data loggers recorded the temperature and humidity of the system at predetermined intervals throughout the testing duration. This was done to keep track of the system's temperature and humidity changes. One logger recorded data for both temperature and humidity using temperature and humidity sensors placed inside the chamber, while another used a temperature sensor placed around the heat sink in the TEC to record temperature. When viewed from the top, the temperature and humidity sensors were located in the center of half of the total storage, to the right. The temperature sensor was placed 13.09cm away from the bottom face. The temperature and humidity sensors were set at a 4.5cm distance from one another. The primary source of power in this case was grid energy, which was used to power the system via an inverter. The system was powered by a 12V lead acid battery as a backup. In addition, one analogue voltmeter and one analogue ammeter were included in the main circuit for recording the battery's current and voltage ratings. A single digital volt-ampere meter was used to assess the current and voltage ratings on the load side. On all four sides of the vaccine box, a Fluke sensor thermometer was utilized to capture the average ambient temperature.

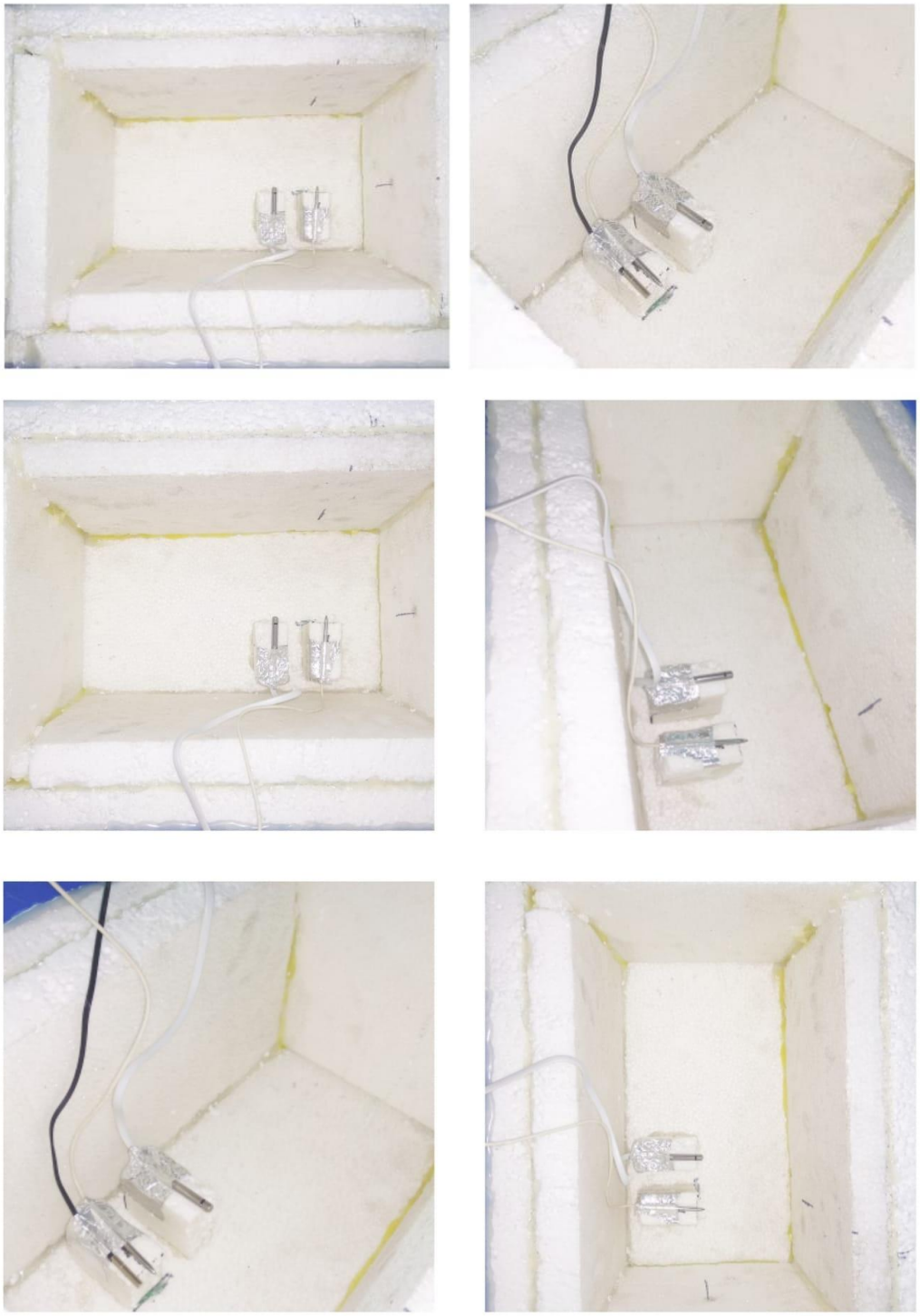

Figure 19: Testing on half volume with insulation.

Based on the results achieved from stage 1, it was evident that the system performed most effectively and reliably in test no.5 that was the case for Half Volume with Insulation. As our aim was to first optimizing the geometry and then moving towards acquiring effective cooling using solar power, we had decided to proceed to the stage 2 of the experimentation - **Photovoltaic Integration.**

In this stage, we incorporated two different cases using two different sets of solar panels. The panels used were Monocrystalline. The two different panels used were – i) Monocrystalline Panel with No Tracking System and ii) Monocrystalline panel with Automatic Tracking System. A Solar Charge Controller was used in the circuit to manage the power flowing to the battery from the solar array. It further ensured that overcharging of the battery was prevented and by no means could it flow backwards to the solar array. In addition, an endoscope camera was placed inside the chamber near the heat sink attached to the TEC module in order to look for any frosting that may occur at any point of the experimentation.

Our aim was to analyze the performance of cooling system on daylong basis to understand whether the solar power can be opted for as a viable energy resource or not.

3.4.2.6 Test Run 6: Solar Direct Drive on the Optimized Volume

This test case had been conducted on the optimal geometry hence the cooling chamber had a volume of 7L. As explained elaborately in test run no. 5, the components incorporated for the experimentation and other proceedings remained exactly the same. Just like all the previous test cases, two sets of data loggers were used to record the temperature and humidity of the system at predetermined intervals throughout the testing duration to keep track of the system's temperature and humidity changes. One logger recorded data for both temperature and humidity using temperature and humidity sensors placed inside the chamber, while another used a temperature sensor placed around the heat sink in the TEC to record temperature. In addition, the current and voltage ratings on the load side were recorded from the digital Volt-Ampere meter. Similar to all the previous cases, the average temperature on the outside faces were recorded using a Fluke Temperature Sensor. For this test case, we also used an Endoscope Camera to observe the frosting and defrosting process of the heat sink adjacent to the TEC module.

The experiment was conducted on a bright sunny day. The primary source of power in this test case was solar energy which was applied through Direct Drive. In this test case, we had utilized a combination of solar panels- three separate panels were used by establishing parallel connection among each other. The panels had been numbered as can be seen from the figure. 20, for establishing convenience at identifying. The figure shows that out of the five panels, the three panels in the middle were selected for the experimentation. The wattage of each panel was 120W. The voltage and current ratings of each of these panels were 18V and 6.7A respectively. No backup system was utilized during the testing process. Hence, effective cooling was achieved via solar direct drive alone.

Figure 20: Panels used in the test case. (Have been numbered sequentially from right corner.)

To understand how the irradiation was varying as the day proceeded forward, a pyranometer was used to record the irradiation on each panels at a specified interval throughout the testing process. As the sunlight did not have a uniform intensity over the entire exposed area, the readings recorded by the pyranometer also varied over the whole exposed surface. Therefore, a number of readings

were taken for each of the panels at a certain interval which was then computed to obtain an average value of irradiation. It is necessary to mention that, as the day proceeded, the shading effect due to adjacent trees and structures covered a large area of the panels. The third panel had fallen under shade during mid-day and stayed in that state for the rest of the duration. The second panel had approximately, more than half of its exposed area fallen under shade and as the sun was approaching towards the west, the exposed area in sunlight gradually reduced. The first panel however, had been affected the least by effect of shading as can be seen from the figure no. 21.

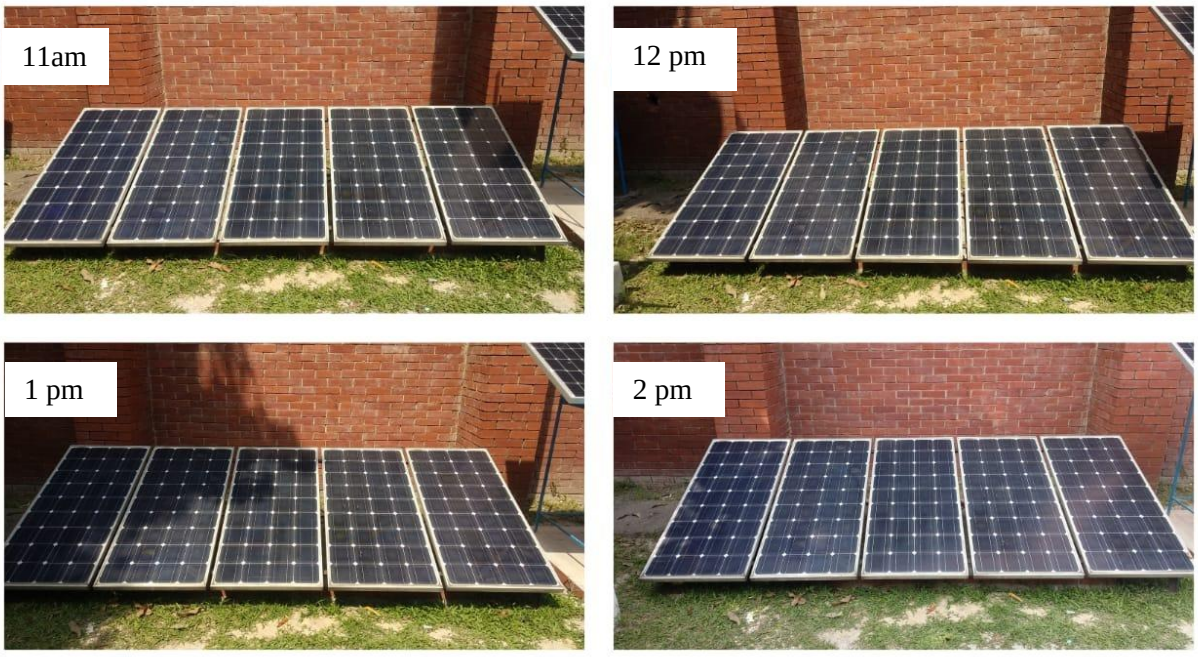

Figure 21: Effect of shading over the panels at different times during the day.

As mentioned earlier, the endoscope camera placed inside the chamber as can be seen from figure no. 22, was used in taking pictures of the heat sink frosting. A couple of pictures had been taken using the camera which showed there was evident frosting over the heat sink when the system produced the highest cooling effect. The frosting sustained for an adequate amount of period and gradually reduced due to reduced power extracted from the panels as the solar irradiation became less and less intensive. From figure no. 23, it can be observed that at low power ratings of the

system, defrosting was taking place on the same heat sink and the presence of ice formations slowly diminished.

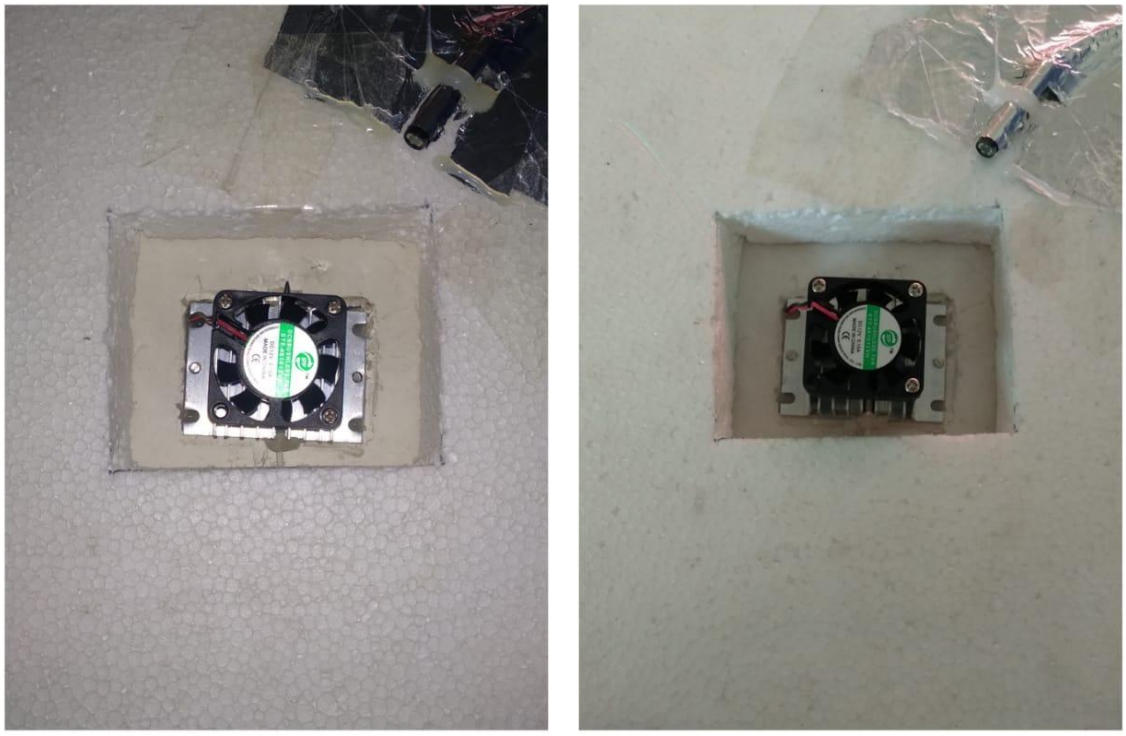

Figure 22: Endoscope camera placed near the heat sink attached to the TEC module.

As the sun was approaching towards the west, with really reduced solar intensity, the system eventually could not produce effective cooling any longer. Therefore, the temperature inside the chamber started rising beyond the desired temperature range. At one point, the power extracted from the panels was just not sufficient in functioning the system therefore the system stopped eventually. It is worth mentioning that, although the power was not considerably sufficient during the later parts of the day, with slight variation in solar intensity, the overall performance by the system was fluctuating as well. Finally, the period of holding the chamber within the desired temperature range by the system was noted down.

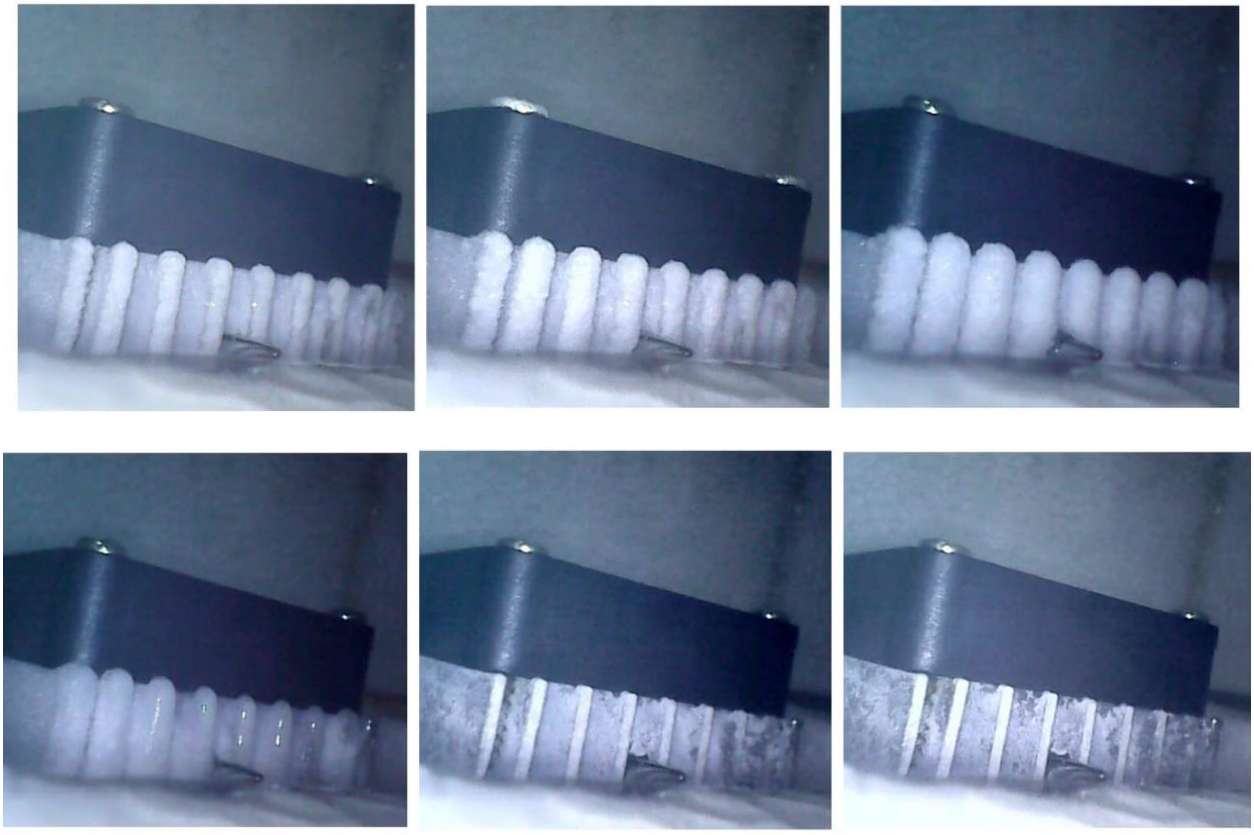

Figure 23: Visible frosting (top three pictures) and defrosting (bottom three pictures) on the heat sink.

3.4.2.7 Test Run 7: Solar Drive with Battery Backup

This test case had also been conducted on the optimal geometry hence the cooling chamber had a volume of 7L. As explained elaborately in test case no. 6, the components incorporated for the experimentation and other procedures remained exactly the same. Just like all the previous test cases, two sets of data loggers were used to record the temperature and humidity of the system at predetermined intervals throughout the testing duration to keep track of the system's temperature and humidity changes. One logger records data for both temperature and humidity using temperature and humidity sensors placed inside the chamber, while another uses a temperature sensor placed around the heat sink in the TEC to record temperature. In addition, the current and

voltage ratings on the source side were recorded from the analog Volt-Ampere meter and for the load side voltage and current readings were recorded using a Solar Charge Controller. Similar to all the previous cases, the average temperature on the outside faces were recorded using a Fluke Temperature Sensor. We also used an Endoscope Camera to observe the frosting and defrosting process of the heat sink adjacent to the TEC module.

For this particular test case we used solar power as the primary power source and a backup battery as the secondary power source. Here we used a 12V, 8-12Ah Lead Acid battery as the backup source. Since a battery was incorporated as the backup power system, a digital Solar Charge Controller was used to regulate the voltage and current drawn from the panels. Besides, we used a 375 W Auto-tracking solar panel (which has three Degrees of Freedom) as the main power source in order to extract the highest possible amount of irradiation according to the inclination of the Sun as the day advances.

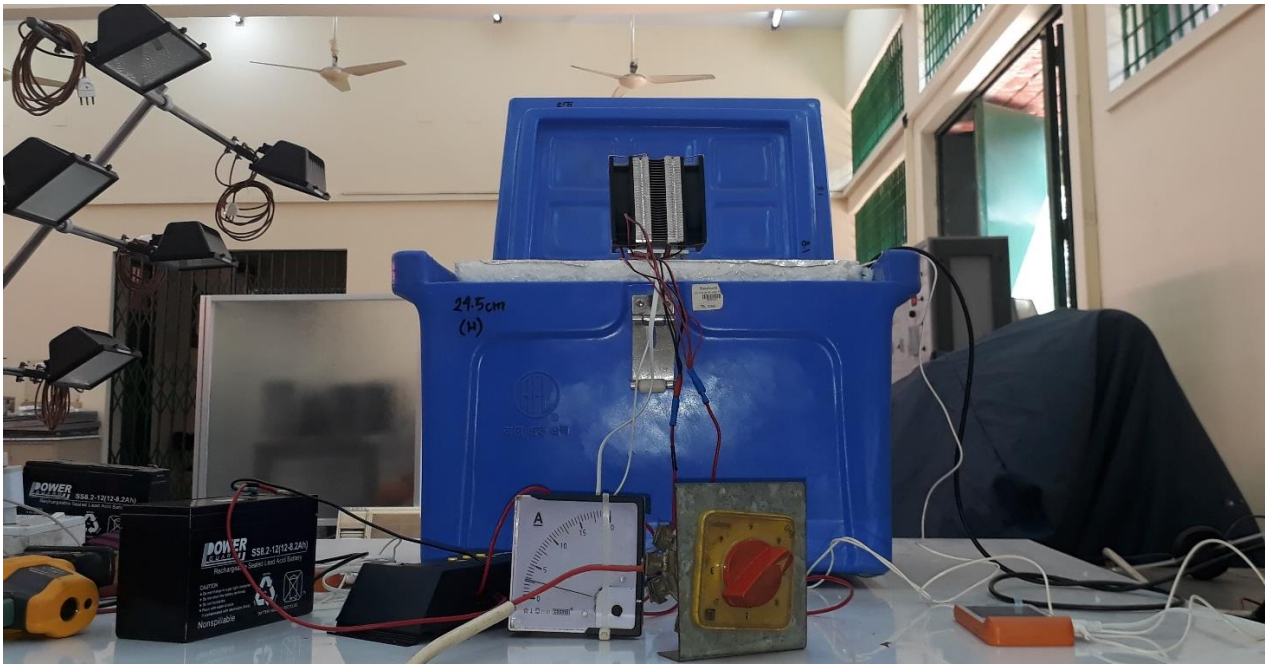

Figure 24: Experimental setup of the complete system.

The readings of solar irradiation was extracted from a software (which is a package built for continuously interfacing and recording data from this particular solar module) throughout the day.

The effect of shading on the Auto-tracking solar panel was also studied during the process. The figure below shows a vivid demonstration of Shading Effect on the panel.

Figure 25: Effect of shading over the panels at different times during the day.

Additionally, similar to the previous case the frosting and defrosting of the fins of heat sink were also observed using an endoscope camera as mentioned earlier. The figure below shows both the

process as the frosting and defrosting rate was changing with respect to the variation of the intensity of solar irradiation.

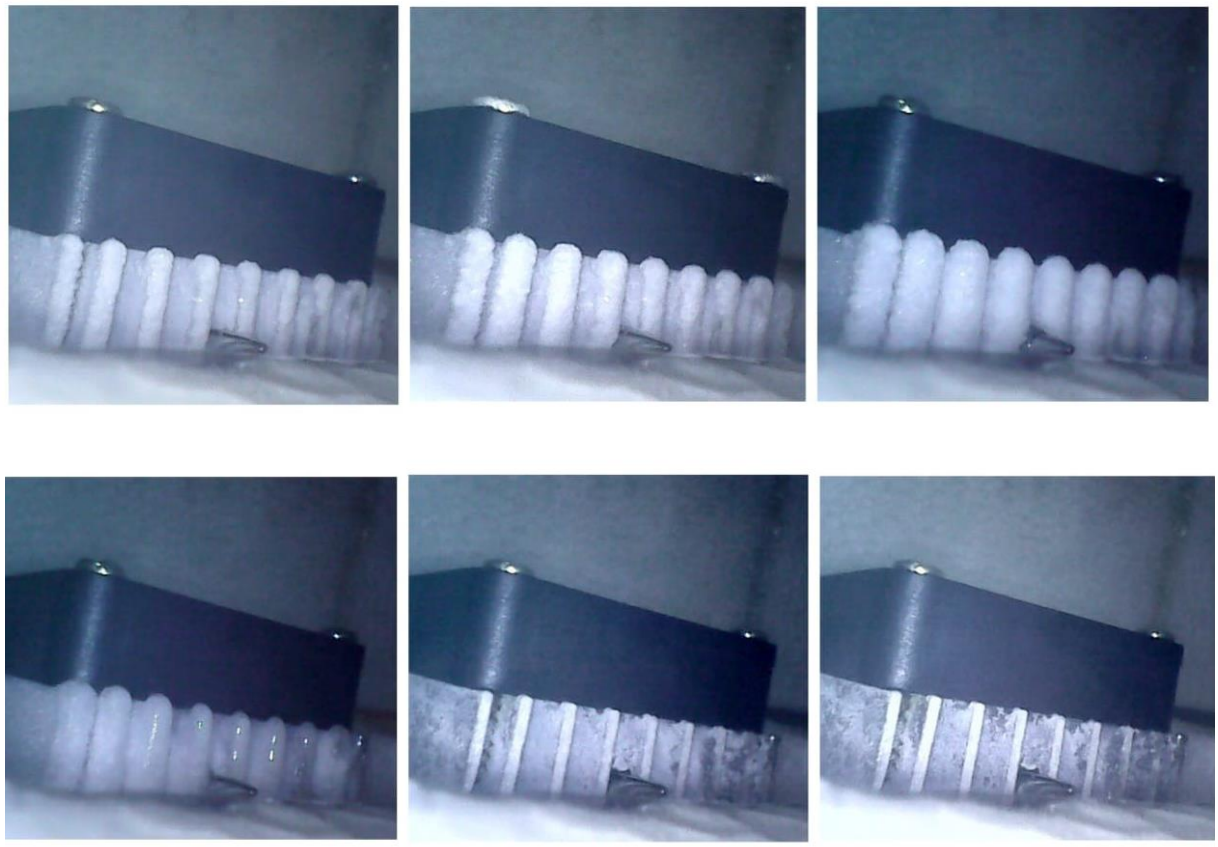

Figure 26: Visible frosting (top three pictures) and defrosting (bottom three pictures) on the heat sink

After completing the complete assembly, a day long study was conducted in order to observe and record the overall thermal performance of the system under the effect of both the primary power source (Solar power) and the backup or secondary power source (Battery power). Finally the period of holding of the desired temperature inside the cooling chamber was documented accordingly as the previous test case. This concluded the study of the stage-2 of the experimentation i.e. Photovoltaic Integration.

Chapter 4

4. Results and Discussions

The purpose of this experiment was to assess the thermal performance of a photovoltaic thermoelectric vaccine refrigerator. To accomplish this, the entire project was divided into two stages. The first stage was to analyze and optimize the geometry of the system (particularly its volume) and the second stage was to monitor the thermal performance of the optimized geometry with photovoltaic integration. This section comprehensively presents the summary of the sets of data extracted from the complete experimentation.

4.1 Results from Stage-1: Volume Optimization

4.1.1 Test Run 1: Full volume without insulation

This test case was conducted on the full volume (volume was 25 L) of the system without the use of any insulation material besides the thermal material of the cold box itself. A constant 12V DC source was provided to the system through a solar charge controller during the process. A 12V-10A Thermoelectric module was used for the cooling of the system. Some of the parameters were recorded and analyzed graphically.

Table 1: Significant Parameters inside the Cooling Chamber and on the cold side of the TEC

Parameters	Chamber	TEC
Initial Time	3:39:25 PM	3:39:25 PM
Initial Temperature	24.7 °C	25.2 °C
Initial Humidity	63.2%	63.5%
During Cooling		
Run Time	60 minutes	60 minutes
Lowest Temperature Achieved	10.3°C	-2.2 °C
Lowest Humidity Achieved	32.9%	62.4%
During Reverse Cooling/Heating		
Run Time	25 minutes	25 minutes
Highest Temperature Reached	24.1°C	22.1°C
Highest Humidity Reached	55.5%	69.8%

The collection of data shown above was extracted from the digital data loggers through a software called **ElitechLogWin V6.2.0.** The temperature sensor or the thermocouple and the humidity sensor were placed inside the chamber and on the cold side of the TEC for this purpose. The graphical data were also extracted from the same software in order to observe the continuous fluctuations of temperature and humidity during the entire process of cooling and reverse cooling. This clarified the validity of the variable thermal performance at different times inside the chamber and on the cold side of the TEC module. Since it was an experimental process, the presence of friction and irreversibility, heat loss and deterioration of efficiency of the TEC module were affecting the overall performance of the system at every instant **[1].**

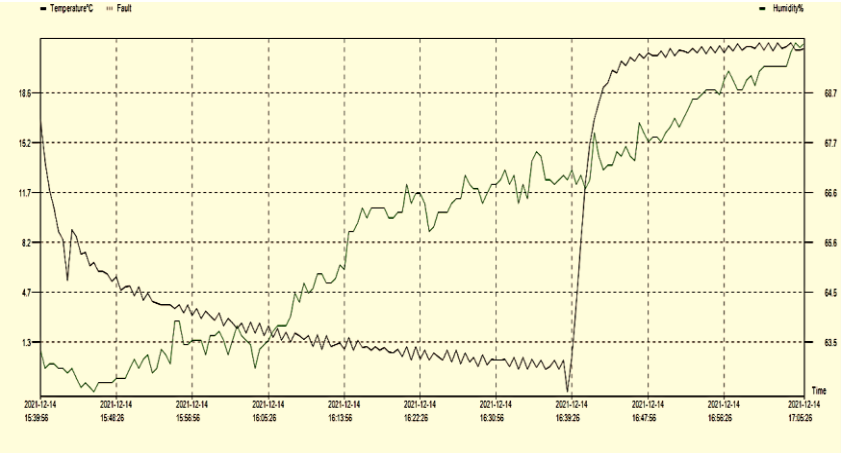

Figure 27: Fluctuation of Temperature and Humidity on the cold side of the TEC. (Sensor Probe placed on the Cold Side of TEC Module)

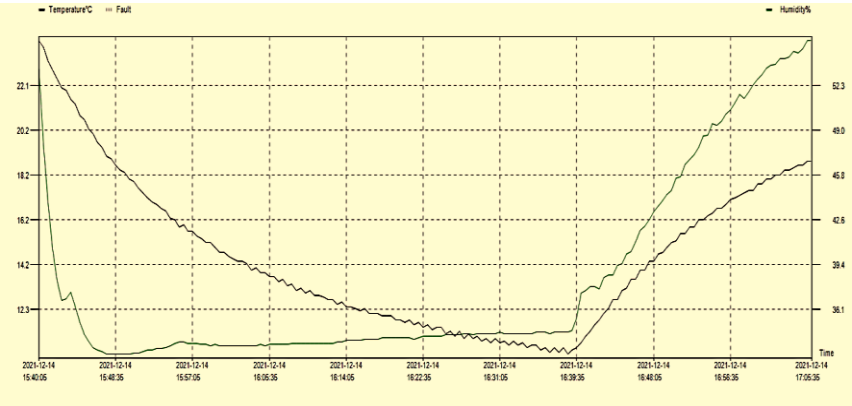

*Figure 28**:** Fluctuation of Temperature and Humidity inside the Cooling Chamber. (Sensor Probe placed inside the chamber in a definite coordinate)*

Additionally the voltage and current readings were taken of both the source (12V DC Battery) and the load (12V-10A TEC module) in order to study the power consumption rate for definite time interval. The average temperature readings of the surfaces exposed to the environment of the cold box were also taken for studying the heat transfer rate and the temperature gradient of the system. The collected data are presented graphically for clear understanding.

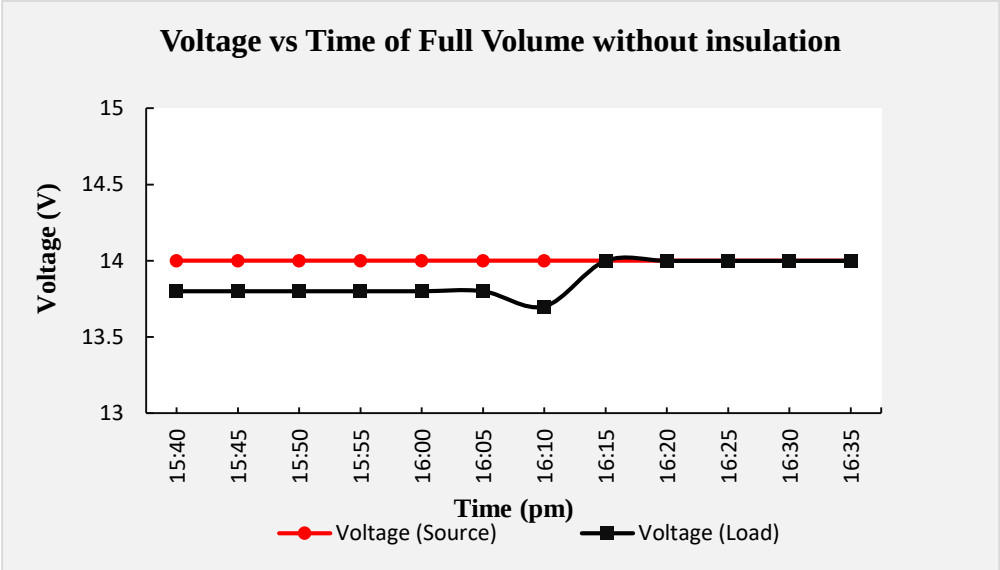

Figure 29: Voltage vs. Time graph of the Source and Load (TEC Module)

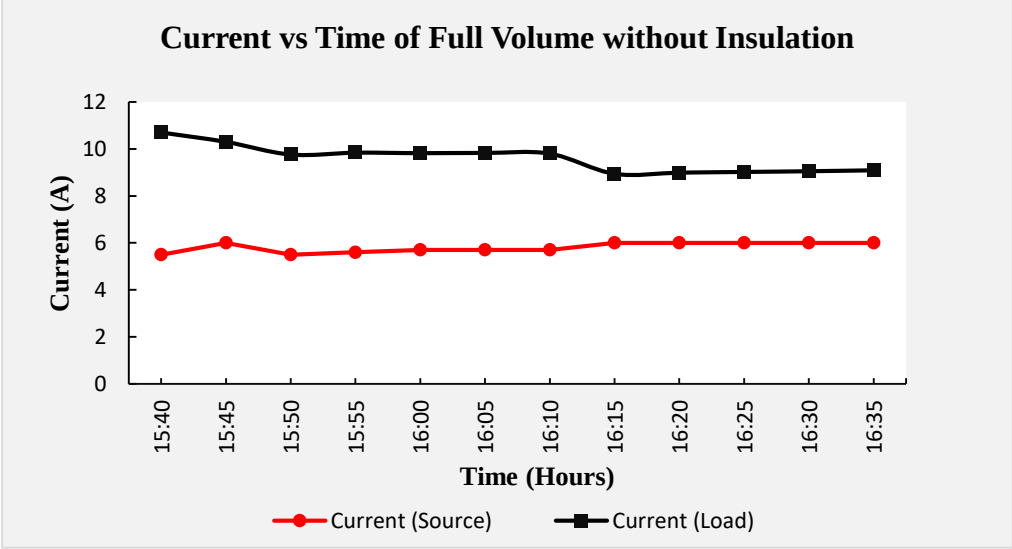

Figure 30: Current vs. Time graph of the Source and Load (TEC Module).

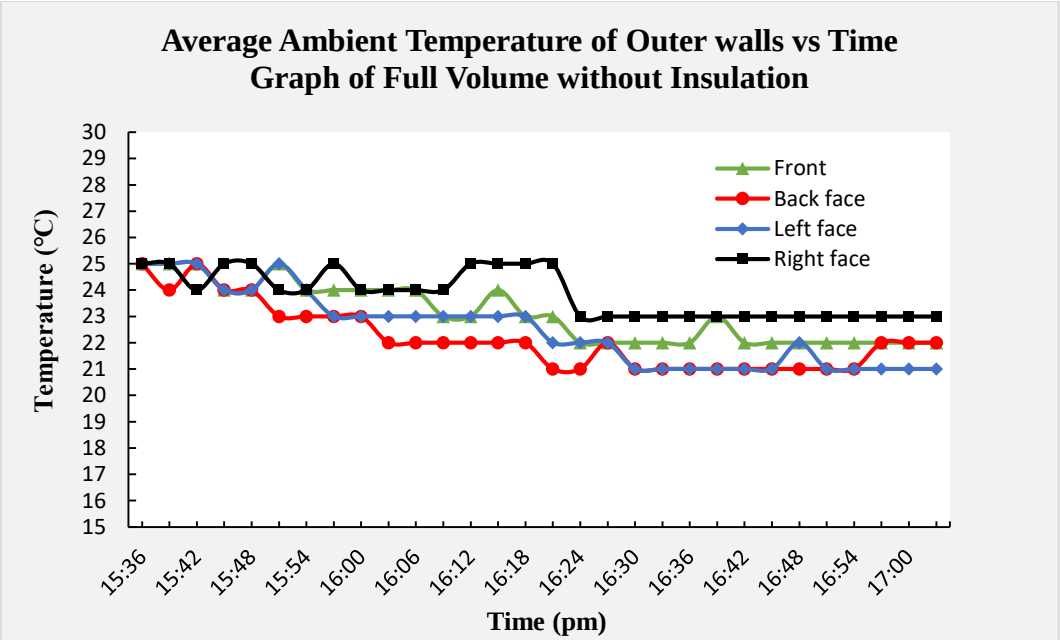

Figure 31: Average Ambient Temperature of the Outer Surfaces vs. Time graph of Full Volume without Insulation

4.1.2 Test Run 2: Full volume with insulation on four sides

This test case was conducted on the full volume with insulation on four sides (volume was 18 L) of the system with a 1 inch layer of Polystyrene sheet as insulation material besides the thermal material of the cold box itself. A constant 12V DC source was provided to the system through a solar charge controller during the process. A 12V-10A Thermoelectric module was used for the cooling of the system. Some of the parameters were recorded and analyzed graphically.

Table 2: Significant Parameters inside the Cooling Chamber and on the cold side of the TEC

Parameters	Chamber	TEC
Initial Time	3:39:25 PM	3:39:25 PM
Initial Temperature	26.2 °C	25.2 °C
Initial Humidity	60.1%	63.5%
During Cooling		
Run Time	57 minutes	57 minutes
Lowest Temperature Achieved	6.3°C	-4.4 °C
Lowest Humidity Achieved	37.1%	62.9%
During Reverse Cooling/Heating		
Run Time	38 minutes	38 minutes
Highest Temperature Reached	26.2°C	26.2°C
Highest Humidity Reached	60.2%	67.6%

The collection of data shown above was extracted from the digital data loggers through a software called **ElitechLogWin V6.2.0.** The temperature sensor or the thermocouple and the humidity sensor were placed inside the chamber and on the cold side of the TEC for this purpose. The graphical data were also extracted from the same software in order to observe the continuous fluctuations of temperature and humidity during the entire process of cooling and reverse cooling. This clarified the validity of the variable thermal performance at different times inside the chamber and on the cold side of the TEC module.

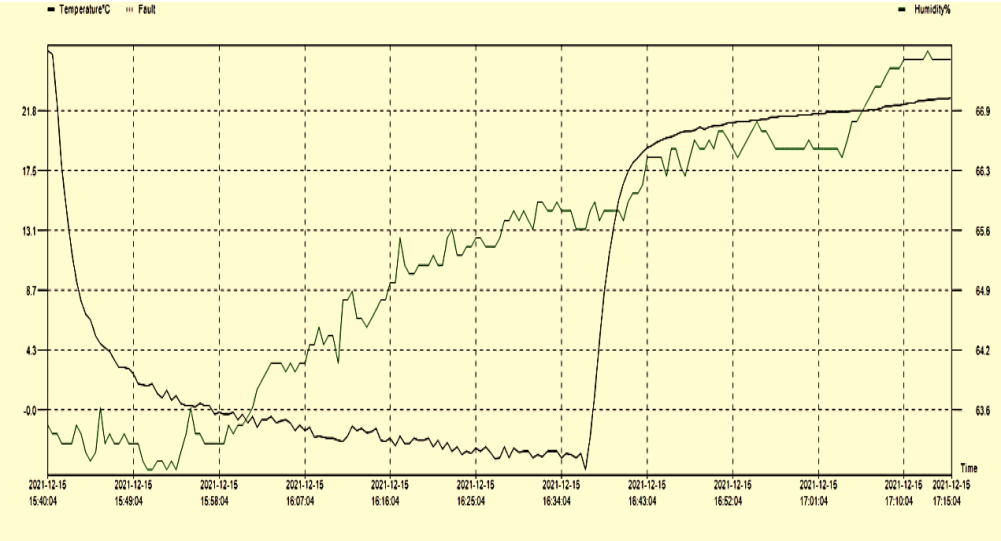

Figure 32: Fluctuation of Temperature and Humidity on the cold side of the TEC. (Sensor Probe placed on the Cold Side of TEC Module)

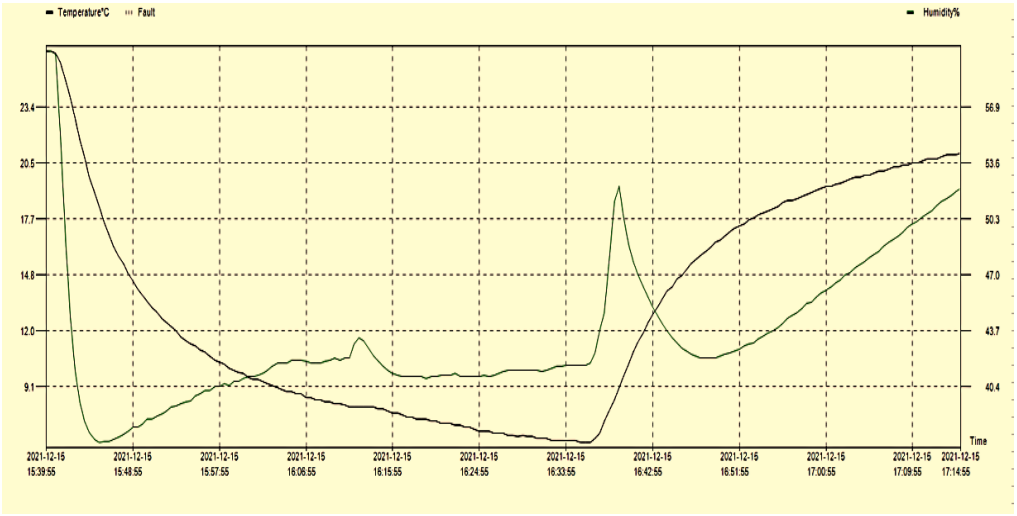

Figure 33: Fluctuation of Temperature and Humidity inside the Cooling Chamber. (Sensor Probe placed inside the chamber in a definite coordinate)

Additionally the voltage and current readings were taken of both the source (12V DC Battery) and the load (12V-10A TEC module) in order to study the power consumption rate for definite time interval. The average temperature readings of the surfaces exposed to the environment of the cold box were also taken for studying the heat transfer rate and the temperature gradient of the system. The collected data are presented graphically for clear understanding.

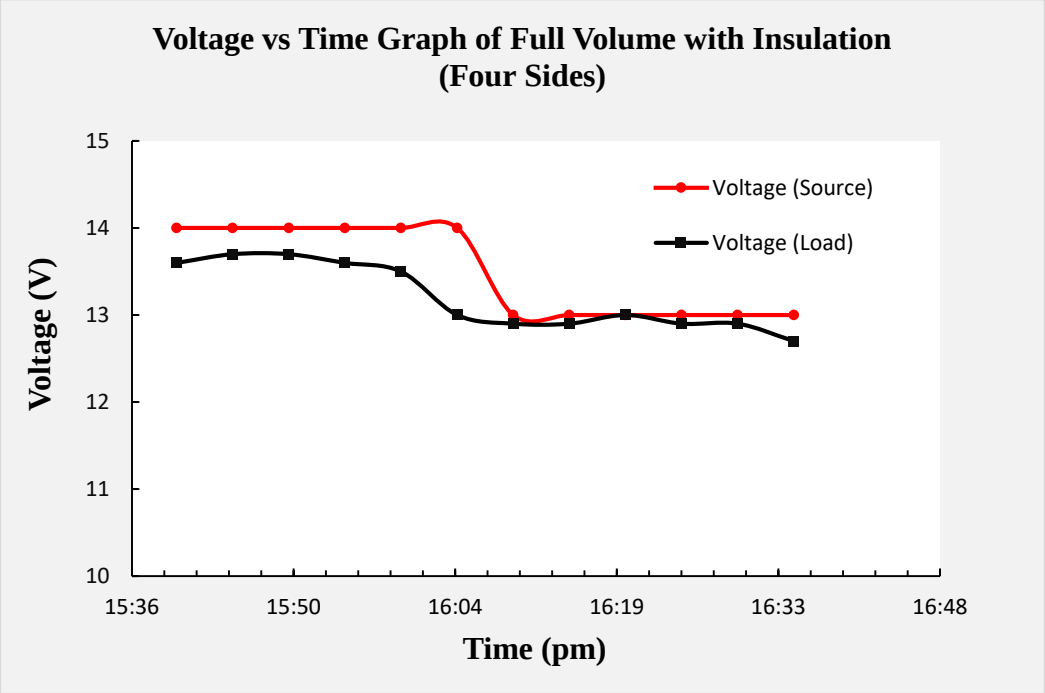

Figure 34: Voltage vs. Time graph of the Source and Load (TEC Module).

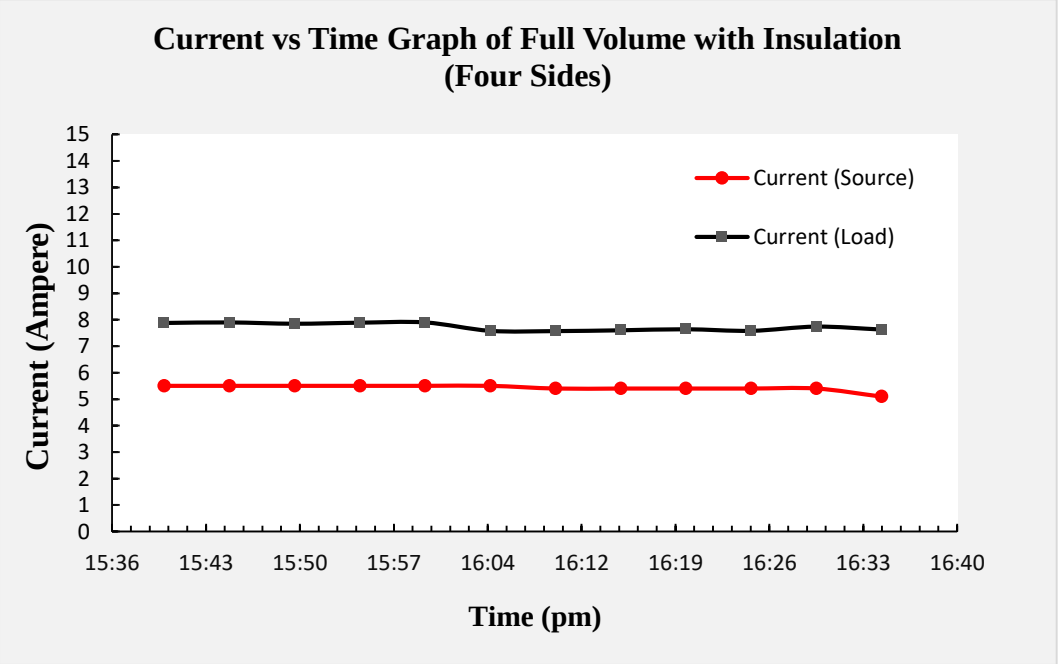

Figure 35: Current vs. Time graph of the Source and Load (TEC Module)

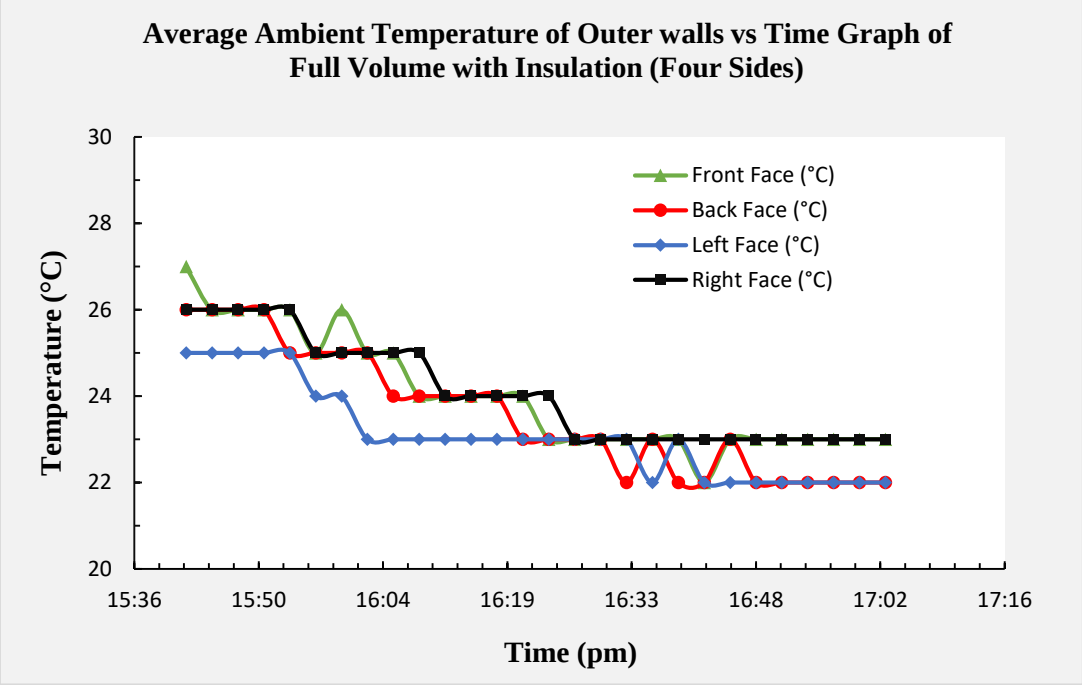

Figure 36: Average Ambient Temperature of the Outer Surfaces vs. Time graph of Full Volume with Insulation on Four Sides.

4.1.3 Test Run 3: Full volume with insulation on five sides

This test case was conducted on the full volume with insulation on five sides (volume was 15 L) of the system with a 1 inch layer of Polystyrene sheets as insulation material besides the thermal material of the cold box itself. A constant 12V DC source was provided to the system through a solar charge controller during the process. A 12V-10A Thermoelectric module was used for the cooling of the system. Some of the parameters were recorded and analyzed graphically.

Table 3: Significant Parameters inside the Cooling Chamber and on the cold side of the TEC

Parameters	Chamber	TEC
Initial Time	2:12:00 PM	2:12:00 PM
Initial Temperature	21.7 °C	22.4 °C
Initial Humidity	66.6%	62.1%
During Cooling		
Run Time	37 minutes	37 minutes
Lowest Temperature Achieved	2.5°C	-7.9 °C
Lowest Humidity Achieved	42.6%	62%
During Reverse Cooling/Heating		
Run Time	43 minutes	41 minutes
Highest Temperature Reached	20.1°C	21.4°C
Highest Humidity Reached	54.9%	61.8%

The collection of data shown above was extracted from the digital data loggers through a software called **ElitechLogWin V6.2.0.** The temperature sensor or the thermocouple and the humidity sensor were placed inside the chamber and on the cold side of the TEC for this purpose. The graphical data were also extracted from the same software in order to observe the continuous fluctuations of temperature and humidity during the entire process of cooling and reverse cooling. This clarified the validity of the variable thermal performance at different times inside the chamber and on the cold side of the TEC module.

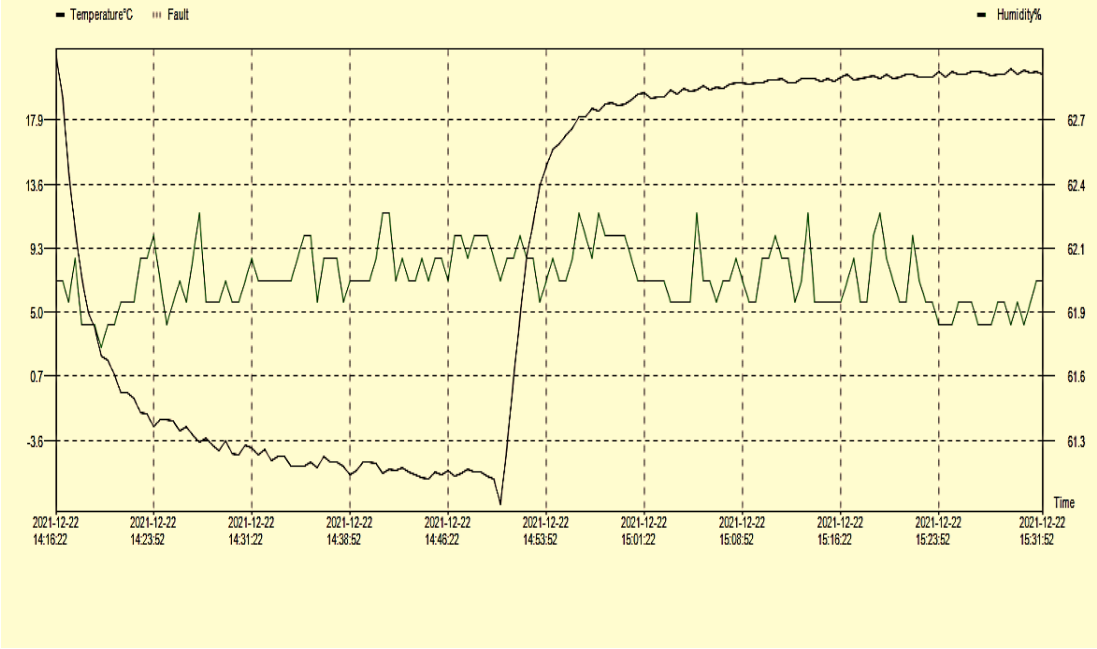

Figure 37: Fluctuation of Temperature and Humidity on the cold side of the TEC. (Sensor Probe placed on the Cold Side of TEC Module)

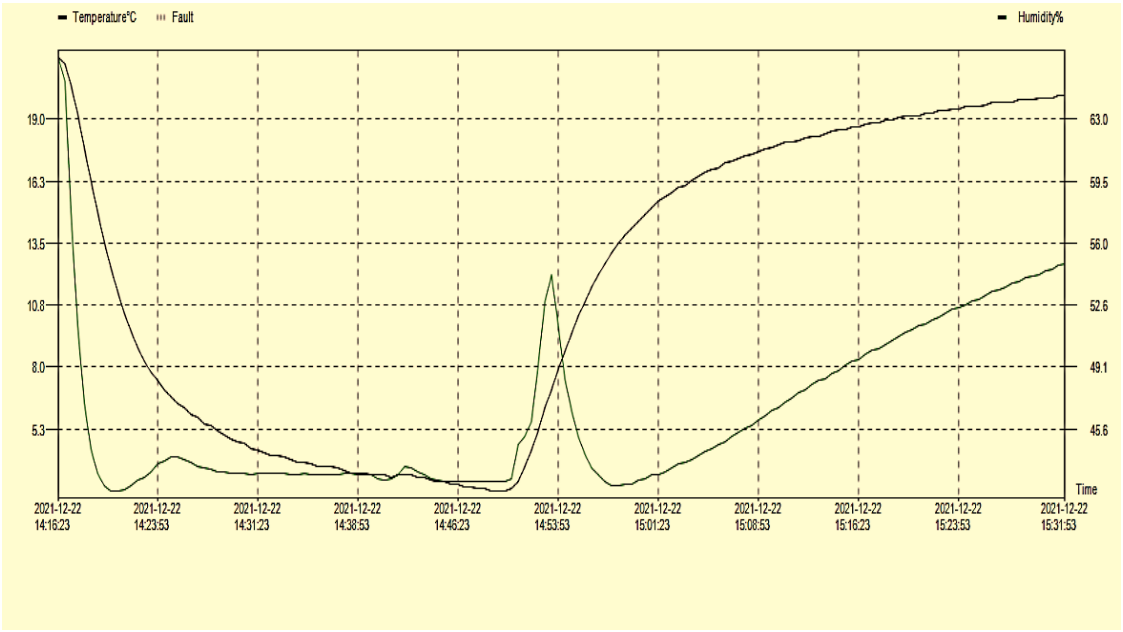

Figure 38: Fluctuation of Temperature and Humidity inside the Cooling Chamber. (Sensor Probe placed inside the chamber in a definite coordinate)

Additionally the voltage and current readings were taken of both the source (12V DC Battery) and the load (12V-10A TEC module) in order to study the power consumption rate for definite time interval. The average temperature readings of the surfaces exposed to the environment of the cold box were also taken for studying the heat transfer rate and the temperature gradient of the system. The collected data are presented graphically for clear understanding.

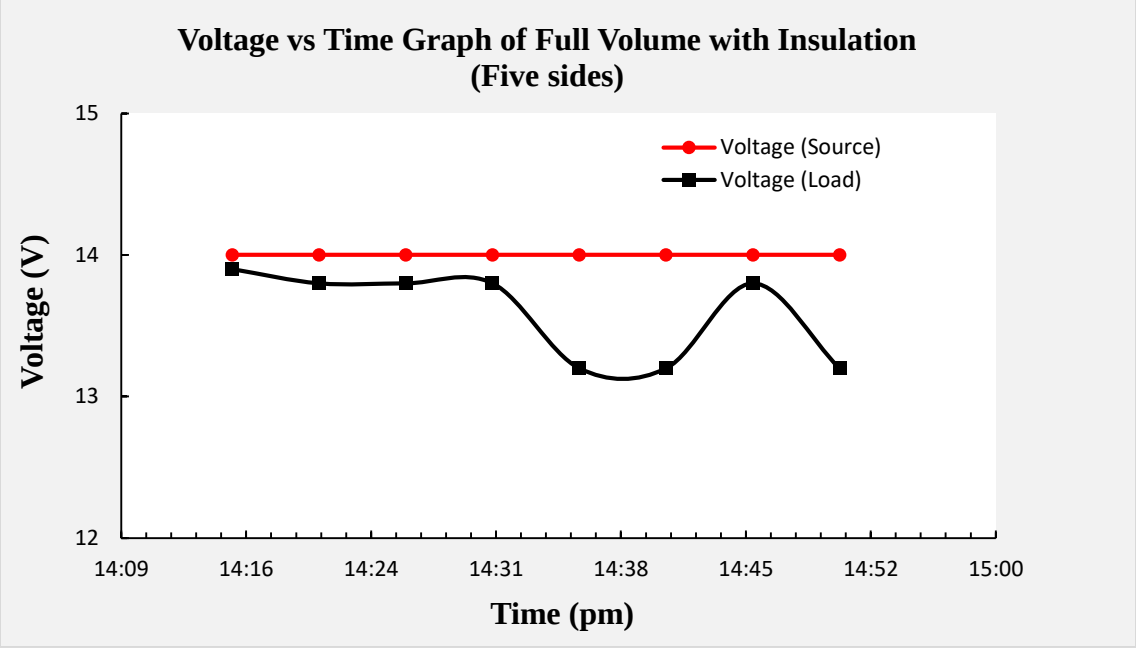

Figure 39: Voltage vs. Time graph of the Source and Load (TEC Module).

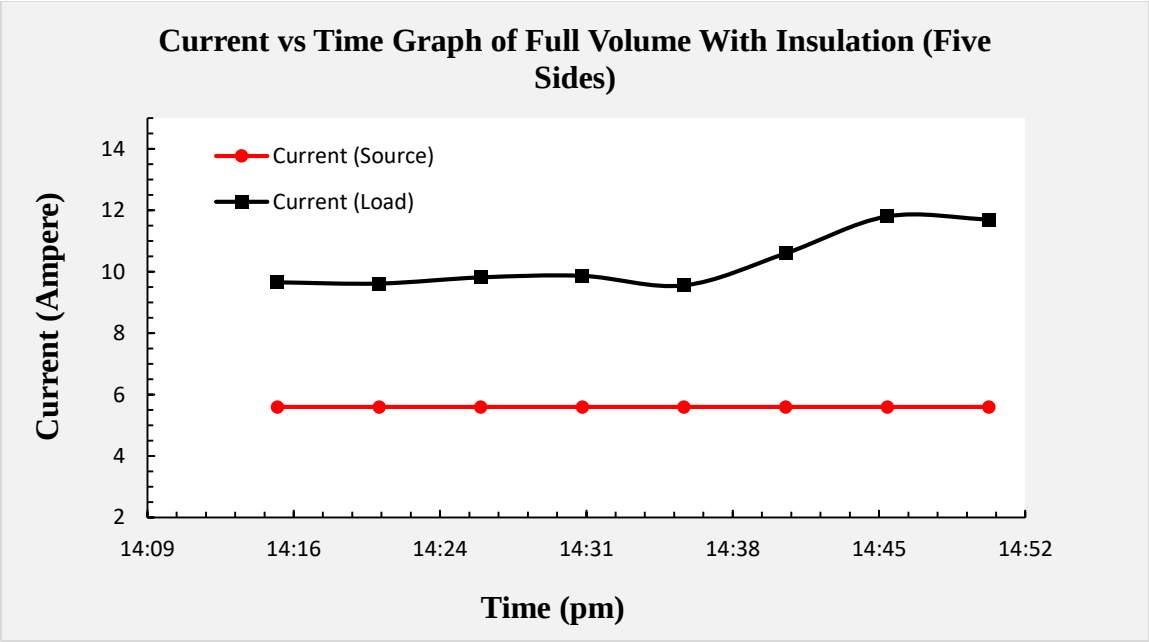

Figure 40: Current vs. Time graph of the Source and Load (TEC Module).

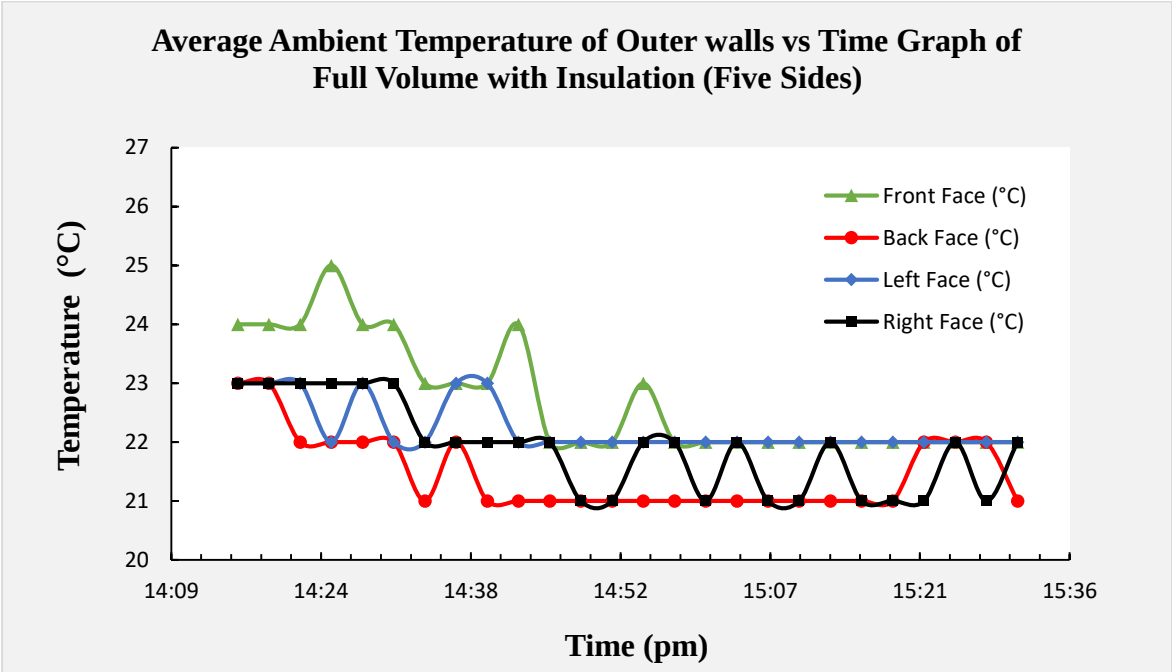

Figure 41: Average Ambient Temperature of the Outer Surfaces vs. Time graph of Full Volume with Insulation on Five Sides.

4.1.4 Test Run 4: Half volume without insulation

This test case was conducted on the half volume (volume was 13.7 L) of the system without the use of any insulation material besides the thermal material of the cold box itself. A constant 12V DC source was provided to the system through a solar charge controller during the process. A 12V-10A Thermoelectric module was used for the cooling of the system. Some of the parameters were recorded and analyzed graphically.

Table 4: Significant Parameters inside the Cooling Chamber and on the cold side of the TEC

Parameters	Chamber	TEC
Initial Time	4:05:00 PM	4:05:00 PM
Initial Temperature	23.1 °C	22.5 °C
Initial Humidity	68.4%	62.5%
During Cooling		
Run Time	45 minutes	46 minutes
Lowest Temperature Achieved	5°C	-4.4 °C
Lowest Humidity Achieved	42.4%	67.5%
During Reverse Cooling/Heating		
Run Time	45 minutes	44 minutes
Highest Temperature Reached	19°C	20.8°C
Highest Humidity Reached	74.5%	71.3%

The collection of data shown above was extracted from the digital data loggers through a software called **ElitechLogWin V6.2.0.** The temperature sensor or the thermocouple and the humidity sensor were placed inside the chamber and on the cold side of the TEC for this purpose. The graphical data were also extracted from the same software in order to observe the continuous fluctuations of temperature and humidity during the entire process of cooling and reverse cooling. This clarified the validity of the variable thermal performance at different times inside the chamber and on the cold side of the TEC module.

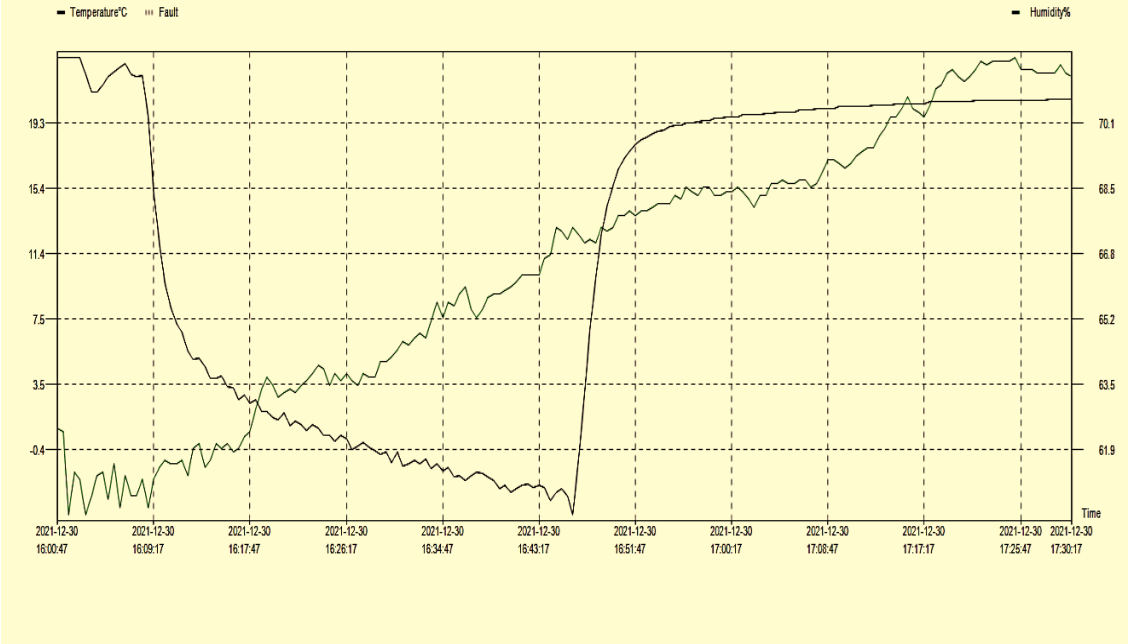

Figure 42: Fluctuation of Temperature and Humidity on the cold side of the TEC. (Sensor Probe placed on the Cold Side of TEC Module)

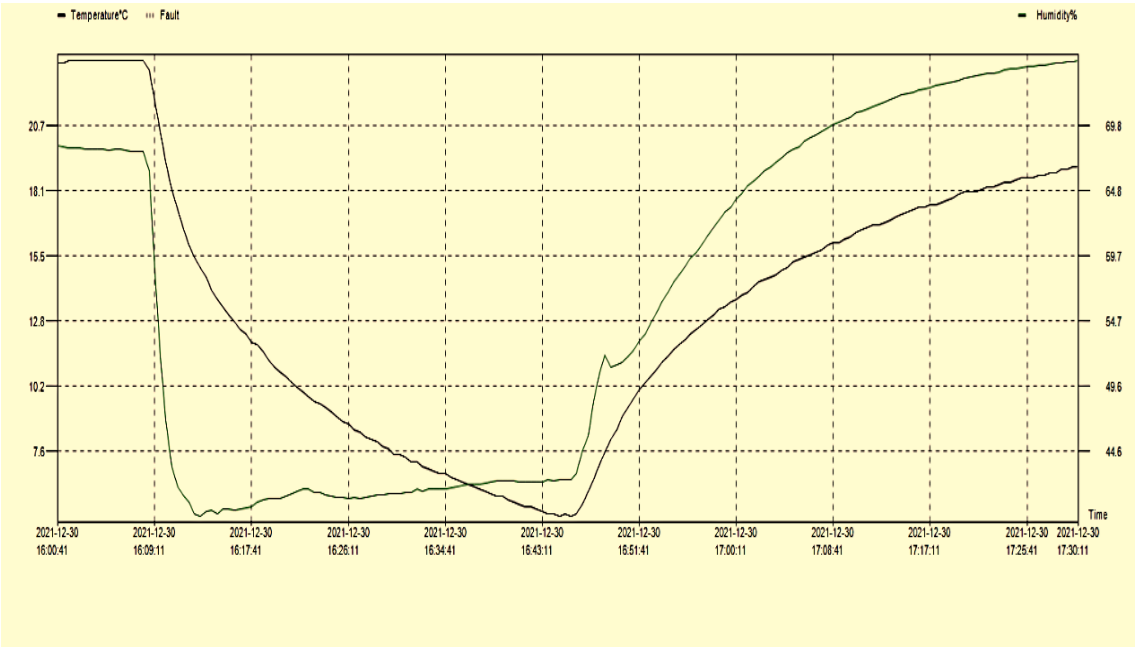

Figure 43: Fluctuation of Temperature and Humidity inside the Cooling Chamber. (Sensor Probe placed inside the chamber in a definite coordinate)

Additionally the voltage and current readings were taken of both the source (12V DC Battery) and the load (12V-10A TEC module) in order to study the power consumption rate for definite time interval. The average temperature readings of the surfaces exposed to the environment of the cold box were also taken for studying the heat transfer rate and the temperature gradient of the system. The collected data are presented graphically for clear understanding.

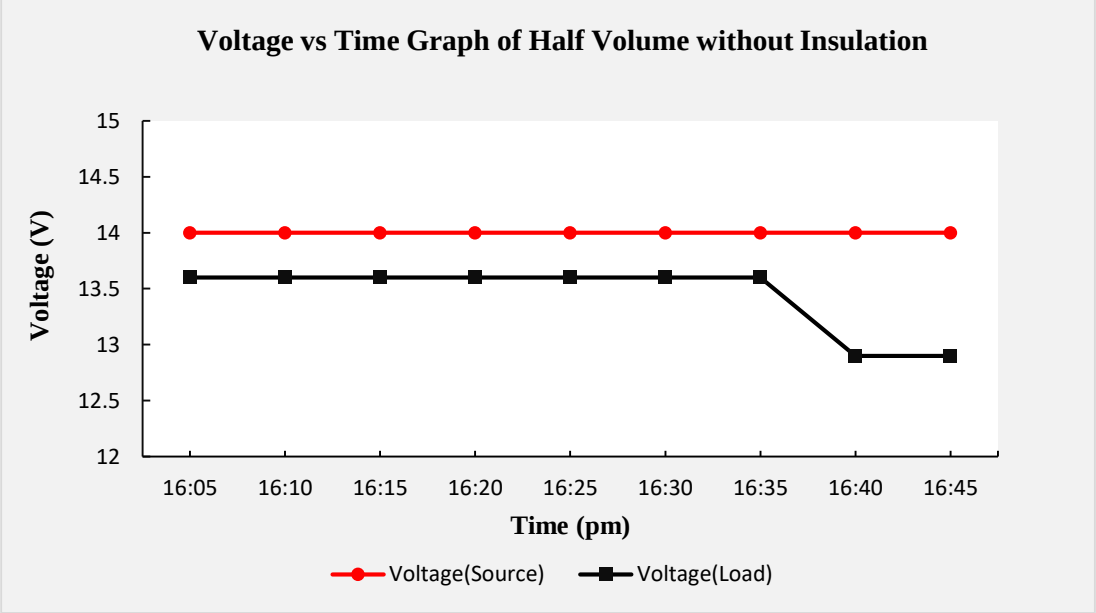

Figure 44: Voltage vs. Time graph of the Source and Load (TEC Module).

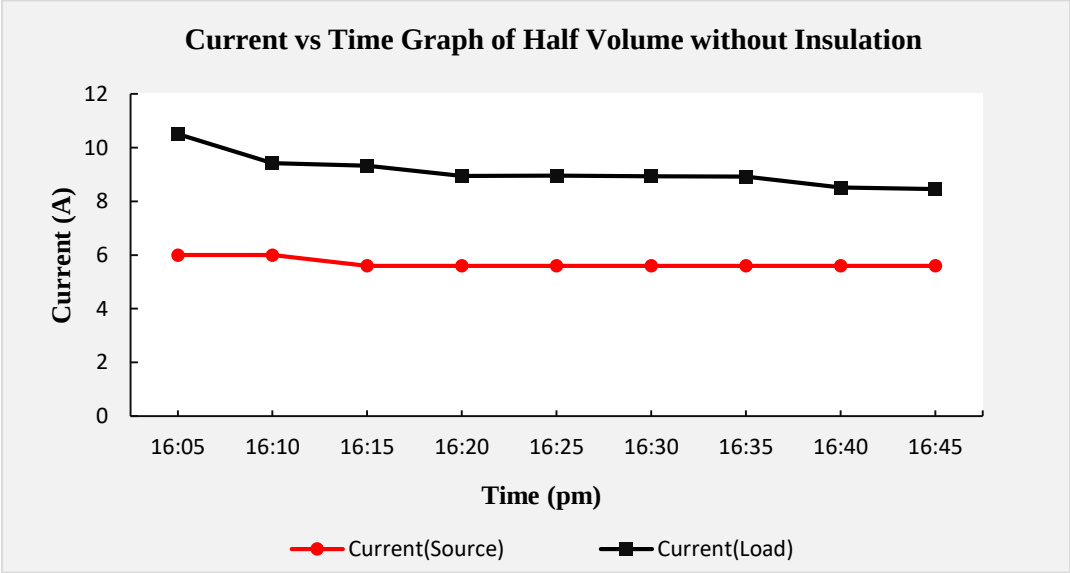

Figure 45: Current vs. Time graph of the Source and Load (TEC Module).

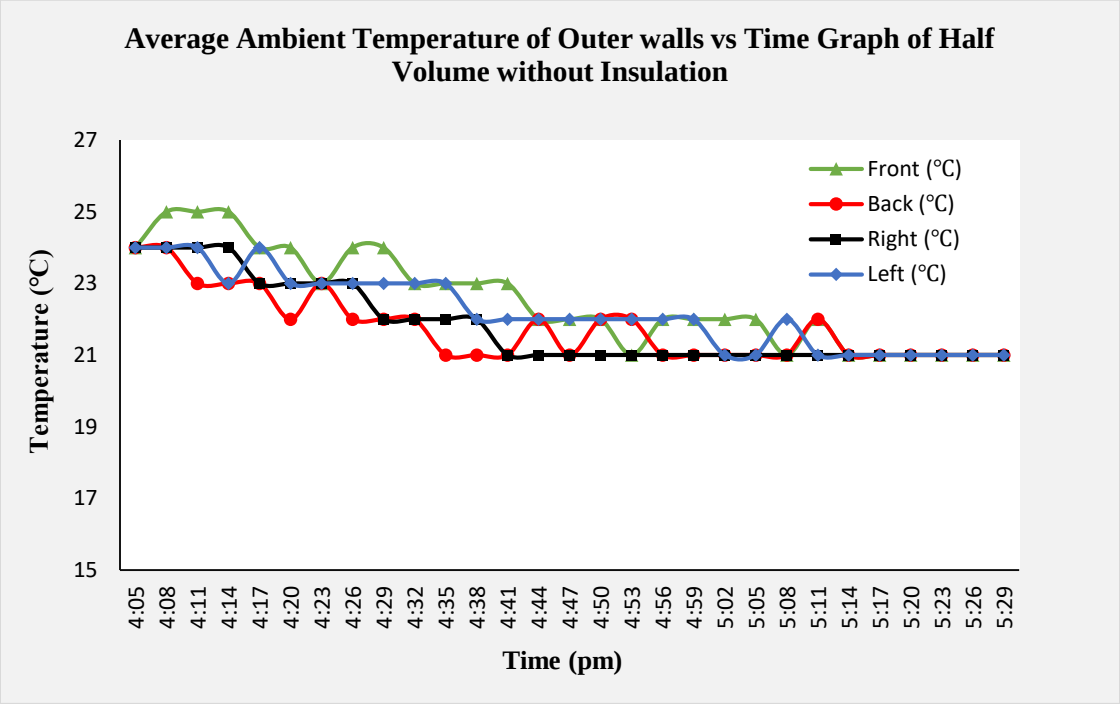

Figure 46: Average Ambient Temperature of the Outer Surfaces vs. Time graph of Half Volume without Insulation

4.1.5 Test Run 5: Half volume with insulation

This test case was conducted on the half volume (volume was 7 L) of the system with the use of two 1 inch layers of Polystyrene sheets as insulation material on five sides besides the thermal material of the cold box itself. A constant 12V DC source was provided to the system through a solar charge controller during the process. A 12V-10A thermoelectric module was used for the cooling of the system. Some of the parameters were recorded and analyzed graphically.

Table 5: Significant Parameters inside the Cooling Chamber and on the cold side of the TEC

Parameters	Chamber	TEC
Initial Time	1:18:00 PM	1:18:00 PM
Initial Temperature	21.5 °C	22.4 °C
Initial Humidity	69.3%	63.5%
During Cooling		
Run Time	10 minutes	10 minutes
Lowest Temperature Achieved	0.9°C	-6.8 °C
Lowest Humidity Achieved	47.7%	62.3%
During Reverse Cooling/Heating		
Run Time	41 minutes	41 minutes
Highest Temperature Reached	21.5°C	22.5°C
Highest Humidity Reached	68.1%	59.8%

The collection of data shown above was extracted from the digital data loggers through a software called **ElitechLogWin V6.2.0.** The temperature sensor or the thermocouple and the humidity sensor were placed inside the chamber and on the cold side of the TEC for this purpose. The graphical data were also extracted from the same software in order to observe the continuous fluctuations of temperature and humidity during the entire process of cooling and reverse cooling. This clarified the validity of the variable thermal performance at different times inside the chamber and on the cold side of the TEC module.

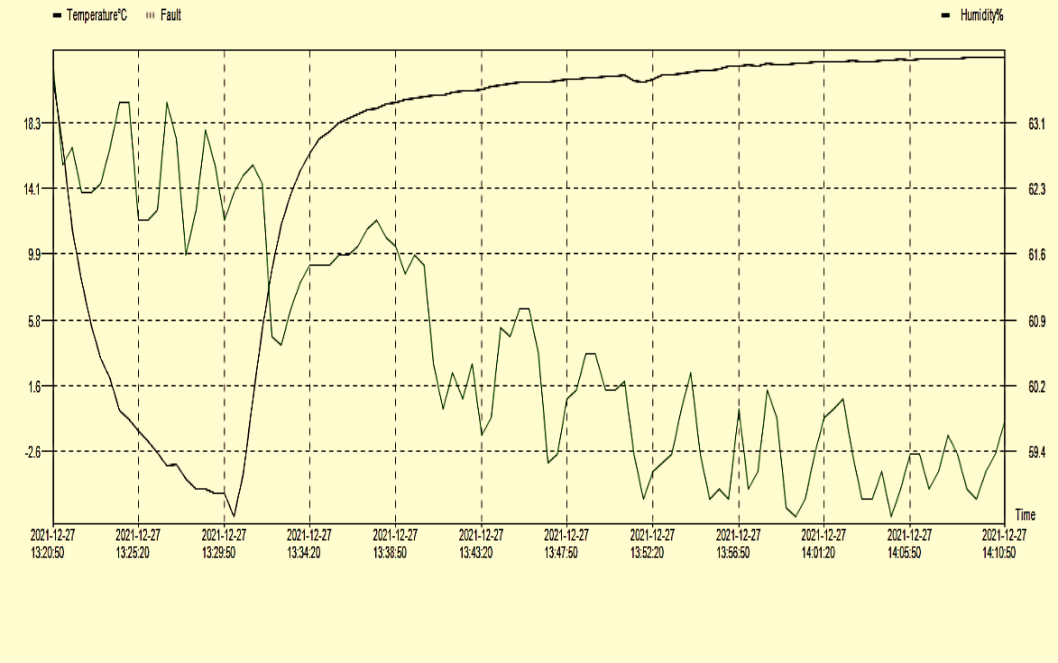

Figure 47: Fluctuation of Temperature and Humidity on the cold side of the TEC. (Sensor Probe placed on the Cold Side of TEC Module)

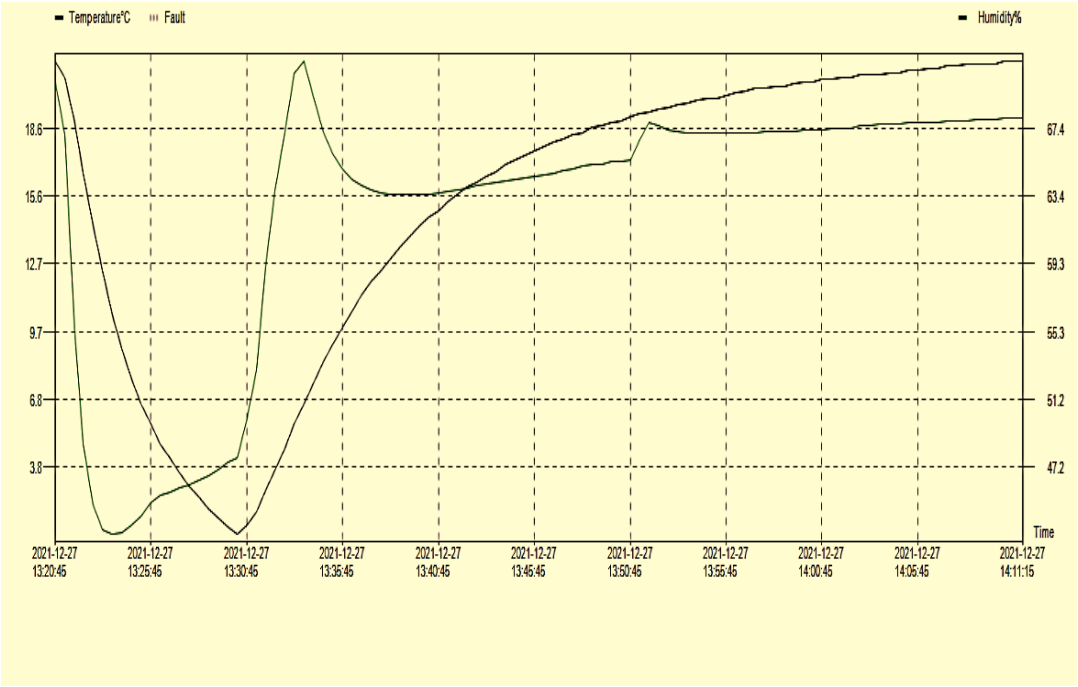

Figure 48: Fluctuation of Temperature and Humidity inside the Cooling Chamber. (Sensor Probe placed inside the chamber in a definite coordinate)

Additionally the voltage and current readings were taken of both the source (12V DC Battery) and the load (12V-10A TEC module) in order to study the power consumption rate for definite time interval. The average temperature readings of the surfaces exposed to the environment of the cold box were also taken for studying the heat transfer rate and the temperature gradient of the system. The collected data are presented graphically for clear understanding.

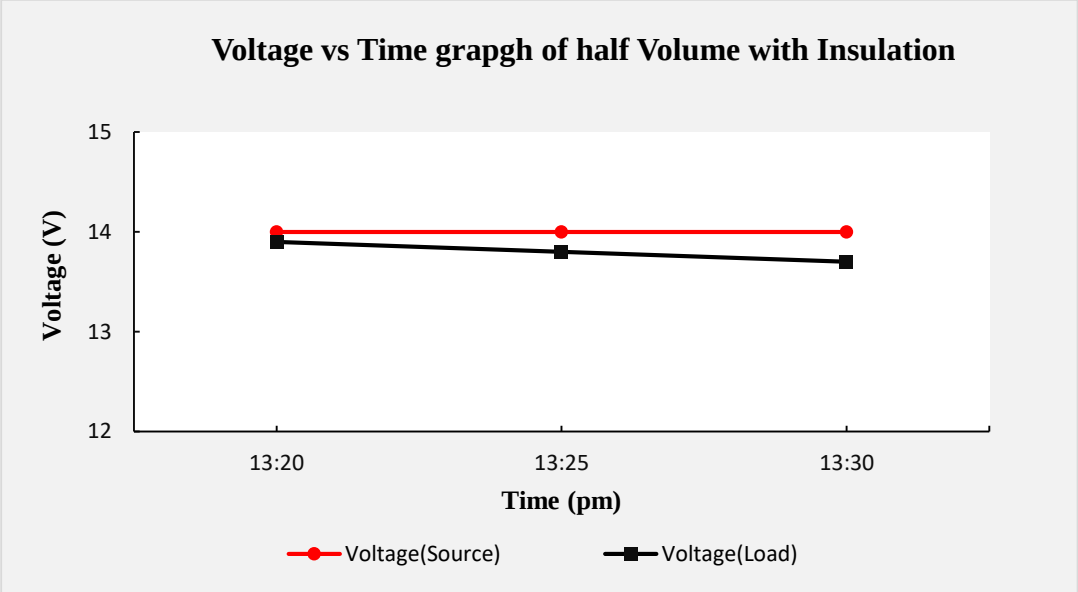

Figure 49: Voltage vs. Time graph of the Source and Load (TEC Module).

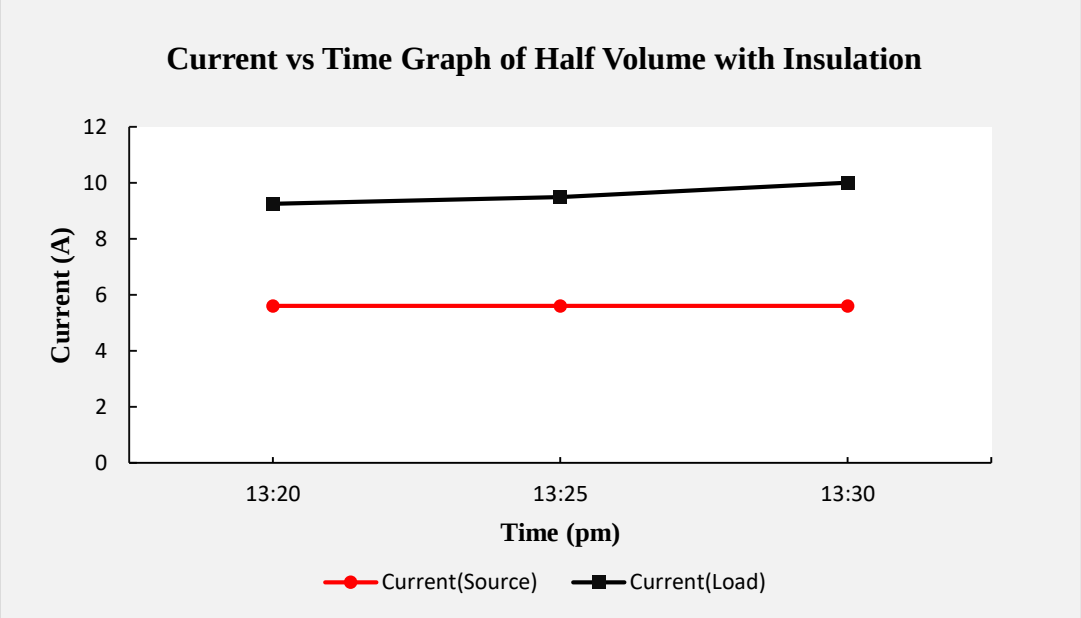

Figure 50: Current vs. Time graph of the Source and Load (TEC Module).

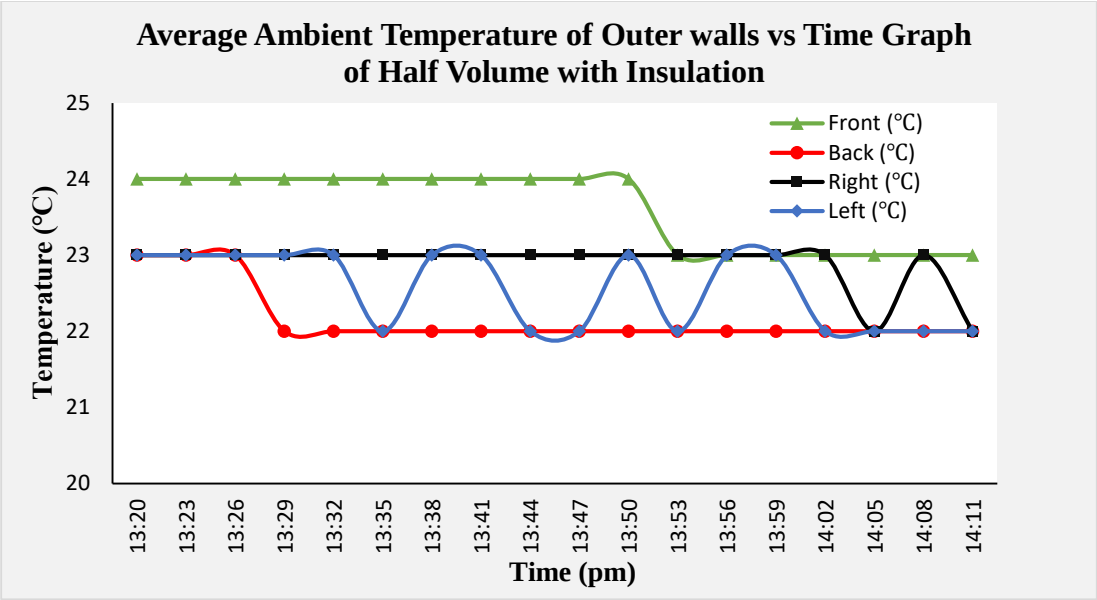

Figure 51: Average Ambient Temperature of the Outer Surfaces vs. Time graph of Half Volume with Insulation.

4.2 Results for Selection Criteria: Volume Optimization Stage

In this section we presented some of the plots with the help of which the best and optimized geometry of the cooling system was determined. For selecting the optimal geometry we considered some parameters to conduct a comparative study among the test cases. Accordingly the best possible geometry was finalized by observing the case where the system performed most efficiently in terms of all the considered parameters. The parameters chosen were mainly Cooling Time and Reverse Cooling Time, Temperature Difference during Cooling and Temperature Difference during Reverse Cooling. After comparing these parameters with respect to all the cases, the optimized geometry was logically determined. Here the optimal geometry was characterized by its best provided thermal performance.

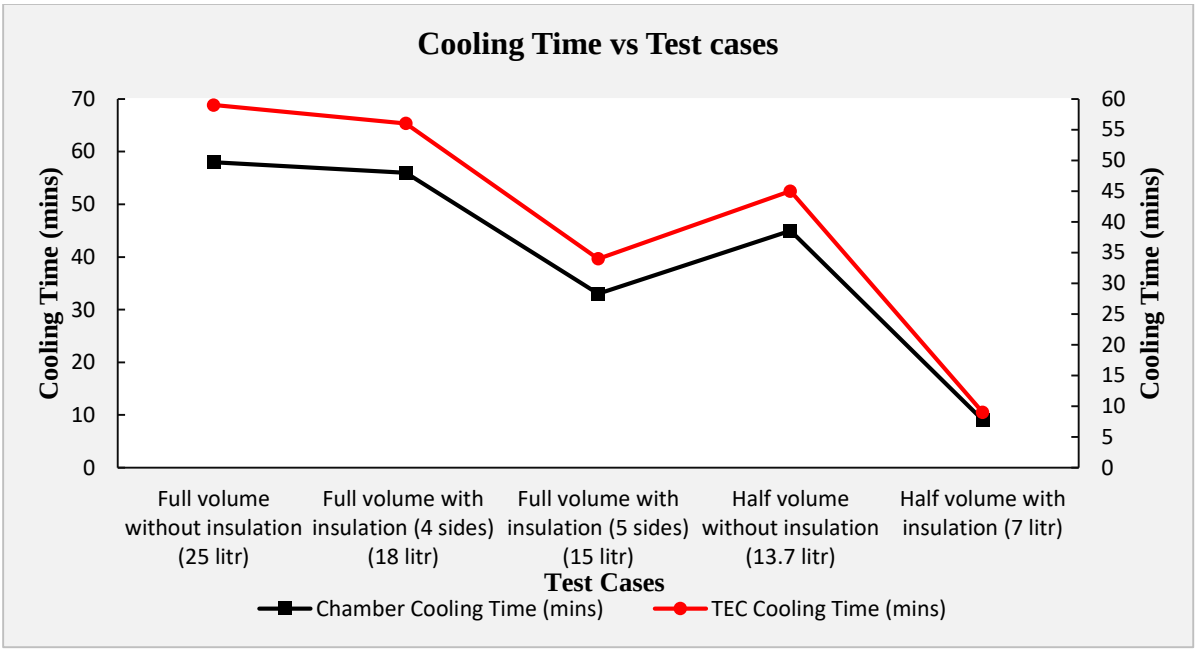

Figure 52: Cooling Time Taken by the TEC Module for different Volumes of the system.

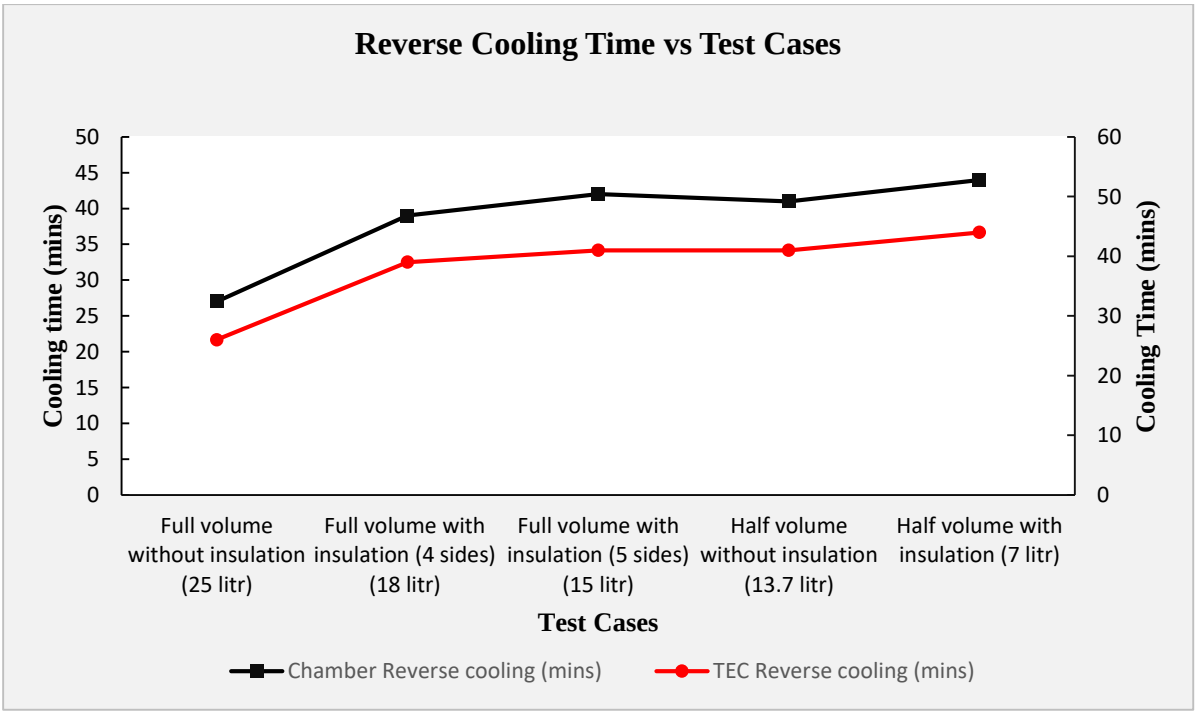

Figure 53: Retention Time of the system for different Volumes of the system.

Cooling Time is the time required by a refrigeration system in order to indicate sensible rate of Heat transfer considering all modes of heat transfer in a particular system. And Retention Time is the period of time during which the system can hold its Heat content as the Heating process accelerates **[2].** From the **(Figure 52)**, it is observed that the lowest amount of cooling time was taken by the Optimal Volume (7L). Similarly from **(Figure 53)**, it is observed that the highest retention period was taken by the Optimal Volume as well.

Another considered parameter was Temperature Difference achieved by the system during both Cooling and Heating process.

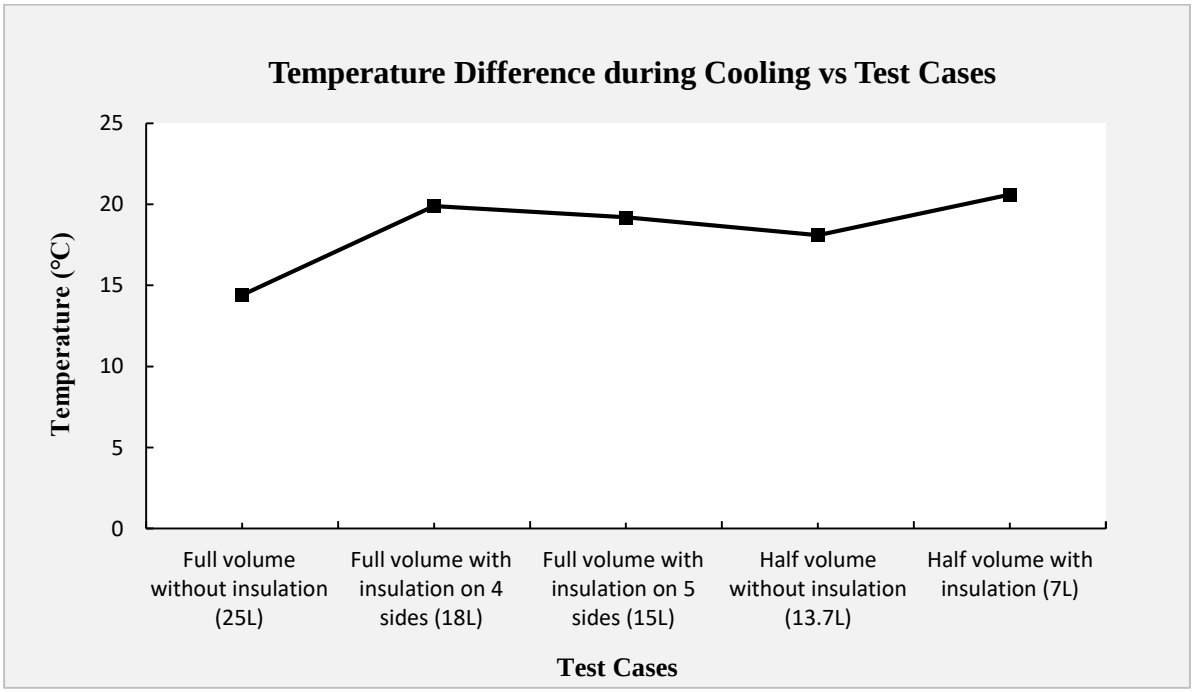

*Figure 54**:** Temperature Difference during cooling process with respect to different Test Cases.*

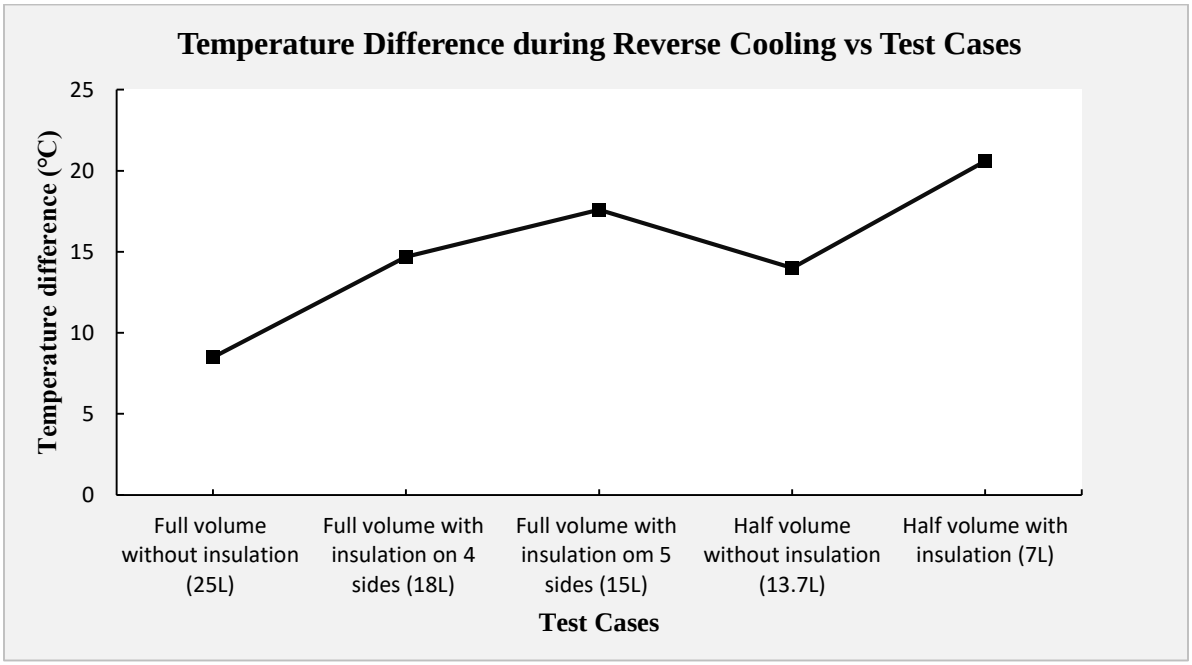

Figure 55: Temperature Difference during Reverse Cooling with respect to different Test Cases.

From **(Figure 54),** it is observed that the highest difference was achieved by the optimal volume during the cooling process. Here the temperature difference indicates the difference between the initial and the lowest temperature in the chamber. From **(Figure 55),** it is observed that the highest difference was achieved by the optimum volume during the reverse cooling process. Here the temperature difference indicates the difference between the lowest temperature in the chamber and the ambient temperature.

4.3 Result Summary from Stage-1: Volume Optimization

Table 6: Summary of Different Parameters from Volume Optimization Stage

Parameters	Test Run 1 (Full Volume without Insulation)	Test Run 2 (Full Volume with Insulation on four sides)	Test Run 3 (Full Volume with Insulation on Five sides)	Test Run 4 (Half Volume without Insulation)	Test Run 5 (Half Volume with Insulation)
Volume of the Chamber	25 ltr	18 ltr	15 ltr	13.7 ltr	**7 ltr**
Initial Temperature (Chamber)	24.7°C	26.2°C	21.7°C	23.1°C	**21.5°C**
Lowest Temperature Reached in the Chamber	10.3°C	6.3°C	2.5°C	5°C	**0.9°C**
Temperature difference achieved in the chamber during cooling	14.4°C	19.9°C	19.2°C	18.1°C	**20.6°C**
Temperature difference achieved in the chamber during reverse cooling	8.5°C	14.7°C	17.6°C	14°C	**20.6°C**
Cooling Run time(Chamber)	58 minutes	56 minutes	33 minutes	45 minutes	**9 minutes**
Cooling Run time(TEC)	59 minutes	56 minutes	34 minutes	45 minutes	**9 minutes**
Reverse Cooling Run time(Chamber)	27 minutes	39 minutes	42 minutes	41 minutes	**44 minutes**
Reverse Cooling Run time(TEC)	26 minutes	39 minutes	41 minutes	41 minutes	**44 minutes**

4.4 Results from Stage-2: Photovoltaic (Solar) Integration

As mentioned earlier, for efficient functioning of the experimentation the entire work-frame was divided into two stages. After completion of the Volume Optimization stage, the system was integrated with solar panels as the main power source. This stage was regarded as Photovoltaic Integration for convenience. In this section results are presented from the study of different parameters significant to the experimentation.

4.4.1 Test Run 6: Solar Direct Drive on Optimized Volume (7L)

This particular case was conducted on the optimized volume of the system i.e. 7L. A Solar array of three 120W Solar panels were used in parallel connection for the study. Each Solar panel was rated to be 18V and 6.7A respectively. These panels were utilized to provide power to the system directly without any Backup and Charge Controller.

Table 7: Significant Parameters inside the Cooling Chamber and on the cold side of the TEC

Parameters	Chamber	TEC
Initial Time	8:35:00 PM	8:35:00 PM
Initial Temperature	23.5°C	23.1°C
Initial Humidity	60.7%	67.1%
	During Cooling	
Run Time	40 minutes	40 minutes
Lowest Temperature Achieved	0.5°C	-6.2 °C
Lowest Humidity Achieved	56.5%	52.6%

The collection of data shown above was extracted from the digital data loggers through a software called **ElitechLogWin V6.2.0.** The temperature sensor or the thermocouple and the humidity sensor were placed inside the chamber and on the cold side of the TEC for this purpose. The graphical data were also extracted from the same software in order to observe the continuous fluctuations of temperature and humidity during the entire process of cooling and reverse cooling. This clarified the validity of the variable thermal performance at different times inside the chamber and on the cold side of the TEC module.

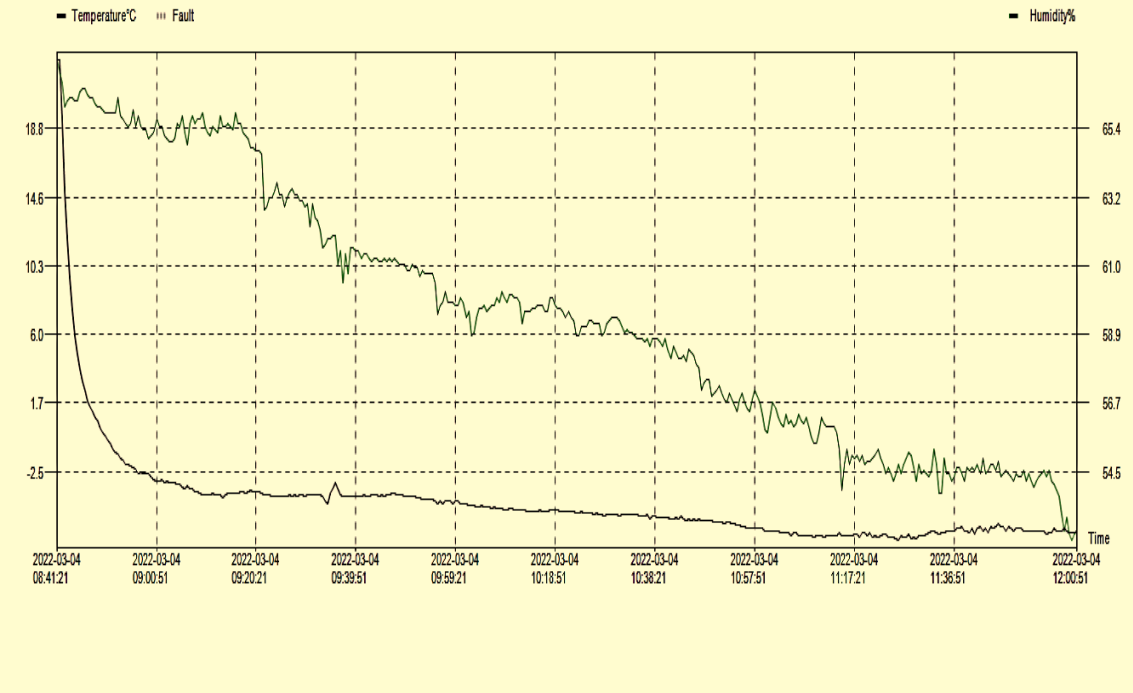

Figure 56: Fluctuation of Temperature and Humidity on the cold side of the TEC. (Sensor Probe placed on the Cold Side of TEC Module)

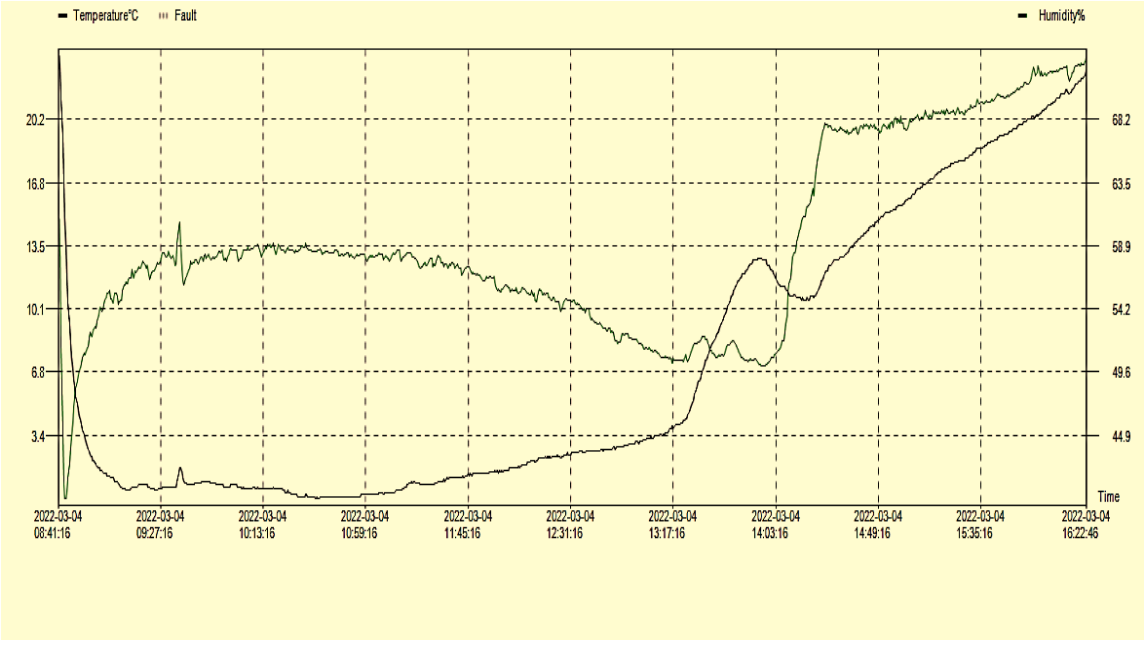

Figure 57: Fluctuation of Temperature and Humidity inside the Cooling Chamber. (Sensor Probe placed inside the chamber in a definite coordinate)

Additionally the voltage and current readings of the load (12V-10A TEC module) were taken in order to study the power consumption rate for definite time interval. The average temperature readings of the surfaces exposed to the environment of the cold box were also taken for studying the heat transfer rate and the temperature gradient of the system. The Solar Irradiation of each panels were recorded by a Pyranometer at definite time intervals in order to study the panel performance and its influence on the thermal performance of the system. The collected data are presented graphically for clear understanding.

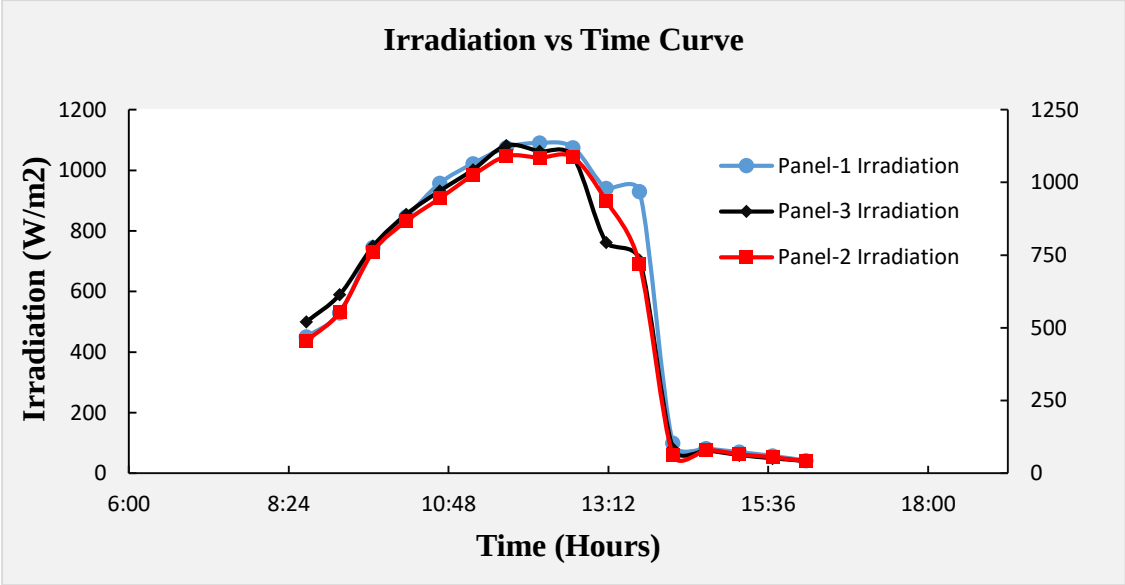

Figure 58: Irradiance profile of 120W Solar panels

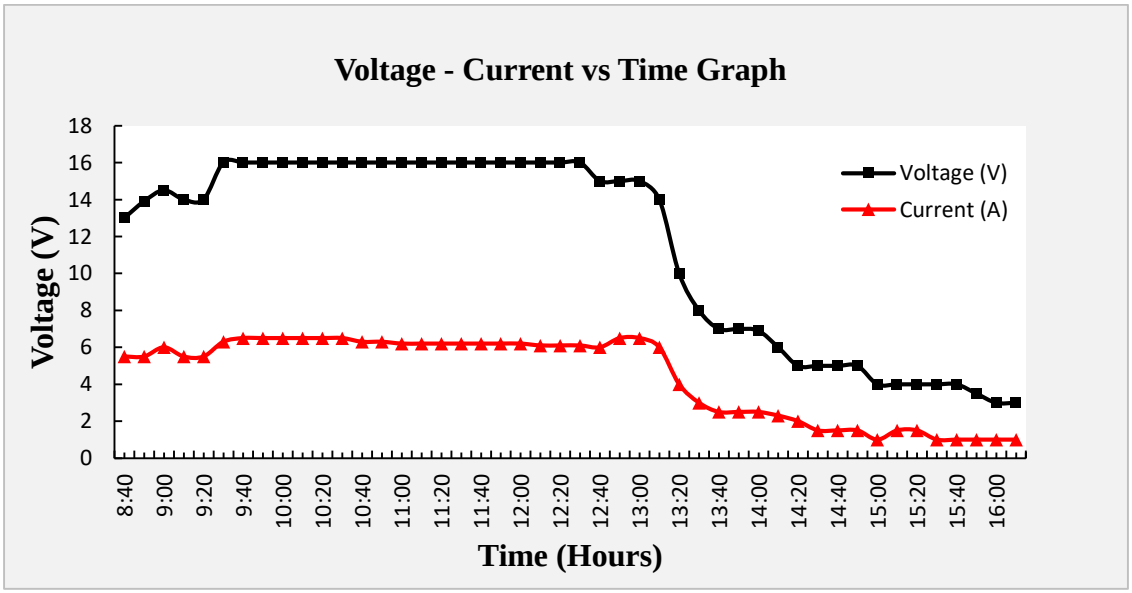

Figure 59: Voltage and Current vs. Time graph during Solar Direct Drive.

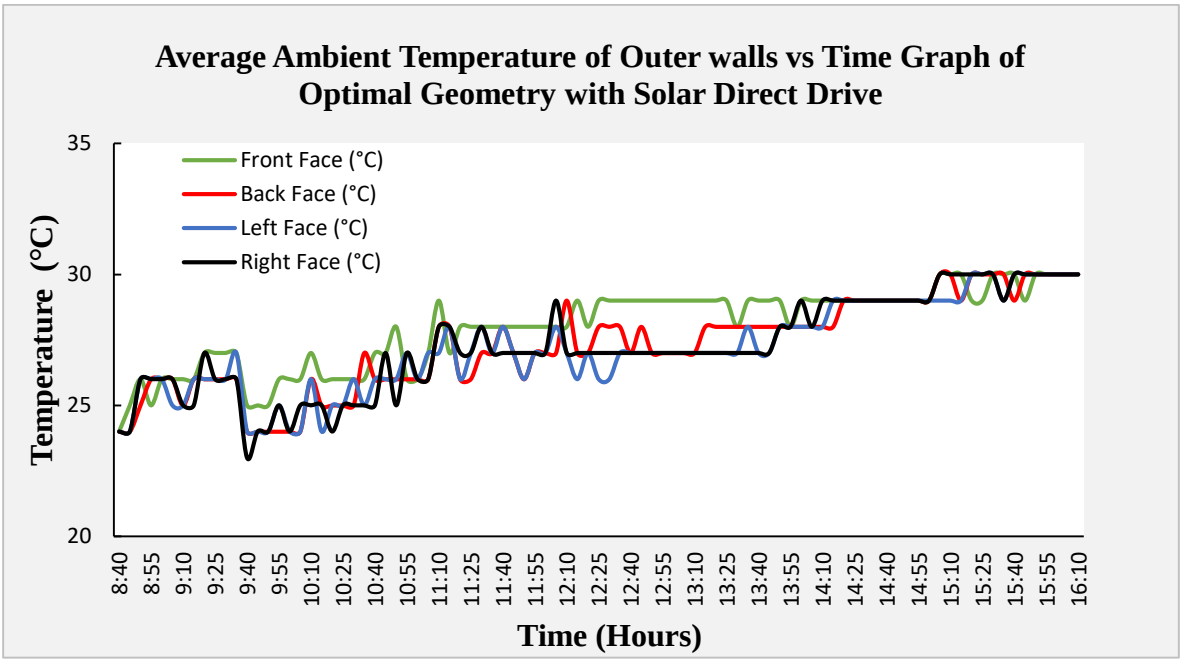

Figure 60: Average Ambient Temperature of Outer Surfaces during Solar Direct Drive.

4.4.2 Test Run 7: Solar Drive with Battery Backup on Optimized Volume (7L)

This particular case was conducted on the optimized volume of the system i.e. 7L. A 375W Auto-tracking Solar panel Module was used for the experimentation. The panel was utilized to provide power to the system along with a 12V, 8.2-12Ah Lead Acid Battery Backup and a Digital Charge Controller.

Table 8: Significant Parameters inside the Cooling Chamber and on the cold side of the TEC

Parameters	Chamber	TEC
Initial Time	10:55:00 PM	10:55:00 PM
Initial Temperature	21.9°C	22.1°C
Initial Humidity	84.1%	59%
	During Cooling	
Run Time	60 minutes	31 minutes
Lowest Temperature Achieved	2°C	-6°C
Lowest Humidity Achieved	61.2%	57.7%

The collection of data shown above was extracted from the digital data loggers through a software called **ElitechLogWin V6.2.0.** The temperature sensor or the thermocouple and the humidity sensor were placed inside the chamber and on the cold side of the TEC for this purpose. The graphical data were also extracted from the same software in order to observe the continuous fluctuations of temperature and humidity during the entire process of cooling and reverse cooling. This clarified the validity of the variable thermal performance at different times inside the chamber and on the cold side of the TEC module.

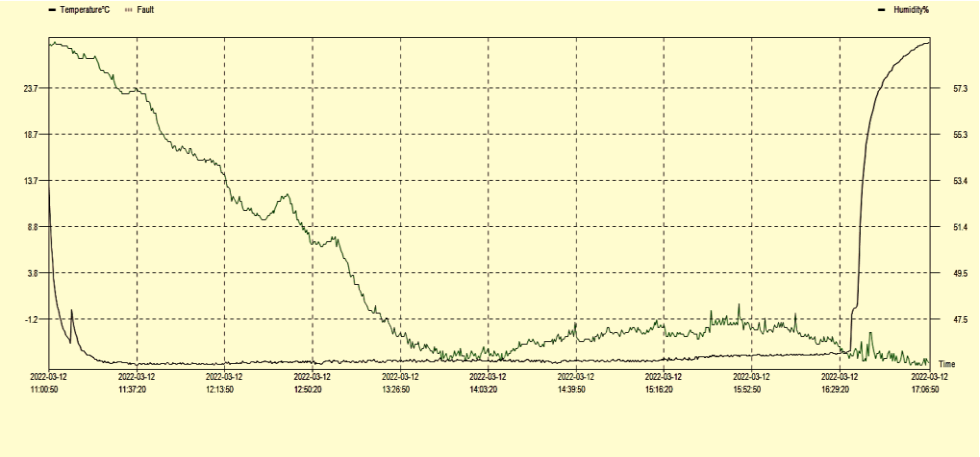

Figure 61: Fluctuation of Temperature and Humidity on the cold side of the TEC. (Sensor Probe placed on the Cold Side of TEC Module)

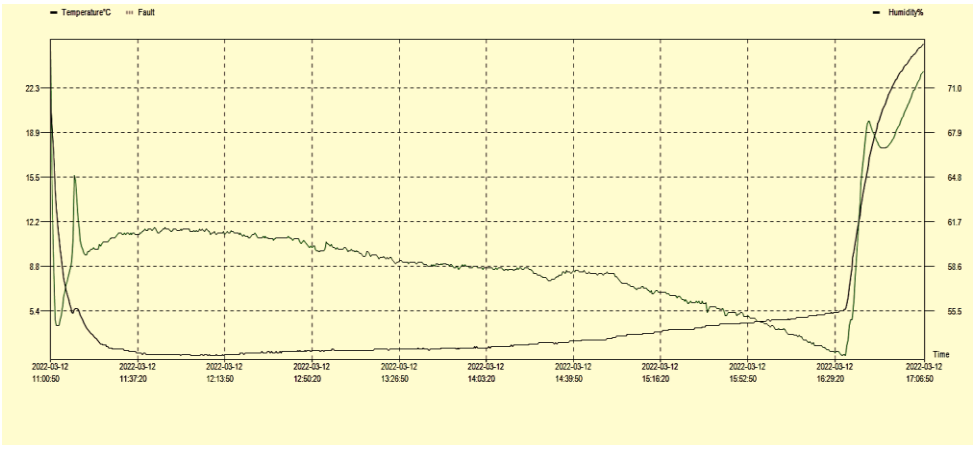

Figure 62: Fluctuation of Temperature and Humidity inside the Cooling Chamber. (Sensor Probe placed inside the chamber in a definite coordinate)

Additionally the voltage and current readings were taken of both the source (12V Lead Acid Battery) and the load (12V-10A TEC module) in order to study the power consumption rate for definite time interval. The average temperature readings of the surfaces exposed to the environment of the cold box were also taken for studying the heat transfer rate and the temperature gradient of the system. The Solar Irradiation of the Auto-tracking panel was recorded by a Software at definite time intervals in order to study the panel performance and its influence on the thermal performance of the system. The collected data are presented graphically for clear understanding.

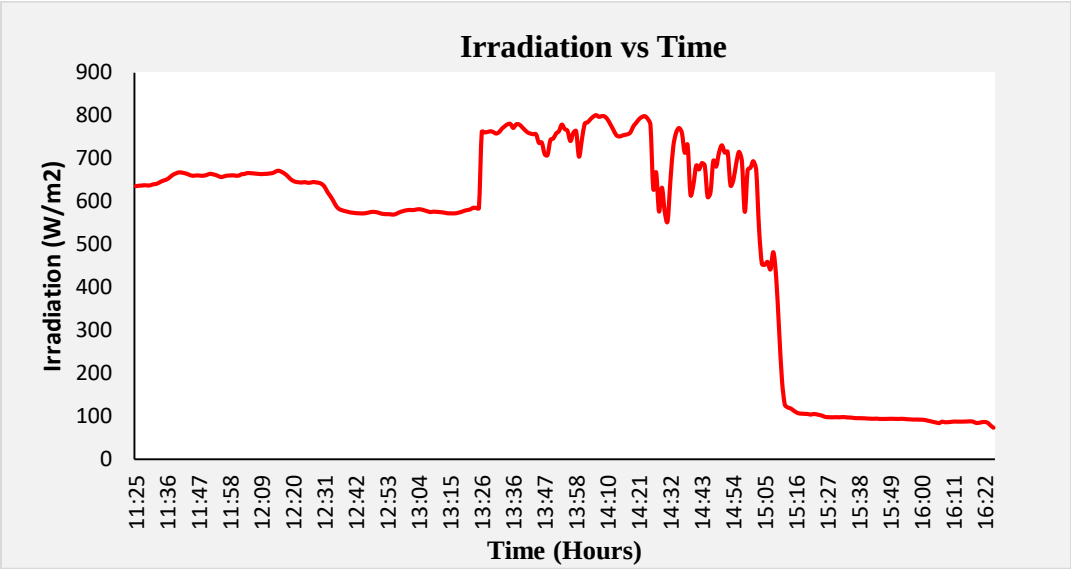

Figure 63: Irradiance profile of 375W Auto-tracking Solar panel.

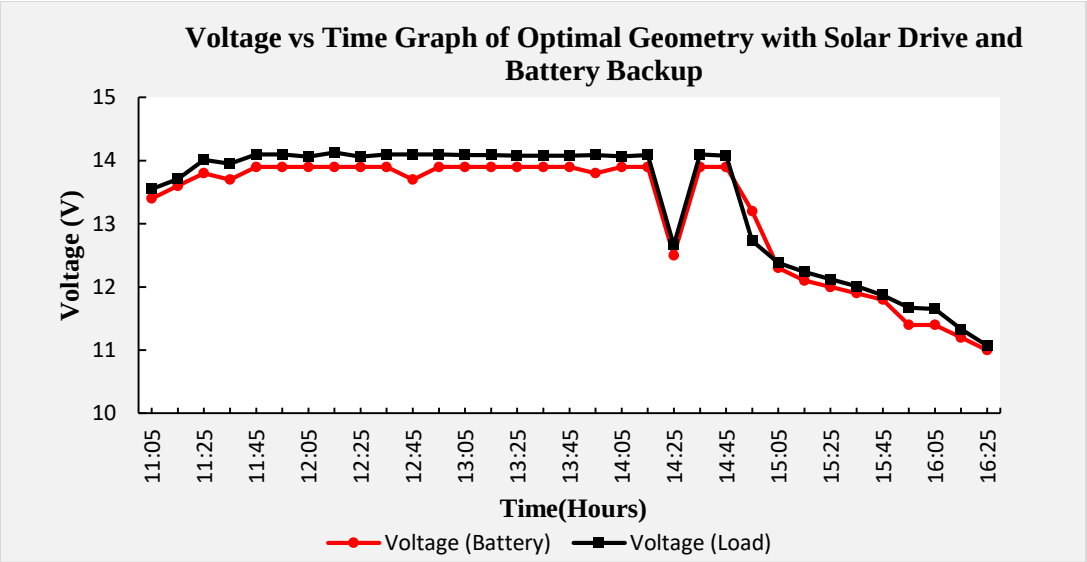

Figure 64: Voltage vs. Time graph during Solar Drive with Battery Backup.

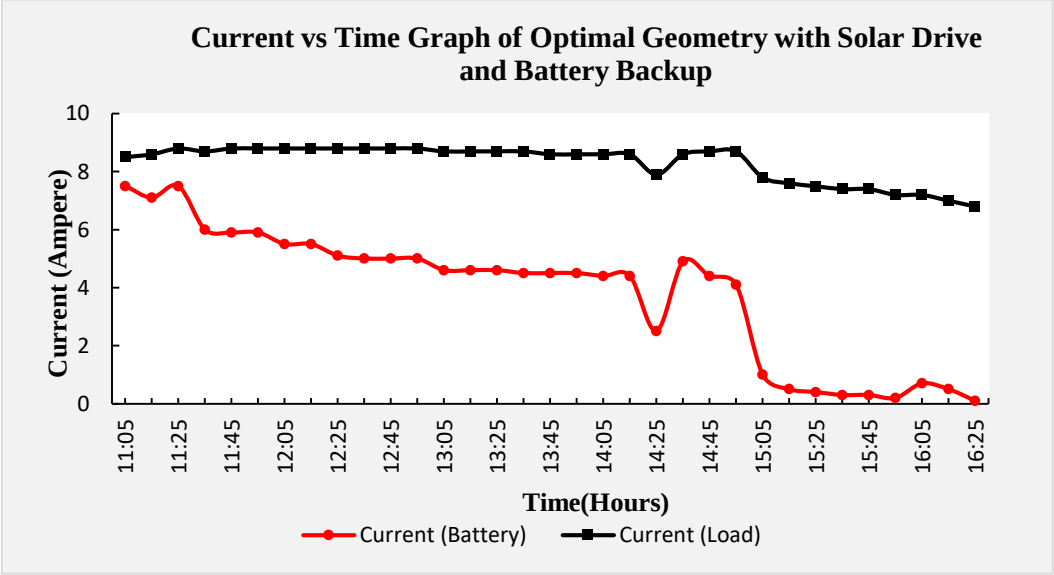

Figure 65: Current vs. Time graph during Solar Drive with Battery Backup.

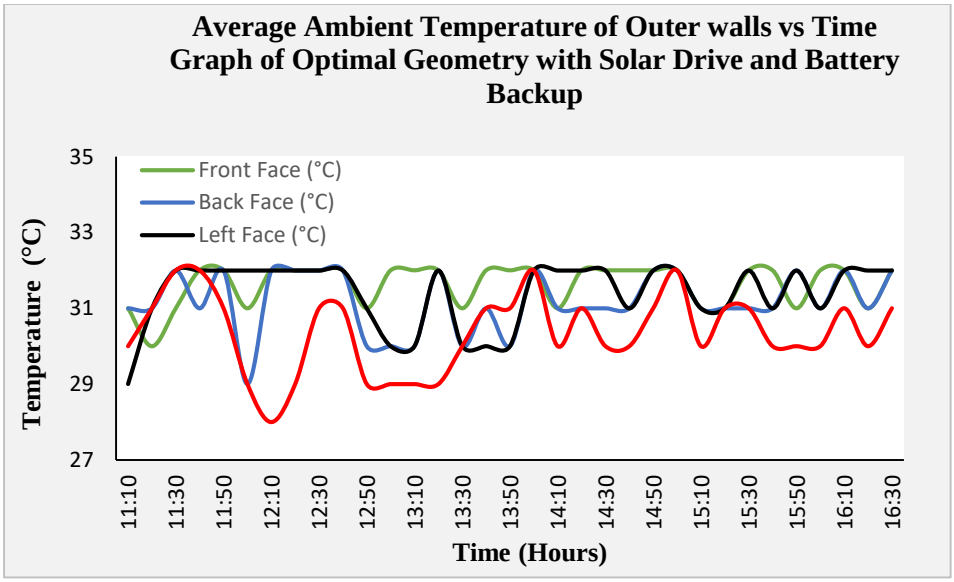

Figure 66: Average Ambient Temperature of Outer surfaces of Optimal Geometry with Solar Drive with Battery backup.

4.5 Result Summary from Stage-2: Photovoltaic Integration

In this section mainly the effect of variable intensity of solar irradiation on the holding period of the system of the desired temperature (2-8°C) is presented graphically and the desired values of some important parameters extracted from the study are summarized.

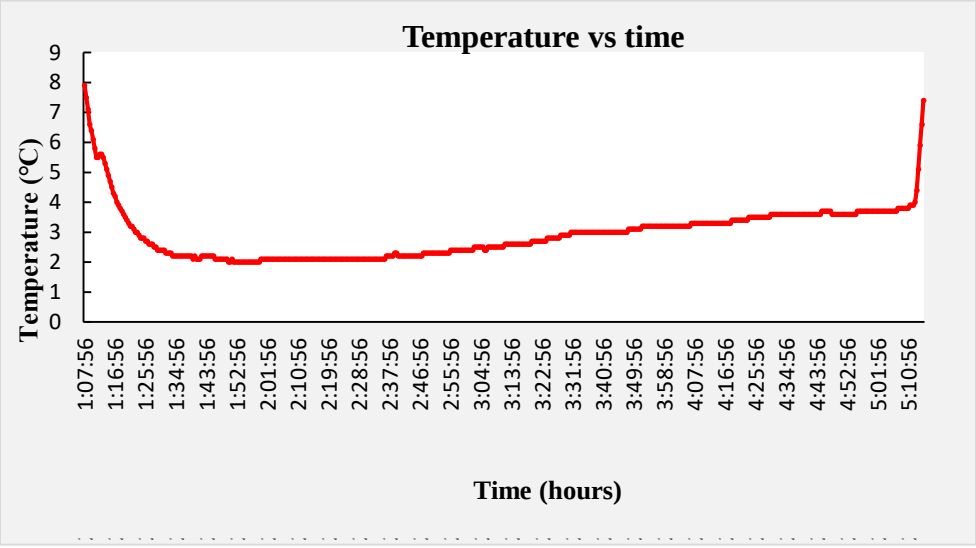

Figure 67: Holding Period of the System During Solar Direct Drive

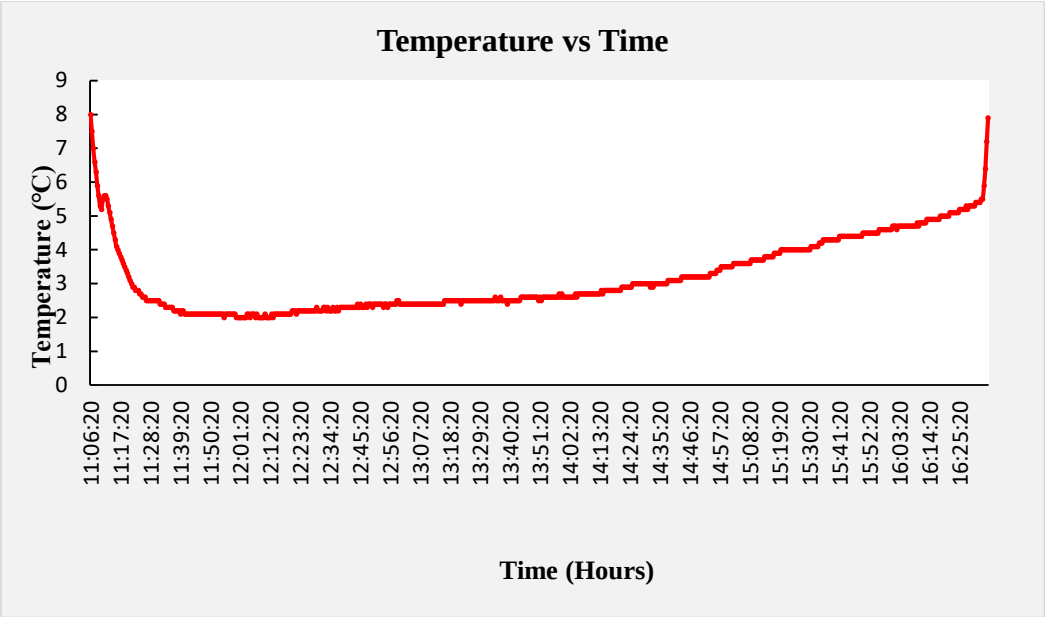

Figure 68: Holding Period of the System During Solar Drive with Battery Backup.

Table 9: Summary of Different Parameters from PV Integration Stage

Parameters	Test Case 6 (Solar Direct Drive)	Test Case 7 (Solar drive with Battery Backup)
Volume of the Chamber	7L	7L
Initial Temperature (Chamber)	23.5°C	21.2°C
Lowest Temperature Reached in the Chamber	0.5°C	2°C
Temperature difference achieved in the chamber during cooling	23°C	19.2°C
Holding Period	**4 Hours 46 Minutes**	**5 Hours 29 Minutes**

Chapter 5

5. Conclusion and Recommendation

5.1 Future Scope

With recent advancements taking place in field of thermoelectric refrigeration and utilization of one of the most valuable source of renewable energy i.e. Solar power, the present study holds wide scopes in future for refined modifications and experimentation. In order to make this system portable and feasible, a better and efficient backup system can be integrated into the design. Additionally use of multiple thermoelectric modules in the system will solve the problem of efficiency loss of TEC which is a common phenomenon. Besides, the incorporation of a temperature control system into the design will assure appropriate adjustment and maintenance of the desired temperature range inside the cooling chamber. For making the present system more efficient with the photovoltaic integration, location of the solar panels can be adjusted in a better position, as well as the orientation of the panels can also be reformed. Finally, further investigation and performance study of the solar panels can be conducted under varying weather conditions, simultaneously performance study of the backup system can be done for proper functioning of the system during night-time applications.

5.2 Conclusion

The objective of the current study was firstly to design a prototype of a cooling system and experimentally optimize its geometry for thermoelectric vaccine refrigerator. Secondly, the thermal performance of the system was investigated with photovoltaic integration into the system, thereby making the system feasible for off-grid areas. The study was rather focused on experimentation and optimization than its commercial applications in practical fields. The system was successfully functional under the applied conditions giving satisfactory results in terms of all desired parameters. It could reach a temperature difference (difference between initial and lowest temperature achieved inside the chamber) in the range of 18-25°C during both categories of Solar Drive incorporated in the system within a very short period of time (less than one hour). Additionally the retention period of the desired temperature was sufficient for a vaccine storage

system. The holding period (indicates the time duration during which the system could maintain the desired temperature range) during solar direct drive was 4 hours 46 minutes and during solar drive with battery backup was 5 hours 29 minutes. Thus the designed cooling system for vaccine storage purpose is fairly efficient and was experimentally verified.

References:

[1] T. J. Scotto, "Book reviews: Book reviews," *Party Polit.*, vol. 17, no. 4, pp. 525–527, 2011, doi: 10.1177/1354068811407546.

[2] S. Jiajitsawat and J. Duffy, "A portable direct-PV thermoelectric vaccine refrigerator with ice storage through heat pipes," *Am. Sol. Energy Soc. - Sol. 2006 35th ASES Annu. Conf., 31st ASES Natl. Passiv. Sol. Conf., 1st ASES Policy Mark. Conf., ASME Sol. Energy Div. Int. Sol. Energy Conf.*, vol. 1, no. January 2008, pp. 242–249, 2006.

[3] J. M. Brewer, "State of the world's vaccines and immunization," *Trans. R. Soc. Trop. Med. Hyg.*, vol. 97, no. 2, p. 181, 2003, doi: 10.1016/s0035-9203(03)90113-1.

[4] U. H. Kartoglu, K. L. Moore, and J. S. Lloyd, "Logistical challenges for potential SARS-CoV-2 vaccine and a call to research institutions, developers and manufacturers," *Vaccine*, vol. 38, no. 34, pp. 5393–5395, 2020, doi: 10.1016/j.vaccine.2020.06.056.

[5] W. H. Organization, "Immunization coverage," *Fact sheet N 378*, 2015. http://www.who.int/mediacentre/factsheets/fs378/en/ (accessed May 10, 2022).

[6] J. L. Silveira, C. E. Tuna, and W. D. Q. Lamas, "The need of subsidy for the implementation of photovoltaic solar energy as supporting of decentralized electrical power generation in Brazil," *Renew. Sustain. Energy Rev.*, vol. 20, pp. 133–141, 2013, doi: 10.1016/j.rser.2012.11.054.

[7] S. G and S. Raj, "Design and Fabrication of Portable Thermoelectric Vaccine Preservator," *Int. J. Res. Aeronaut. Mech. Eng.*, vol. 3, no. 12, pp. 50–62, 2015.

[8] R. L. Field, "Photovoltaic/Thermoelectric refrigerator for medicine storage for developing countries," *Sol. Energy*, vol. 25, no. 5, pp. 445–447, 1980, doi: 10.1016/0038-092X(80)90452-1.

[9] GAVI, "Cold Chain Equipment Optimisation Platform," *Technol. Guid.*, no. October 2019, pp. 27–28, 2019, Accessed: May 11, 2022. [Online]. Available: www.gavi.org.

[10] H. Ritchie, "Access to Energy - Our World in Data," *OurWorldInData.org.*, 2019. https://ourworldindata.org/energy-access#access-to-electricity%0Ahttps://ourworldindata.org/energy-access (accessed May 10, 2022).

[11] The World Bank, *Access to electricity (% of population) | Data*. 2019.

[12] S. B. Riffat and X. Ma, "Improving the coefficient of performance of thermoelectric cooling systems: A review," *Int. J. Energy Res.*, vol. 28, no. 9, pp. 753–768, 2004, doi: 10.1002/er.991.

[13] M. Gökçek and F. Şahin, "Experimental performance investigation of minichannel water

cooled-thermoelectric refrigerator," *Case Stud. Therm. Eng.*, vol. 10, no. September 2016, pp. 54–62, 2017, doi: 10.1016/j.csite.2017.03.004.

[14] D. M. Matthias, J. Robertson, M. M. Garrison, S. Newland, and C. Nelson, "Freezing temperatures in the vaccine cold chain: A systematic literature review," *Vaccine*, vol. 25, no. 20, pp. 3980–3986, 2007, doi: 10.1016/j.vaccine.2007.02.052.

[15] M. Bilgili, "Hourly simulation and performance of solar electric-vapor compression refrigeration system," *Sol. Energy*, vol. 85, no. 11, pp. 2720–2731, 2011, doi: 10.1016/j.solener.2011.08.013.

[16] S. Clara *et al.*, "(2) Patent Application Publication (10) Pub . No .: US 2016 / 0003503 A1 | _ < Heat pipe – TEC Conductive He ; at sink," vol. 1, no. 19, 2016.

[17] S. McCarney, J. Robertson, J. Arnaud, K. Lorenson, and J. Lloyd, "Using solar-powered refrigeration for vaccine storage where other sources of reliable electricity are inadequate or costly," *Vaccine*, vol. 31, no. 51, pp. 6050–6057, 2013, doi: 10.1016/j.vaccine.2013.07.076.

[18] D. Astrain, A. Martínez, and A. Rodríguez, "Improvement of a thermoelectric and vapour compression hybrid refrigerator," *Appl. Therm. Eng.*, vol. 39, pp. 140–150, 2012, doi: 10.1016/j.applthermaleng.2012.01.054.

[19] A. F. Ioffe, "Semiconductor Cooling," *Semicond. THERMOELEMENTS Thermoelectr. Cool.*, 1957.

[20] D. Zhao and G. Tan, "A review of thermoelectric cooling: Materials, modeling and applications," *Appl. Therm. Eng.*, vol. 66, no. 1–2, pp. 15–24, 2014, doi: 10.1016/j.applthermaleng.2014.01.074.

[21] I. Sarbu and A. Dorca, "A comprehensive review of solar thermoelectric cooling systems," *Int. J. Energy Res.*, vol. 42, no. 2, pp. 395–415, 2018, doi: 10.1002/er.3795.

[22] X. Ma, H. Zhao, X. Zhao, G. Li, and S. Shittu, "Building integrated thermoelectric air conditioners—a potentially fully environmentally friendly solution in building services," *Futur. Cities Environ.*, vol. 5, no. 1, pp. 1–13, 2019, doi: 10.5334/fce.76.

[23] G. T. Craven and A. Nitzan, "Wiedemann-Franz Law for Molecular Hopping Transport," *Nano Lett.*, vol. 20, no. 2, pp. 989–993, Feb. 2020, doi: 10.1021/acs.nanolett.9b04070.

[24] T. P. Hogan *et al.*, "Nanostructured thermoelectric materials and high-efficiency power-generation modules," *J. Electron. Mater.*, vol. 36, no. 7, pp. 704–710, 2007, doi: 10.1007/s11664-007-0174-9.

[25] L. E. Bell, "Cooling, heating, generating power, and recovering waste heat with thermoelectric systems," *Science (80-.).*, vol. 321, no. 5895, pp. 1457–1461, 2008, doi: 10.1126/science.1158899.

[26] F. J. Disalvo, "Thermoelectric cooling and power generation," *Science (80-.).*, vol. 285, no.

5428, pp. 703–706, 1999, doi: 10.1126/science.285.5428.703.

[27] A. Elghool, F. Basrawi, T. K. Ibrahim, K. Habib, H. Ibrahim, and D. M. N. D. Idris, "A review on heat sink for thermo-electric power generation: Classifications and parameters affecting performance," *Energy Convers. Manag.*, vol. 134, pp. 260–277, 2017, doi: 10.1016/j.enconman.2016.12.046.

[28] N. Zhu, P. Hu, L. Xu, Z. Jiang, and F. Lei, "Recent research and applications of ground source heat pump integrated with thermal energy storage systems: A review," *Appl. Therm. Eng.*, vol. 71, no. 1, pp. 142–151, 2014, doi: 10.1016/j.applthermaleng.2014.06.040.

[29] Y. Choi *et al.*, "Effect of the carbon nanotube type on the thermoelectric properties of CNT/Nafion nanocomposites," *Org. Electron.*, vol. 12, no. 12, pp. 2120–2125, 2011, doi: 10.1016/j.orgel.2011.08.025.

[30] S. A. Abdul-Wahab *et al.*, "Design and experimental investigation of portable solar thermoelectric refrigerator," *Renew. Energy*, vol. 34, no. 1, pp. 30–34, 2009, doi: 10.1016/j.renene.2008.04.026.

[31] J. Chen, Z. Yan, and L. Wu, "The influence of Thomson effect on the maximum power output and maximum efficiency of a thermoelectric generator," *J. Appl. Phys.*, vol. 79, no. 11, pp. 8823–8828, 1996, doi: 10.1063/1.362507.

[32] D. Enescu and E. O. Virjoghe, "A review on thermoelectric cooling parameters and performance," *Renew. Sustain. Energy Rev.*, vol. 38, pp. 903–916, 2014, doi: 10.1016/j.rser.2014.07.045.

[33] D. Astrain, A. Martínez, and A. Rodríguez, "Improvement of a thermoelectric and vapour compression hybrid refrigerator," *Appl. Therm. Eng.*, vol. 39, pp. 140–150, 2012, doi: 10.1016/j.applthermaleng.2012.01.054.

[34] A. Martínez, D. Astrain, A. Rodríguez, and G. Pérez, "Reduction in the electric power consumption of a thermoelectric refrigerator by experimental optimization of the temperature controller," *J. Electron. Mater.*, vol. 42, no. 7, pp. 1499–1503, 2013, doi: 10.1007/s11664-012-2298-9.

[35] X. Liu and J. Yu, "Numerical study on performances of mini-channel heat sinks with non-uniform inlets," *Appl. Therm. Eng.*, vol. 93, pp. 856–864, 2016, doi: 10.1016/j.applthermaleng.2015.09.032.

[36] Y. J. Dai, R. Z. Wang, and L. Ni, "Experimental investigation on a thermoelectric refrigerator driven by solar cells," *Renew. Energy*, vol. 28, no. 6, pp. 949–959, 2003, doi: 10.1016/S0960-1481(02)00055-1.

[37] M. Saifizi, M. S. Zakaria, S. Yaacob, and K. Wan, "Development and Analysis of Hybrid Thermoelectric Refrigerator Systems," *IOP Conf. Ser. Mater. Sci. Eng.*, vol. 318, no. 1, 2018, doi: 10.1088/1757-899X/318/1/012036.

[38] J. A. Gastelo-Roque and A. Morales-Acevedo, “Design of a photovoltaic system using thermoelectric Peltier cooling for vaccines refrigeration,” *2017 IEEE MIT Undergrad. Res. Technol. Conf. URTC 2017*, vol. 2018-Janua, no. February, pp. 1–4, 2018, doi: 10.1109/URTC.2017.8284211.

[39] F. Hidayanti, “The effect of monocrystalline and polycrystalline material structure on solar cell performance,” *Int. J. Emerg. Trends Eng. Res.*, vol. 8, no. 7, pp. 3420–3427, 2020, [Online]. Available: https://doi.org/10.30534/ijeter/2020/87872020.

[40] V. P. Anand, E. Ameen, and B. Pesala, “Experimental investigation of the shading losses on solar module system performance,” *2014 Int. Conf. Adv. Electr. Eng. ICAEE 2014*, 2014, doi: 10.1109/ICAEE.2014.6838548.

[41] A. Ghazali M. and A. M. Abdul Rahman, “The Performance of Three Different Solar Panels for Solar Electricity Applying Solar Tracking Device under the Malaysian Climate Condition,” *Energy Environ. Res.*, vol. 2, no. 1, pp. 235–243, 2012, doi: 10.5539/eer.v2n1p235.